2011-01-01

Aerosol Characterizaton In El Paso-Juarez Airshed Using Optical Methods

Angel E. Esparza
University of Texas at El Paso, eangel@miners.utep.edu

AEROSOL CHARACTERIZATON IN EL PASO-JUAREZ AIRSHED USING OPTICAL METHODS

ANGEL EDUARDO ESPARZA

Environmental Science and Engineering Doctoral Program

APPROVED:

_____
Rosa M. Fitzgerald, Ph.D., Chair

_____
Russell Chianelli, Ph.D.

_____
Luis Rene Contreras, Ph.D.

_____
Sergio Flores, Ph.D.

_____
Benjamin C. Flores, Ph.D.
Interim Dean of the Graduate School

DEDICATION

I dedicate my dissertation work to my family. A special feeling of gratitude to my loving parents, Blanca Estela and Telésforo whose words of encouragement and example make me be always on top of any issue.

I also dedicate this work to my aeonian girlfriend and now wife, Ana Gabby, for being there throughout the entire doctorate program. I cannot imagine my life without her presence.

I want to thank all the people that directly or indirectly have provided me with all their support.

Papi, thank you. Mami, Eduardo, Maria Luisa, Julia and Conchita, thank you and I miss you.

I have found profound inspiration in these quotes. Somehow, I feel they are beautifully intertwined; holistically, they have helped me in this wonderful endeavor.

"Go confidently in the direction of your dreams! Live the life you've imagined.
As you simplify your life, the laws of the universe will be simpler."
-Henry David Thoreau

"If one does not know to which port one is sailing, no wind is favorable."
-Lucius Annaeus Seneca

"I am an idealist. I don't know where I am going but I am on my way."
-Carl Sandburg

“I asked God for strength that I might achieve.
I was made weak that I might learn humbly to obey.

I asked for health that I might do greater things.
I was given infirmity that I might do better things.

I asked for riches that I might be happy.
I was given poverty that I might be wise.

I asked for power that I might have the praise of men.
I was given weakness that I might feel the need of God.

I asked for all things that I might enjoy life.
I was given life that I might enjoy all things.

I got nothing that I asked for, but everything I hoped for.
Almost despite myself, my unspoken prayers were answered.
I am, among all men, most richly blessed.

- *The prayer of an unknown confederate soldier*

AEROSOL CHARACTERIZATON IN EL PASO-JUAREZ AIRSHED USING OPTICAL METHODS

BY

ANGEL EDUARDO ESPARZA, MSME & MSIE, EIT

DISSERTATION

Presented to the Faculty of the Graduate School of

The University of Texas at El Paso

in Partial Fulfillment

of the Requirements

for the Degree of

DOCTOR OF PHILOSOPHY

Environmental Science and Engineering Doctoral Program

THE UNIVERSITY OF TEXAS AT EL PASO

DECEMBER 2011

ACKNOWLEDGEMENTS

I wish to thank Dr. Rosa Fitzgerald, my committee chairwoman for her hours of reflecting, reading and most of all, for the patience throughout the entire process. A special thanks to my committee members who were more than generous with their expertise and valuable time. I would like to thank Dr. Chianelli, Dr. Contreras and Dr. Flores for agreeing to serve in my committee.

I would like to acknowledge and thank the ESE program and the Physics department for allowing me to conduct my research and providing any assistance requested.

I wish to thank Dr. Ralph Kahn, Dr. David Diner and Dr. Olga Kalashnikova from the MISR team for providing me with the satellite data. Also, to the USDA-UVB monitoring stations program for providing the MFRSR data. Additionally, special thanks to the TCEQ and AERONET teams for providing ground and columnar measurements of aerosols.

Finally I would like to thank the beginning teachers, mentor-teachers and administrators in our school division that assisted me with this project. A special thanks to Dr. Barry Benedict for his vision, candidness and pragmatism. Their excitement and willingness to provide feedback made the completion of this research an unforgettable experience.

ABSTRACT

The assessment and characterization of atmospheric aerosols and their optical properties are of great significance for several applications such as air pollution studies, atmospheric visibility, remote sensing of the atmosphere, and impacts on climate change. Decades ago, the interest in atmospheric aerosols was primarily for visibility impairment problems; however, recently interest has intensified with efforts to quantify the optical properties of aerosols, especially because of the uncertainties surrounding the role of aerosols in climate change. The main objective of the optical characterization of aerosols is to understand their properties. These properties are determined by the aerosols' chemical composition, size, shape and concentration.

The general purpose of this research was to contribute to a better characterization of the aerosols present in the Paso del Norte Basin. This study permits an alternative approach in the understanding of air pollution for this zone by analyzing the predominant components and their contributions to the local environment.

This dissertation work had three primary objectives, in which all three are intertwined by the general purpose of the aerosol characterization in the Paso del Norte region. The first objective was to retrieve the columnar aerosol size distribution for two different cases (clean and polluted scenarios) at each season (spring, summer, fall and winter) of the year 2009. In this project, instruments placed in buildings within the University of Texas at El Paso (UTEP) as well as a monitoring site (CAMS 12) from the Texas Commission on Environmental Quality (TCEQ) provided the measurements that delimited the aerosol size distribution calculated by our model, the Environmental Physics Inverse Reconstruction (EPIRM) model. The purpose of this objective was to provide an alternate method of quantifying and size-allocating aerosols *in situ*,

by using the optical properties of the aerosols and inversely reconstruct and retrieve the size distribution of them. This method permits the assessment of aerosols in the ambient *in-situ*, without physically extracting them from their current state, as the filter technique does.

The second objective was an analysis and comparison of the aerosol optical thickness (AOT) data between ground-based instruments and satellite data. In this project, the ground-based instruments are the Multi Filter Rotating Shadowband Radiometers (MFRSR) installed at UTEP and the nearest sun photometer facility, a NASA's Aerosol Robotic Network (AERONET), located at White Sands, New Mexico. The satellite data is provided by the NASA's Multi-angle Imaging Spectro-radiometer (MISR) instrument located in the Terra satellite.

Finally, the third objective was to estimate ground particulate matter concentration of particles no greater than 2.5 μm in diameter ($PM_{2.5}$) by using the MISR's satellite data. This objective was achieved by implementing an empirical mathematical model that includes measured data. In addition, this model addressed the geographic characteristics of the region as well as several factors such as season, relative humidity (RH) and the height of the planetary boundary layer (PBL).

TABLE OF CONTENTS

LIST OF TABLES

Page

LIST OF FIGURES

Page

INTRODUCTION

The assessment and characterization of atmospheric aerosols and their optical properties are of great significance for several applications such as atmospheric visibility studies, remote sensing of the atmosphere, impacts on climate change, as well as particulate matter monitoring *in situ* and from space (Kokhanovsky 2008). Also, the influence of aerosols in the flux of solar radiation as well as in its extinction plays a fundamental role that could have important relations in the understanding of air pollution.

Decades ago, the interest in atmospheric aerosols was primarily for visibility impairment problems; however, recently interest has intensified with efforts to quantify the optical properties of aerosols, especially because of the uncertainties surrounding the role of aerosols in climate change (Malm and Hand 2007). The main objective of the optical characterization of aerosols is to understand their properties. These properties are determined by the aerosols' chemical composition, size, shape and concentration. Determination of the aerosol optical thickness, single scattering albedo, extinction and absorption coefficients, asymmetry parameter and angstrom exponent, are fundamental values in the aerosol characterization.

In recent years, there has been substantial progress in the understanding of aerosol optical properties. Nonetheless, more work is required in determining the effects of light interaction with non-spherical aerosol particles, and also the retrieval of aerosol optical thickness and optical particle sizing using satellite observations (Kokhanovsky 2008).

The general purpose of this research is to contribute to a better understanding of the aerosols present in the Paso del Norte Basin. This study permits an alternative approach in the understanding of air pollution for this zone by analyzing the predominant components and their

contributions to the local environment. Nonetheless, this study sets another silo in the general comprehension of the local, regional, and global contribution of the aerosols.

This dissertation work had three primary objectives, in which all three are intertwined by the general purpose of the aerosol characterization in the Paso del Norte region. The first objective was to retrieve the columnar aerosol size distribution for two different cases (clean and polluted scenarios) at each season (spring, summer, fall and winter) of the year 2009. In this project, instruments placed in buildings within the University of Texas at El Paso (UTEP) as well as a monitoring site (CAMS 12) from the Texas Commission on Environmental Quality (TCEQ) provided the measurements that delimited the aerosol size distribution calculated by our model called Environmental Physics Inverse Reconstruction (EPIRM). The purpose of this objective was to provide an alternate method of quantifying and size-allocating aerosols *in situ*, by using the optical properties of the aerosols and inversely reconstruct and retrieve the size distribution of them. This method permits the assessment of aerosols in the ambient without physically extracting them from their current state, as the filter technique does.

The second objective was an analysis and comparison of the aerosol optical thickness (AOT) data between ground-based instruments and satellite data. In this project, the ground-based instruments are the Multi Filter Rotating Shadowband Radiometers (MFRSR) installed at UTEP and the nearest sun photometer facility, a NASA's Aerosol Robotic Network (AERONET), located at White Sands, New Mexico. The satellite data is provided by the NASA's Multi-angle Imaging Spectroradiometer (MISR) instrument located in the Terra satellite.

Finally, the third objective was to estimate particulate matter concentration of particles no greater than 2.5 μm in diameter ($PM_{2.5}$) by using the MISR's satellite data. This objective was

achieved by implementing an empirical mathematical model that includes measured data. Also, this model addressed the geographic characteristics of the region as well as several factors such as season, relative humidity (RH) and the height of the planetary boundary layer (PBL).

The first objective provided a methodology for the optical characterization of the aerosols in the site; by the ascertained of this methodology, it will be very relevant to reproduce it in other parts of the world by using fixed or dynamic instruments. With the advent of new remote sensing technologies, this objective could be achieved practically at no expense for the researchers. Therefore, the second objective provided an analysis of the MISR's satellite data against ground instruments (MFRSR and AERONET) in terms of the validity and correlation between the satellite and ground values. By understanding the differences between ground and satellite data, the direct conversion of satellite values into ground values by using a mathematical model is of high relevance. Consequently, the third objective was the creation of an empirical model that, by inputting certain conditions, converts satellite optical depth values into ground $PM_{2.5}$ values for this zone.

The Paso del Norte Airshed is comprised by three cities: El Paso, Texas; Sunland Park, New Mexico; and Ciudad Juarez, Chihuahua Mexico. This air basin frequently exceeds the ambient particulate matter (PM) concentration of the national air quality standards of both countries (Li et al. 2001). PM in the region derives from geological sources, industrial sources, vehicle exhaust, residential cooking and heating, and other unidentified sources; the arid weather, occasional high winds, frequent stagnations, shallow nighttime and morning mixing depths, and complex topography preclude simple explanations for excessive PM levels (Li et al. 2001).

The city of El Paso along with its neighboring city of Ciudad Juarez is the area of study for this research. Figure 1 shows the spatial location of El Paso-Juarez region.

Figure 1. Spatial location of El Paso-Juarez airshed excerpted from google ® (Google n.d.).

The two cities have a population of more than 2 million, where about 1.4 million live in Juarez, Mexico (INEGI n.d.) and about 750,000 live in El Paso, Texas (US Census Bureau n.d.). Geographically, these cities are surrounded by mountains on three sides, and share a common Airshed which makes a relatively homogenous physical environment. Generally, this region has more than 300 days of sunshine a year. The annual mean temperature ranges from -3 °C in winter to 38 °C in summer (Ordieres et al. 2005). The annual rainfall is 23.95 cm (9.43 inches), July and August being the months with the maximum rainfall (National Weather Service Weather Forecast Office 2009).

BACKGROUND

Initially air pollution was an indoor phenomenon, caused by open fires without controlled venting. Ambient urban air pollution, is as old as cities, however, this issue have been underestimated, because generally people were less critical about their living conditions and they had no means of evaluating long-term impacts (Baltensperger et al. 2009). Early documented air pollution episodes such as the London smog of 1952 led to the premature deaths of thousands of people, and prompted governments of many countries to create and enforce environmental policies that contributed to reduce their urban levels of air pollution (Gouveia and Fletcher 2000). Since 1950 global urbanization, defined as the fraction of people living in settlements above 2000 inhabitants, has risen from below 30 to 45%; in the more developed countries it is now around 75% and in the less developed 37% (Baltensperger et al. 2009).

Particulate matter (PM) was originally determined as soot or black smoke. Starting in 1971, the Ambien Air Quality Standard (NAAQS) for PM was based on the mass concentration of total suspended particulate (TSP). In 1987, this indicator was replaced with PM_{10} because TSP levels were often driven by a few very large particles, while health effects generally correlated with smaller particles, indeed those particles in the respirable size range, which is generally characterized by PM_{10}. Finally in the light of health effects data, United States Environmental Protection Agency revised the PM NAAQS in 1997 to include an indicator for the fine mode only, namely a $PM_{2.5}$ standard (Baltensperger et al. 2008).

In summary the following size ranges are defined:

TSP	Total suspended particulate matter (up to 35 μm in diameter)
PM 10	Particulate matter smaller than 10 μm in diameter
PM 2.5	Particulate matter smaller than 2.5 μm in diameter

Fine PM	Particles smaller than about 1-3 μm in diameter; defined as $PM_{2.5}$
Coarse PM	Particles larger than 1-3 μm in diameter; defined as $PM_{10} - PM_{2.5}$
Ultrafine PM	Particles smaller than about 100 nm
Nuclei mode	Particles in the range 5 – 100 nm
Accumulation	Particles in the range 100 nm – 2 μm

Particulate matter in the region

In 1978 a study to quantify pollutants emitted into the air in the Paso del Norte region was performed, showing that particulate emissions were the second highest pollutants for the zone, just preceded by sulfur oxides (Applegate and Bath 1978). In this study the found that unpaved streets and vehicular transportation were line sources of pollution, and that commercial areas were more polluted than residential and rural areas; overall, this study concluded that the city of Juarez was more polluted than El Paso and Las Cruces.

In 1981, a study in the Paso-Juarez area tried to relate vehicular emissions to carbon monoxide, as a possible explanation of the nonattainment status for the gas. Here, the author analyzed CO data emitted by vehicles registered in and driving the streets of El Paso, as well as the vehicles waiting to pass through customs on the international bridges and vehicles registered in and driving on Fort Bliss (Applegate 1981).

In 1983, the Agreement for the Protection and Improvement of the Environment in the Border Area (La Paz agreement) was signed. This agreement defined the US-Mexico border region as the area within 100 km on either side of the international boundary (Mukerjee 2001).

1990s were characterized by more research and higher level of citizen and nongovernmental agencies participation (Parks et al. 2005). On these years, the awareness of PM increased, relating the PM_{10} and $PM_{2.5}$ to health problems (Shwartz and Neas 2000).

In 1996, the Paso del Norte Ozone study was performed, with the objective of understanding the chemical and physical processes that provoked high ozone concentrations in this area (MacDonald et al. 2001). They found that this high ozone concentration was due in part to anthropogenic contribution of ozone precursors at ground level as well as atmospheric conditions such as high surface temperatures, strong sunlight with few clouds and slow convective boundary layer growth.

Li et al. have made studies using gravimetric and chemical analyses to determine the temporal and spatial variations of $PM_{2.5}$ and $PM_{2.5-10}$ mass concentrations, using the 24-hr average dichotomous samples collected from sites in the El Paso- Cd. Juarez air quality basin.

Frames of reference

According to Lynch and Cassano, the Eulerian and Lagrangian frames of reference are the two ways in which the motion of a fluid such as the Earth's atmosphere can be described. In a Eularian frame of reference, the flow quantities such as temperature or velocity are defined as functions of position in space and time. The primary flow quantity is the velocity vector field, but the complete description includes the spatial distribution of other quantities of interest such as temperature, pressure, and density. On the other hand, the Lagrangian acknowledges that some of the dynamical and physical quantities refer not only to certain positions in space but also to identifiable pieces of matter. The flow quantities here are defined as functions of time and the choice of the piece of matter, or parcel, and thus describe the dynamical history of the selected parcel. In this description then, any flow variable (including the location of a parcel) is expressed as a function of time only, since parcels change shape as they move, parcels must be chosen such that they are considered to be small, and that smallness must continue throughout time (Lynch and Cassano 2006).

PROBLEM

The recent attention that climate change and adverse health effects of traffic-related air pollution, aerosol research has progressively increased over the last twenty years.

Particles in the atmosphere are distinguished by their size, shape and composition. They can be directly emitted from sources and can be formed in the atmosphere by chemical reactions and physical processes. Once particles are formed, their properties can be modulated in space and time by atmospheric physical and chemical processes, such as condensation, evaporation and coagulation (Baltensperger et al. 2008). In time, the particles are removed from the atmosphere by wet or dry deposition, with such removal occurring minutes to weeks after their release or formation, and after travelling meters to thousands of kilometers.

Particles in the atmosphere are directly emitted by sources (primary emissions) or formed in the atmosphere by physicochemical processes (secondary formation). Combustion and other high-temperature processes are largely responsible for primary emissions of fine-mode particles, while mechanical processes such as grinding, entrainment of dust and soil and droplet formation by waves generate coarse-mode particles (Baltensperger et al. 2008). Condensable gases can homogenously nucleate to form new particles in the atmosphere if there is insufficient surface area for their uptake. Heterogeneous condensation is the uptake of vapor by pre-existing particles, with the reverse process of evaporation also important.

A summary of the atmospheric aerosol properties must necessarily reflect upon the methods used to arrive at the current state of knowledge. The dimensions of size, composition, space and time, observational data collected from measurements integrate the aerosol

characterization. Most observational data have been collected at fixed locations, however more data are being retrieved from satellite and other profiling instruments that provide wider spatial resolution.

Time resolution of the measurements also shapes the understanding of dynamical aspects of aerosol properties. Routine networks for particle mass and, more recently, composition collect samples periods with frequency of every day to once every several days. Continuous monitoring of particle mass concentration is now common with data typically reported as hourly averages. This has been used in real-time health advisory reporting and to bring the particle mass measurements closer to the characteristics timescales for variations in the weather, emission rates and atmospheric processes that drive variations in particle properties.

Monte Carlo methods have been used extensively to model the forward problem of electromagnetic scattering from aerosols of known properties; however, their use in solving the inverse scattering problem has not been appropriately verified. Ligon et al., did a research work in determining aerosol parameters from light-scattering data using an inverse Monte Carlo technique (Ligon, Chen, and Gillespie 1996). Here, the authors solve the electromagnetic problem from generally complex distributions of dielectric particles. This method was found to give accurate inversion results even when the data have a signal-to-noise ratio as low as 3:1. Still, this technique used simulated scattering data from aerosols composed of spherical dielectrics.

There is also research in optical characterization of metallic aerosols. Airborne metallic particulates are highly conducting aerosols that are frequently observed in the urban setting produced by industry and other urban sources. Metallic particulates are highly reflective,

affecting local weather or regional radiation budget. Sun and Lin studied the light scattering characteristics of metallic aerosols using exact solutions on perfectly conducting spherical and cylindrical particles in order to provide results that permit metallic aerosol detection and monitoring for environmental protection (Sun and Lin 2006).

Many physical properties of ambient aerosols can be estimated from their size distribution and chemical properties. Examples include light scattering and absorption properties that are important in both visibility and climate change contexts.

The distribution of aerosol properties as function of size has significant implications to behavior of the ensemble of particles. There are various approaches to characterizing such behavior. For a given property of interest, it might be possible to directly measure that property for size-selected aerosols. Alternatively, if the functional relationship between particle size and the property of interest is known, then a measurement of the number size distribution can be used to determine the ensemble behavior. In situ measurements are the least invasive whereby measurements, generally by optical techniques, are made without moving a sample from a flowing aerosol stream (Baltensperger et al. 2008).

Research budget

In September 2001, the NOAA Center for Atmospheric Sciences (NCAS) was awarded a cooperative agreement with the Department of Commerce National Oceanic and Atmospheric Administration-Educational Partnership Program. The goal of the Educational Partnership Program is to increase the number of students from underrepresented communities who are educated, trained and graduated in fields that directly support NOAA's mission.

NCAS is a cooperative partnership between four minority-serving institutions: Howard University (HU), Jackson State University (JSU), the University of Puerto Rico at Mayaguez (UPRM), and the University of Texas at El Paso (UTEP), and two majority universities; the University of Illinois at Urbana-Champaign (UIUC), and the State University of New York at Albany (SUNYA). The four MSI partners possess the highest concentrations of African American and Hispanics students in the physical sciences, engineering, and atmospheric-related disciplines at the undergraduate and graduate levels.

The mission of NCAS is to increase the number of highly qualified, well-trained graduates in NOAA-related sciences, with particular emphasis on the atmospheric sciences, for career opportunities with NOAA, NOAA contractors, other Federal agencies, and academia. NCAS enhances the implementation of comprehensive academic and research-training programs, which capitalize on the strength of the university partners. All partners contribute to training workshops and professional conferences, shared courses and seminars, outreach activities, student recruitment and mentoring, and conduct and present NOAA related research at professional meetings.

NCAS has developed two primary research themes: a) Advancing the understanding of air quality-climate-health interactions and b) improving prediction of precipitation through integrated measurements, models and data analyses. The center supports three activities under these themes;

1. Infrastructure development for weather-related research and applications, with a specific focus on urban and transitional regions within the United States.

2. Production of a domestic corps of highly trained atmospheric and environmental specialists to support the professional workforce at NOAA, other Federal agencies, academic institutions, and within the private sector, and.
3. Research and applications in support of NOAA's strategic goals, specifically those of the National Weather service (NWS).

The research goals are pursued through the development, validation and application of weather research and forecast models. NCAS and NOAA researchers collaborate in the development of improved physical parameterization for weather, climate, and air quality forecast models with the aim to improve weather and climate model predictions. Another unique aspect of NCAS is the development of observational programs in climate and air quality in support of model development and satellite data analysis.

CHAPTER 1

Use of the EPIRM model to study aerosols and retrieve aerosol size distribution in the Paso del Norte Airshed

Introduction

Atmospheric aerosols, principally those proximate to the surface, have a strong direct and indirect influence on the environment, air quality, visibility and human health (Raghavendra Kumar et al. 2009). However, the aerosol radiative forcing has not being studied extensively, causing a lack of thorough knowledge of the optical properties of aerosols (Hansen, Sato, and Ruedy 1997). Nevertheless, it is known that they alter the radiation budget of the earth-atmosphere system through radiative forcing thereby distressing the climate and the environment (Intergovernmental Panel in Climate Change (IPCC) 2007).

In situ characterization of aerosols present in the atmosphere using optical methods is of great relevance to the understanding of airborne particulates and their optical properties (Toledano et al. 2009), since aerosols can directly and indirectly affect human health, air quality, meteorology and climate (Jacobson 1999).

El Paso is situated at the extreme western tip of the state of Texas. With a population of over 600,000, the city is contiguous with the industrial city of Juarez, Mexico (population over 1 million) and some adjacent suburbs in the state of New Mexico. The combined urban area, known as the Paso del Norte, is one of the largest bi-national metropolitan areas in the world, and one of the fifty largest metropolitan areas in the Western Hemisphere. The Paso del Norte metro area is isolated, more than 500 km away from the nearest urban area of comparable size, thus making it an ideal location for air quality studies of an isolated urban environment.

The area is in the heart of the Chihuahuan Desert (an area of 362,000 km^2), which is otherwise sparsely populated. The climate is characterized by well-defined seasons, with hot summers and cold winters and with an average of approximately 22 cm of annual precipitation. The metropolitan area contains the river valley of the Rio Grande (Rio Bravo del Norte), as well as the Franklin Mountains which bisect the city of El Paso and the Sierra de Juarez in the city of Juarez. This complex topography and location of the mountains and river valley result in a constrained air basin where, on calm days, especially in the winter, anthropogenic air pollution is trapped over the metropolitan area (Noble et al. 2003). Moreover, this region is located in a combined urban/rural semi-arid region which frequently observes high concentrations of particulate matter (Svendsen et al. 2009). This airborne particulate matter (PM) has been identified as the major air pollutant in the Paso del Norte region. (Garcia et al. 2004) It has been stated that arid and semi-arid regions often exhibit relatively high concentration of mineral dust particles. (Huang, Zhang, and Prospero 2009) On windy days, especially during the winter and early spring, mineral dust and sand blowing out of the surrounding desert cause high particulate matter concentrations (Rivera Rivera et al. 2009). Both low-wind inversions and high-wind dust events lead to reduced visibility, occasional exceedances of air quality regulations, and potential concerns for the health of the Paso del Norte's residents (Staniswalis et al. 2005). The combination of a topographically-restricted urbanized air basin surrounded by a dust-producing desert also makes the Paso del Norte an ideal location for the study of aerosols from different sources. Furthermore, the air quality is among the worst along the U.S-Mexico border.

In 1990, the Paso del Norte Airshed was designated as non-compliant with U.S. Standards for particulate matter, with frequent days of severe air pollution (Texas Commission on Environmental Quality 2009).

Likewise, one of the effects of being in this type of setting is the high probability of a high concentration of fuel combustion particles such as soot. It is known that one of the most significant sources of fine and ultrafine aerosol particulates in an urban setting come from motor vehicle emissions. Hitherto little has been known about their concentration and size distribution (Zhu et al. 2002). For this reason, numerous studies have been undertaken to identify the causes and sources of contamination in this complex region. Research is currently being conducted to characterize the size distribution of aerosols in the Paso del Norte Airshed and neighboring cities under different conditions. US State agencies have ambient air monitoring programs that include particulate matter, in which the method of collecting data is to allow the passage of air through a series of air filters with successively smaller pores. This method is of high relevance since particle size is the most important parameter for characterizing the behavior of aerosols. All properties of aerosols depend on particle size as well as on other properties, but some are strongly subject to particle size (Hinds 1998).

Ground-based optical instruments are an alternative approach that permits the retrieval of aerosol information and its characterization (Alexandrov et al. 2007); (Alexandrov et al. 2008). In this research work, a light-scattering method for monitoring aerosols in-situ is used in conjunction with a robust inverse reconstruction model to retrieve aerosol size distribution. An alternative and complimentary method to the filter approach is presented to study aerosols, and is applied to the Paso del Norte area. A comparison of four different scenarios, for four different seasons, was performed for this region.

Methodology

The Environmental Physics Inverse Reconstruction Model (EPIRM) (Pearson, Fitzgerald, and Polanco 2007), in conjunction with Multi Filter Rotating Shadowband Radiometer (MFRSR)

optical depth data, was used to retrieve the aerosol size distribution for two different scenarios and for two different seasons of the year for the Paso del Norte region.

The MFRSR instruments are located at the University of Texas at El Paso (UTEP) campus (31° 46' 06.79" N, 106° 30' 21.99" W). They measure solar irradiance at seven narrowband wavelengths (332, 368, 415, 500, 610, 665 and 860 nanometers) in the ultraviolet and visible regions. From this data, total optical depths were calculated using the standard Beer's Law approach (Bigelow et al. 1998); (Hand et al. 2004). Optical depth due to water vapor and other molecules as well as Rayleigh and ozone optical depths are subtracted from the total optical depth to obtain the aerosol optical depth (Slusser et al. 2000) as shown in equation 1.

$$\tau_A = \tau_T - \tau_R - \tau_O - \tau_{WM} \quad (1)$$

These instruments are linked to a nationwide network of MFRSR radiometers (Bigelow et al. 1998). The network is part of the USDA UV-B Monitoring Program that was established in 1992 by the U.S. Department of Agriculture (USDA), with the purpose of determining possible temporal trends and the UV climatology (Slusser et al. 1999). Currently, the network of standard climatological monitoring sites includes thirty five locations in the U.S. (including Alaska and Hawaii), two in Canada and one in New Zealand (Mckenzie et al. 2006).

The scenarios were classified as clean (low polluted), and polluted days, as described in the text. In order to provide the greatest contrast, comparisons between winter and summer were performed; then comparison of between spring and fall followed. Representative winter days were January 28, 2009 (clean day) and February 5, 2009 (polluted day); representative summer days were June 5, 2009 (polluted day) and July 5, 2009 (clean day); representative spring days

were May 26, 2009 (clean day) and May 20, 2009 (polluted day); representative fall days were October 14, 2009 (clean day) and November 28, 2009 (polluted day).

The Environmental Physics Inverse Reconstruction model (EPIRM) was developed to solve the following general equation:

$$\tau_A(\lambda) = \int_0^\infty \int_0^\infty C_{ext}(r, \lambda, m) n(r, z) dz dr \quad (2)$$

For the case of aerosols represented by spheres it becomes:

$$\tau_A(\lambda) = \int_0^\infty \int_0^\infty \pi r^2 Q_{ext}(r, \lambda, m) n(r, z) dz dr \quad (3)$$

in which $\tau_A(\lambda)$ is the aerosol optical depth (AOD), $C_{ext}\ (r, \lambda, m)$ is the particle extinction cross-sections, $Q_{ext}\ (r, \lambda, m)$ is the extinction efficiency of the atmosphere, n(r, z) is the height-dependent aerosol number density in the radius range r *to* $r+dr$, m is the complex refractive index of the aerosol particles and λ is the wavelength of the incident light. This problem is ill-posed, having the form of a Fredholm integral equation of the first kind and requiring a constrained, regularized solution (Twomey 1977); (Liu, Arnott, and Hallett 1999); (Pearson, Fitzgerald, and Polanco 2007). The regularized solution is obtained by solving the following equation:

$$f = (A^T A + \gamma H)^{-1} A^T g \quad (4)$$

where f is the size distribution array, A is the kernel matrix, γ the Lagrange multiplier, H is the smoothing matrix and g is the optical depth data. The Lagrange multiplier weights the smoothing matrix to provide unwavering size distributions.

The particle extinction cross-sections (C_{ext}) values were calculated using Mishchenko's T-matrix code (Mishchenko, Travis, and Mackowski 1996); (Mishchenko et al. 2010) for each of

the MFRSRs' wavelengths. These values are related to the extinction efficiency by the following equation, which is valid for the case of spheres:

$$C_{ext} = \pi r^2 Q_{ext} \tag{5}$$

A maximum radius of 1.5 micrometers (μm) and a minimum radius of 0.1 μm were selected for the calculations. A representative composite index of refraction for this region, which is wavelength dependent, was constructed. This was achieved using a volume-weighted approach (Hand et al. 2004) in which the major contributors to aerosol loading in the Paso del Norte region are mineral dust and soot (Li et al. 2001). Mineral dust does not show significant spectral variability, except in the infrared regime (Seinfield and Pandis 2006), which is not within the scope of this study. Soot, on the other hand, shows spectral variability according to the type of source producing it (Kokhanovsky 2008). One of the main contributors of soot in this region is the use of scrap tires as a source of heat for improvised furnaces during the winter months, primarily in the pauper zones of Juarez, and by traditional brick manufacturing which frequently burns the tires at high temperatures in kilns (Blackman and Palma 2002). Another contributor is particulate matter from wood burning (Murr et al. 2006).

The size distribution is obtained by discretizing Equation 2 into a matrix equation, where, the computed extinction cross-sections are obtained using the T-matrix code (applicable to irregularly shaped and spherical particles) in terms of wavelength and effective radius, with the composite refractive index specified beforehand. The midpoint rule was used in a log-scale, whereas extinction cross-sections were calculated uniformly in a linear scale, hence the need for interpolation. Since there are more radii than wavelengths, a least squares approach together with a regularization scheme for different Lagrange multipliers was utilized. In particular, the L-

curve method was used to determine the best Lagrange multiplier that leads to the best solution (Hansen 1992); (Hansen 1994); (Rodriguez and Theis 2005).

The scattering of light by a particle depends on several physical variables, such as the wavelength of the incident radiation, the particle refractive index and the size of the particle. The wavelength dependence of the aerosol optical depth (AOD) varies because of the aerosols' type, and their physical and chemical characteristics. This wavelength dependence is expressed by the Angstrom exponent (α), which is given by:

$$\alpha = -\partial ln\tau / \partial ln\lambda \tag{6}$$

This value is inversely related to the average size of the aerosols present. Characteristic values of α for fresh smoke particles (accumulation mode aerosols) range from 2.0 or greater, whereas α values from 2.0 to near zero are typical for Saharan desert dust events (coarse mode aerosols) (Eck et al. 1999).

A laser particle counter (LPC) was used to correlate surface aerosol size distribution with the columnar aerosol size distribution obtained with the EPIRM code. The LPC utilized was a Climet, CI-150t. The CI-150t is a laser diode based aerosol particle counter that monitors particles in four size ranges: 0.3, 0.5, 1, and 5 μm in diameter. This instrument operates on the light scattering principle. It uses a Sharp 50 mW laser diode as the light source at a wavelength of 654 nm, and an elliptical mirror collection system. The light, scattered by particles and collected by the elliptical mirrors, is focused onto a solid-state photo detector, which converts the electromagnetic energy into electrical current.

Figure 1-1 shows a diagram of the sequence of operations for the aerosol size distribution retrieval.

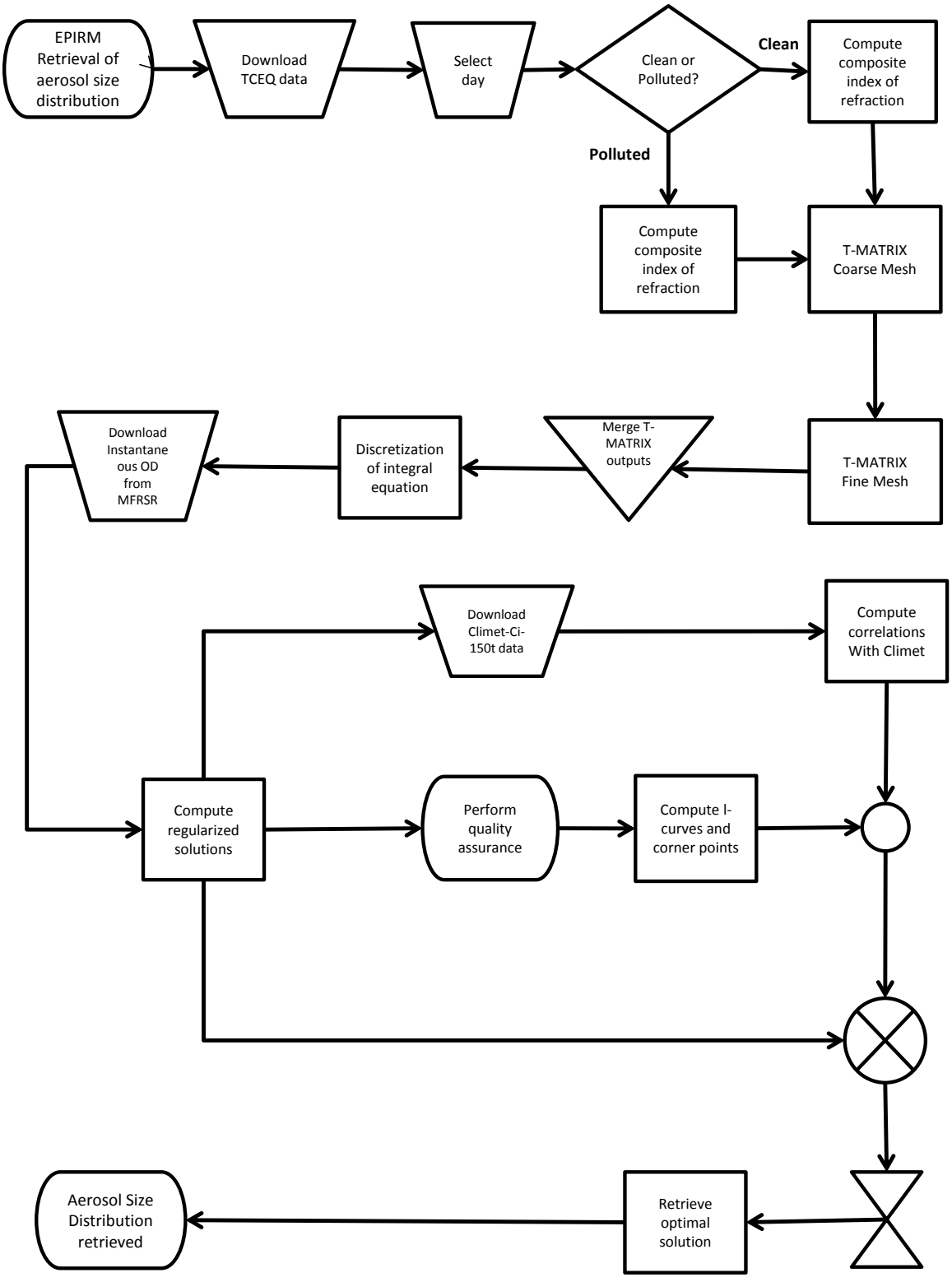

Figure 1-1. Diagram of the sequence of operations for the EPIRM model.

Day classification

Two different types of day were considered in this research. The first classification was a "clean day", in which low concentration of particulate matter, with diameter equal to or less than 2.5 μm ($PM_{2.5}$) was observed. The second classification was a "polluted day", in which high concentration of $PM_{2.5}$ was detected. Data retrieved from the TCEQ provided information on particulate matter concentration, which allowed the classification of days. Table 1-1 provides the basic descriptive statistics of $PM_{2.5}$ concentration for the winter and summer seasons, which enabled the day classification.

Table 1-1. Descriptive statistics of hourly $PM_{2.5}$ concentration values for winter and summer seasons.

Descriptive statistics of PM 2.5 concentration (μg/m^3)										
	Winter (2009)					**Summer (2009)**				
	Maximum	**Second Highest**	**Minimum**	**Avg.**	**Std. Deviation**	**Maximum**	**Second Highest**	**Minimum**	**Avg.**	**Std. Deviation**
Maximum	89.69	67.77	7.28	19.10	20.00	44.45	38.50	7.88	14.65	10.90
Minimum	6.18	5.19	0.02	2.55	1.00	5.19	4.96	0.00	3.21	1.00
Average	26.89	20.17	1.72	8.02	6.19	15.96	12.94	2.92	7.34	3.21
Std. Deviation	16.87	11.76	1.42	3.38	3.90	7.80	5.34	1.73	2.14	1.61
Median	21.90	17.31	1.66	8.22	4.80	13.62	11.51	2.77	7.09	2.90
Mode	6.18	17.66	0.09	3.76	4.80	12.35	10.68	3.61	6.08	2.90
Clean Day	12.74	12.69	0.44	4.97	3.5	5.89	5.22	1.39	3.21	1.10
Polluted Day	89.69	67.77	5.15	18.8	20	42.94	21.50	7.09	14.38	7.40

Considering Table 1-1, it can be seen that the average concentrations of $PM_{2.5}$ in the winter and summer seasons were 8.02 and 7.34 μg m^{-3} respectively. Therefore, the days selected for this study, labeled as clean and polluted days, clearly represent the lowest and highest concentrations for the seasons.

Table 1-2 provides the basic descriptive statistics of $PM_{2.5}$ concentration for the spring and fall seasons, which enabled the day classification.

Table 1-2. Descriptive statistics of hourly $PM_{2.5}$ concentration values for spring and fall seasons.

Descriptive statistics of PM 2.5 concentration (μg/m^3)										
	Spring (2009)					Fall (2009)				
	Maximum	Second Highest	Minimum	Avg.	Std. Deviation	Maximum	Second Highest	Minimum	Avg.	Std. Deviation
Maximum	54.17	39.56	7.37	16.15	12.40	49.61	39.77	8.04	15.35	12.00
Minimum	6.95	6.54	0.34	4.14	1.00	3.36	3.06	0.03	1.89	0.60
Average	18.24	14.91	3.51	8.17	3.73	17.50	14.46	2.55	7.36	3.81
Std. Deviation	9.65	7.19	1.64	2.81	2.39	9.13	6.96	1.62	2.77	2.21
Median	15.49	12.84	3.36	7.65	2.90	15.26	13.30	2.42	7.19	3.30
Mode	25.56	14.93	3.49	4.98	2.20	13.90	14.47	2.25	9.36	2.20
Clean Day	7.46	7.08	1.54	4.88	1.6	8.90	7.10	0.08	2.36	2.20
Polluted Day	25.81	16.96	6.92	11.16	4.5	28.57	26.14	2.65	12.45	7.10

By inspecting table 1-2, it can be seen that the average concentrations of $PM_{2.5}$ in the spring and fall seasons were 8.17 and 7.36 μg m^{-3} respectively. Therefore, the days selected for this study, labeled as clean and polluted days, certainly are representatives of the low and high concentrations for the seasons.

Days were also classified by the diffuse irradiances using the MFRSR. However, this was not the main criterion used in the selection of days, due to the fact that the diffuse irradiance increases with increasing AOD in the range of 0.64 to 1.19, then decreases beyond these range (Cho, Jeong, and Kim 2003). In summary, the criteria for clean days were low values of $PM_{2.5}$ (from the TCEQ) and low values of horizontal diffuse irradiance and AOD less than 2.0 (from

the MFRSRs). Conversely, a polluted day was defined by identifying high values of $PM_{2.5}$ and high values of horizontal diffuse irradiance and AOD greater than 2.0.

The cleanest or the most polluted days during a season were not necessarily the ones selected for the retrieval. An overriding criterion was that only days having the most high quality experimental data were selected for the study. Mostly cloud-free days were also selected to obtain more accurate experimental data.

Results

The values for the composite index of refraction used for each pollution scenario, as well as the calculated single scattering albedo (SSA), and asymmetry parameter (g) are shown in table 1- 3.

Table 1-3. Average values of composite refractive index, single scattering albedo and asymmetry parameter for the visible wavelengths for the clean and polluted day scenarios.

Calculated optical parameters (daily average)								
	Clean day Scenario				Polluted day Scenario			
Wavelength (nm)	Composite Refractive Index				Composite Refractive Index			
	Real	Imaginary	Single Scattering Albedo	Asymmetry Parameter	Real	Imaginary	Single Scattering Albedo	Asymmetry Parameter
415	1.617	0.240	0.487	0.813	1.651	0.332	0.477	0.807
500	1.623	0.240	0.482	0.790	1.659	0.333	0.468	0.785
610	1.629	0.239	0.477	0.761	1.668	0.331	0.459	0.756
665	1.631	0.236	0.476	0.747	1.671	0.327	0.456	0.743
860	1.638	0.225	0.476	0.699	1.681	0.311	0.447	0.697

The values of the imaginary part of the refractive index for the polluted day scenario were greater than those for the clean day scenario. Therefore the particles were more absorbent, due to a higher concentration of soot particles. The most significant absorbing component in atmospheric particles is soot (Seinfield and Pandis 2006). The values of SSA in both scenarios

were very similar, yet those values were higher for the clean than for the polluted scenario. The *g* values for the clean scenario were slightly higher than for the polluted scenario, signifying more light scattered in the forward direction as opposed to the backward direction.

The AOD experimental values provided by the MFRSR instruments were used as input entries for the EPIRM code. Table 1-4 summarizes the average values of optical depth for each of winter and summer days that were selected. Table 1-5 summarizes the average values of optical depth for the days in spring and fall.

Table 1-4. Average values of optical depths for seven narrowband wavelengths for the clean and polluted day scenarios.

	Measured optical depth (daily average)			
	Clean days		**Polluted days**	
Wavelength (nm)	***Winter***	***Summer***	***Winter***	***Summer***
	28-Jan-09	*5-Jul-09*	*5-Feb-09*	*5-Jun-09*
332	0.762	1.248	0.858	2.494
368	0.497	0.983	0.583	2.216
415	0.344	0.844	0.375	1.988
500	0.198	0.727	0.215	1.726
610	0.137	0.664	0.143	1.619
665	0.094	0.634	0.103	1.658
860	0.056	0.594	0.062	1.590

Table 1-5. Average values of optical depths for seven narrowband wavelengths for the clean and polluted day scenarios.

	Measured optical depth (daily average)			
	Clean days		**Polluted days**	
Wavelength (nm)	***Spring***	***Fall***	***Spring***	***Fall***
	26-May-09	*14-Oct-09*	*20-May-09*	*28-Nov-09*
332	1.031	0.771	1.828	1.973
368	0.741	0.499	1.533	1.688
415	0.557	0.336	1.337	1.451
500	0.394	0.181	1.185	1.290
610	0.331	0.120	1.122	1.210
665	0.285	0.078	1.078	1.164
860	0.247	0.039	1.069	1.124

Clean day scenario

As defined in the day classification section, a "clean day" scenario is denoted by low concentrations of $PM_{2.5}$ and generally corresponding low values of AOD and of horizontal diffuse irradiance.

The EPIRM model was used to calculate the size distributions for the selected days in this scenario. These results were compared to the size distribution values recorded at the surface on the corresponding days by the CI-150t, which gave correlation factors of 0.9986 for the winter, 0.9988 for the summer and 0.9966 for the spring cases. Figure 1-2, 1-3 and 1-4 show these comparisons (on a linear scale) between the Climet and EPIRM model for the winter, summer, and spring selected clean days respectively. The values for the fall season were not compared, since the Climet instrument was turned off due to construction operations in the building and in the surrounding areas, which provoked false particle readings.

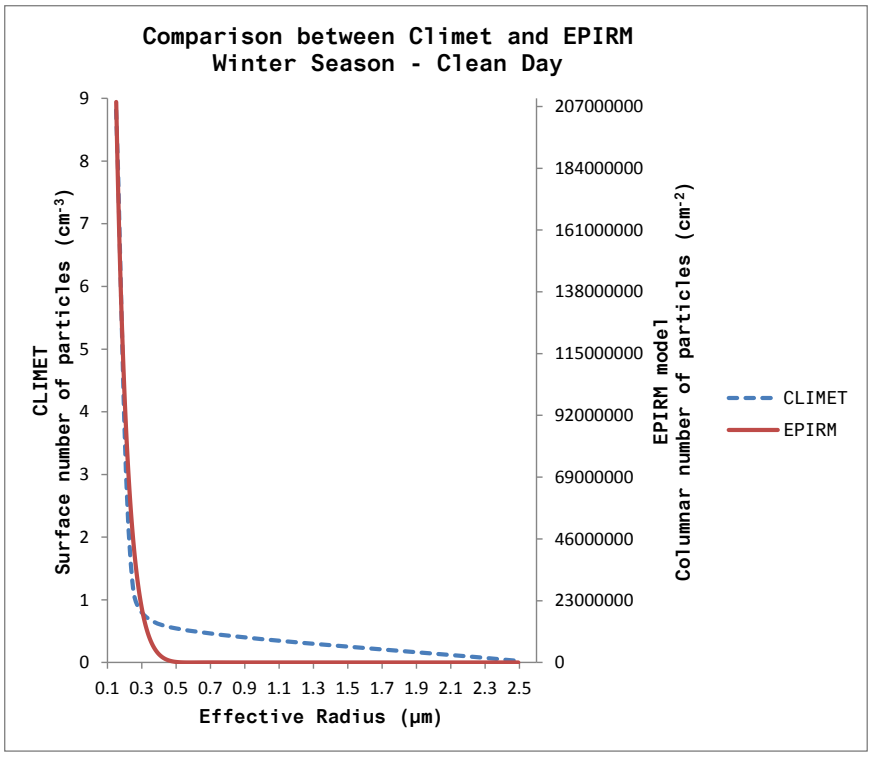

Figure 1-2. Comparison of aerosol size distribution between Climet (ground measurements) and the EPIRM model (columnar calculations) for the clean day of the winter season.

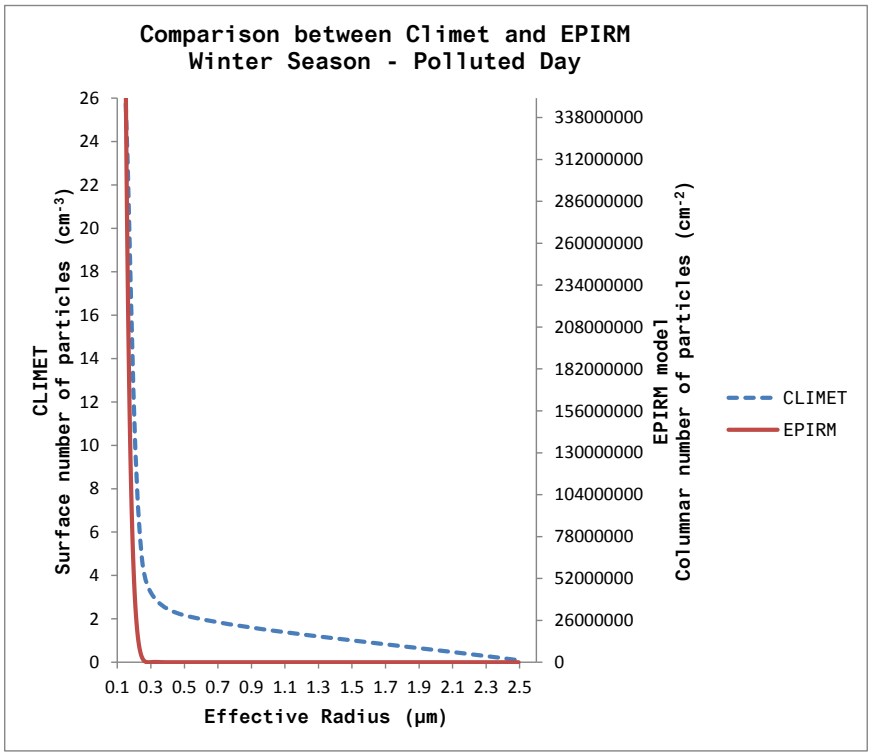

Figure 1-3. Comparison of aerosol size distribution between Climet (ground measurements) and the EPIRM model (columnar calculations) for the clean day of the summer season.

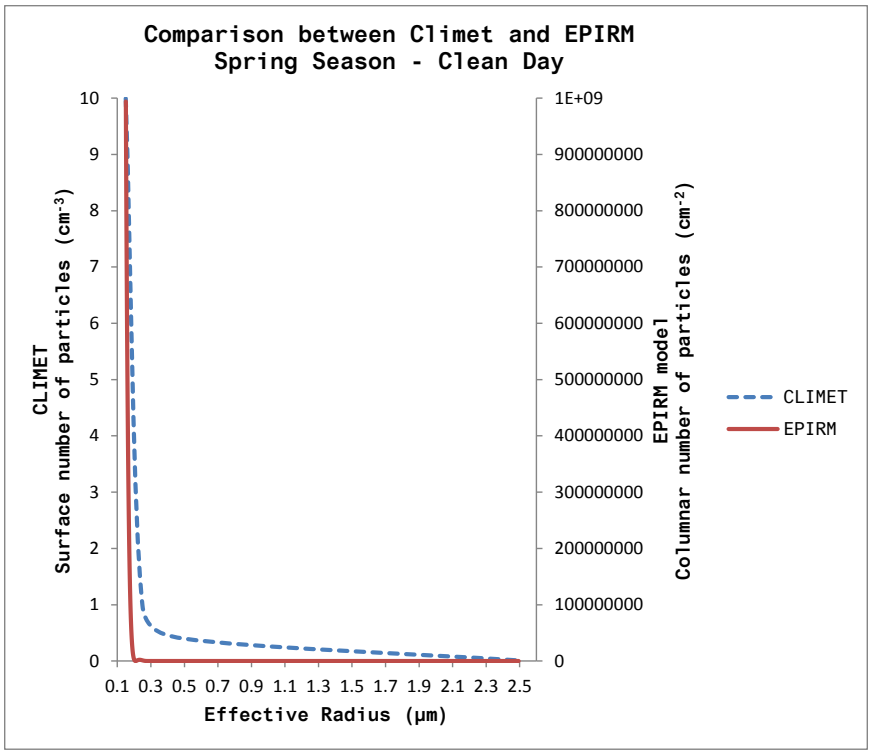

Figure 1-4. Comparison of aerosol size distribution between Climet (ground measurements) and the EPIRM model (columnar calculations) for the clean day of the spring season.

Winter and summer comparison

Figure 1-5 depicts the columnar aerosol size distribution by number and figure 1-6 shows the aerosol size distribution by volume for the selected clean days in winter and summer. These figures show a log-log plot of the columnar number distribution $dN_c/d\ln r_{reff}$ [cm^{-2}] as well as the columnar volume distribution $dV_c/d\ln r_{reff}$ [μm^3 cm^{-2}] with respect to the effective radius (µm). Several maxima and minima are observed in this graph. It is seen that in the lower limit of the fine particle range, values of the columnar number of particles were close to 1 $x10^9$ and 1 x 10^{10} [cm^{-2}] for the winter and summer days respectively. The summer case exhibits in general a larger concentration of particles. Table 1-3 shows that the AOD was higher for summer than for winter, indicative of the presence of more aerosol particles in the summer than in the winter, as

observed in the graph. However, for the largest size particles within the fine particle range, the winter case exhibits a larger concentration.

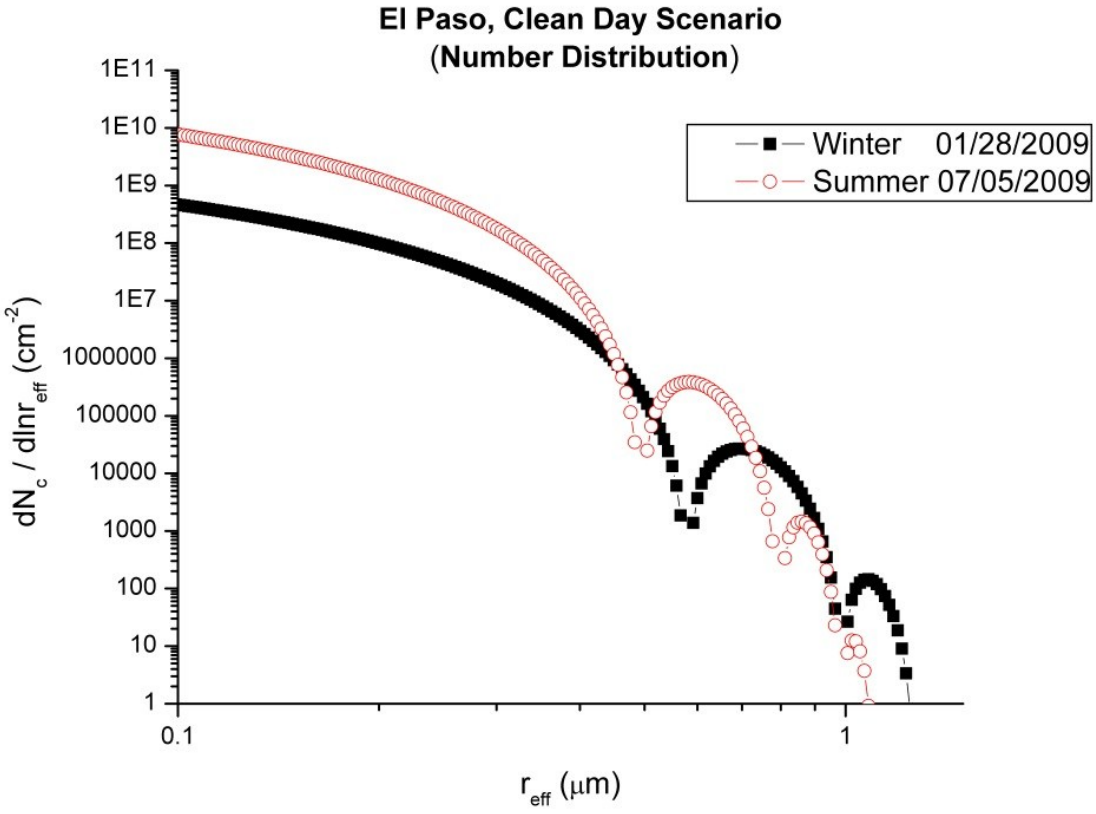

Figure 1-5. Columnar aerosol size distribution (number distribution) for the clean scenario in the winter and summer seasons (January, 28, 2009 and July 5, 2009 respectively).

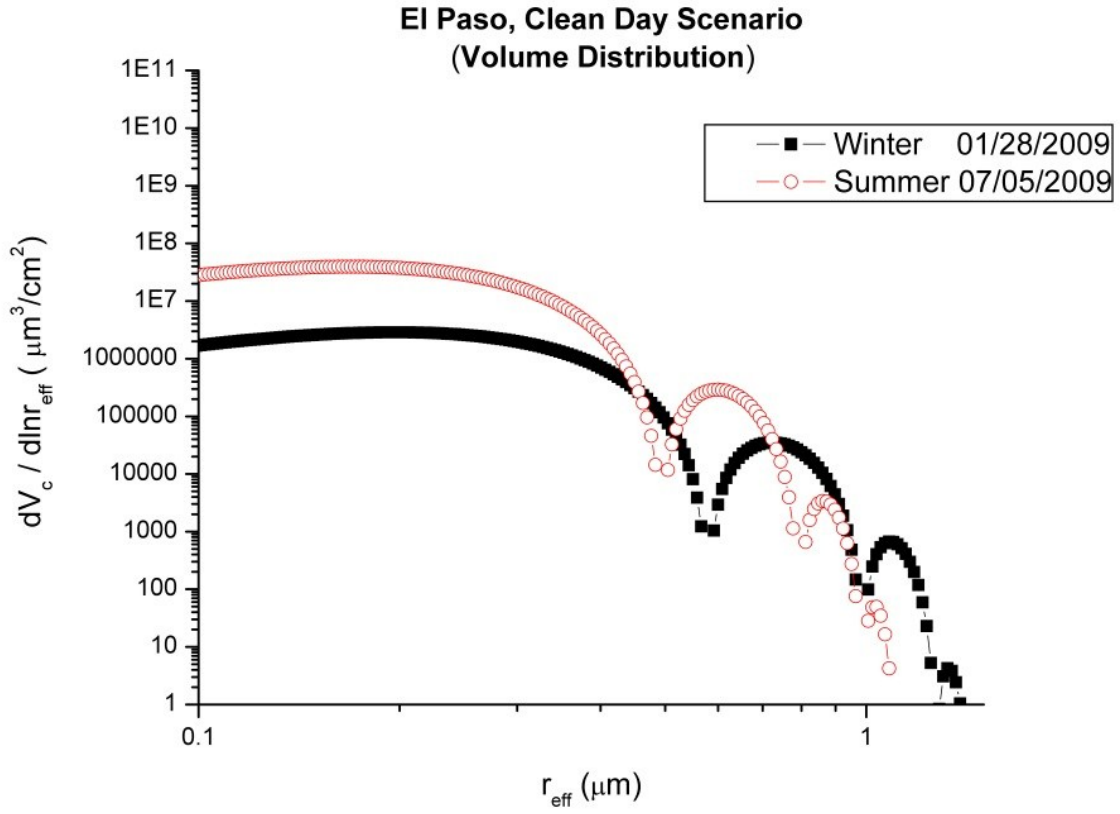

Figure 1-6. Columnar aerosol size distribution (volume distribution) for the clean scenario in the winter and summer seasons (January, 28, 2009 and July 5, 2009 respectively).

Figure 1-7 depicts the Hybrid Single-Particle Lagrangian Integrated Trajectory model (HYSPLIT) graph (Draxler and Rolph 2010) for the winter case, which was used to determine the movement of the air parcels from the day of the event to 48 hours prior. Back trajectories integrate back in time to track the path of an air parcel arriving at a receptor location at a given time (Stohl 1998). However, back trajectories do not take into account mixing between air masses at various heights (Verma et al. 2007). This backward trajectory was at 50, 500 and 1,000 meters above ground level (AGL), all of them showing that the air parcels came from the northwestern part of the United States. From this figure it was inferred that some bigger size

particles, e.g., mineral dust from the Chihuahuan desert (northwest of El Paso) as well as other particles, were transported to the location of study. This explains why the winter case exhibits a greater concentration of largest size particles within the fine particle range.

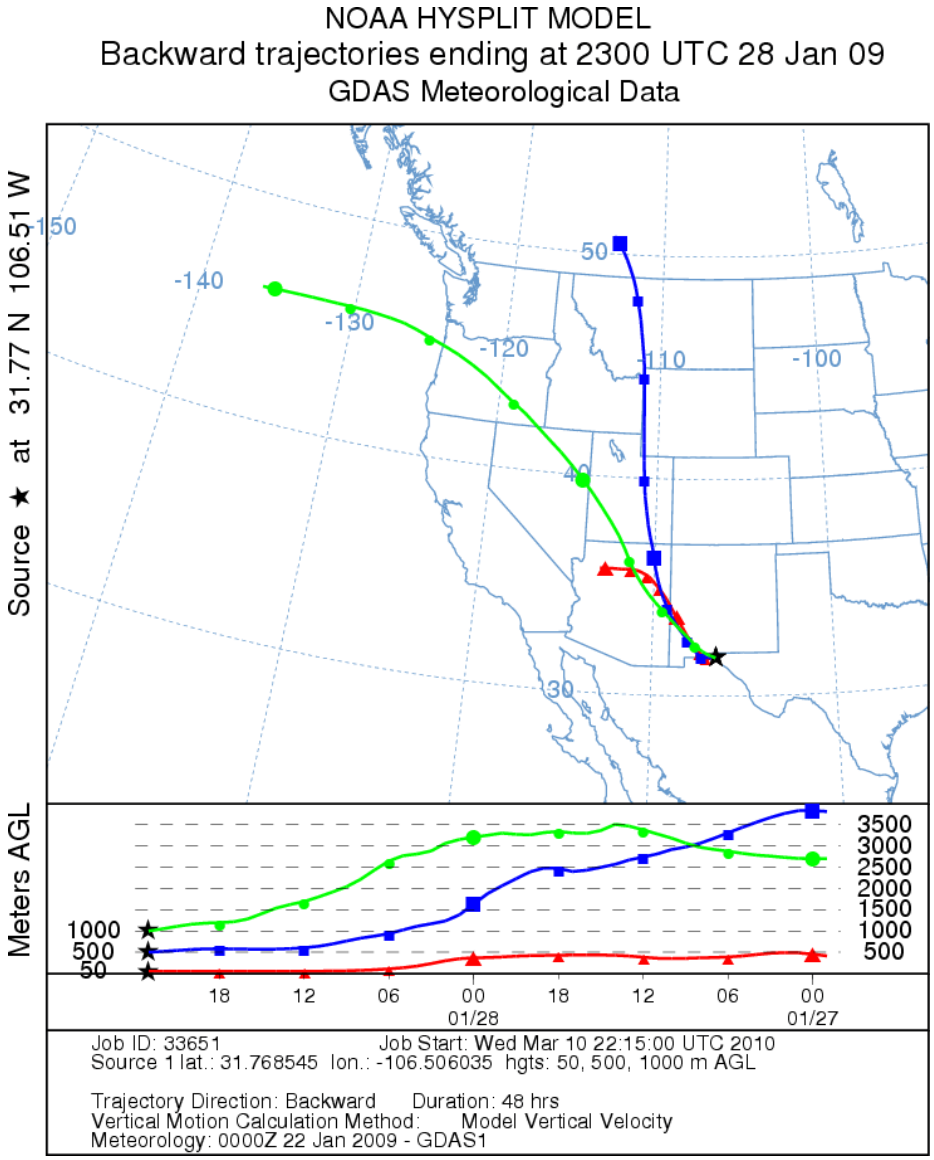

Figure 1-7. HYSPLIT 48-hour backward trajectory for a clean day in the winter (January 28, 2009) at 50, 500 and 1,000 meters above ground level (AGL).

Figure 1-8 illustrates the HYSPLIT backward trajectory for the summer case, in which the same parameters were used. It was observed that the near-surface air parcels were not

transported long distances, and spent a relatively longer time over the urban and rural areas of the El Paso-Juarez metropolitan area, which may result in an increase in soot particles for this day. This caused a higher concentration of smaller size particles in the summer case, as shown in figure 1-4. In particular, this HYSPLIT graph shows that there was an important contribution from air parcels at 50 m AGL that originated from the Chihuahuan desert zone, as well as from the urban region of El Paso-Juarez.

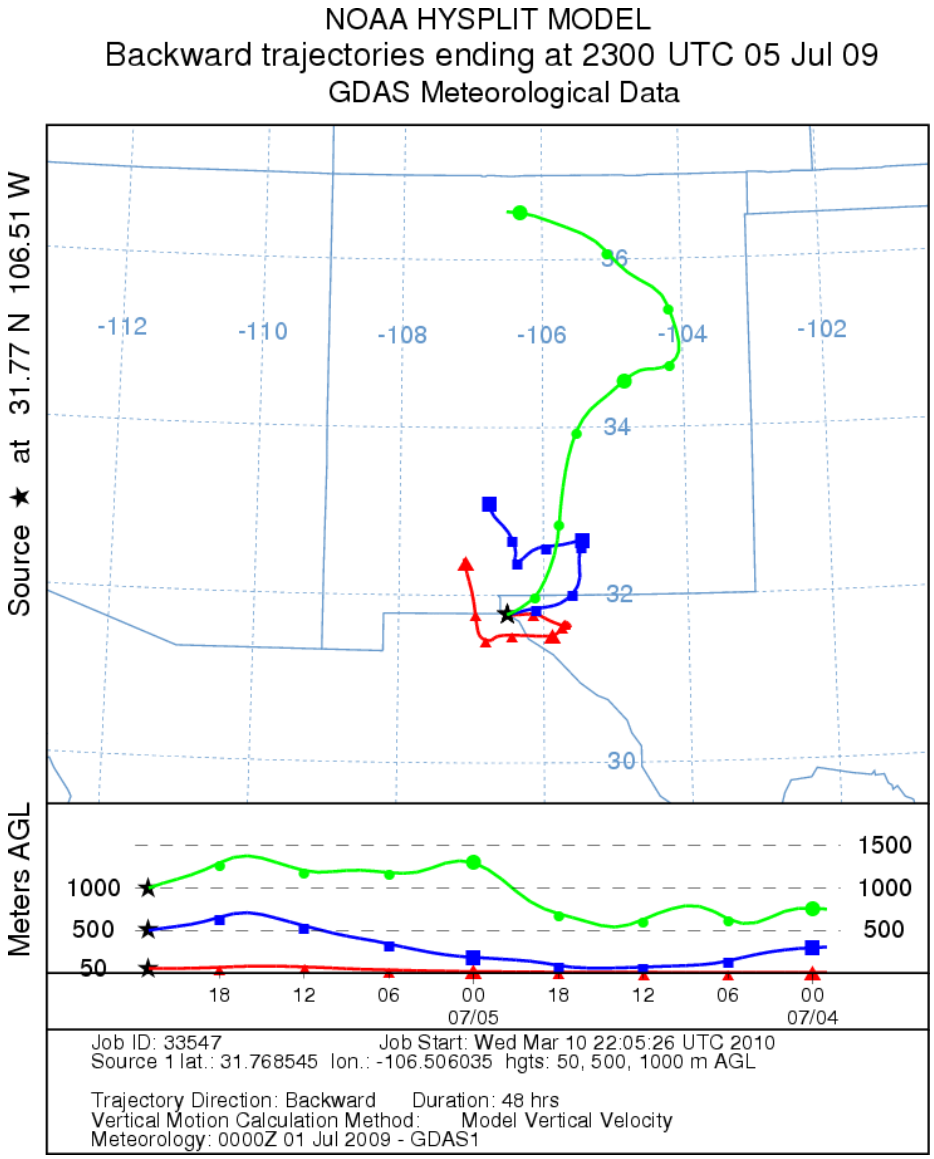

Figure 1-8. HYSPLIT 48-hour backward trajectory for a clean day in the summer (July 5, 2009) at 50, 500 and 1,000 meters above ground level (AGL).

Spring and fall season comparison

The comparison of particle size distribution of the spring (May 26, 2009) and fall (October 14, 2009) days is shown in figure 1-9 (number distribution) and in figure 1-10 (volume distribution). The number distribution graph is a log-log plot of particles over an area against the particles' effective radius in μm. At 0.1 μm of radius, the spring day showed greater number of particles than the day in fall, with 1.8 x 10^{10} [cm^{-2}] and 9.8 x 10^{9} [cm^{-2}] respectively. Consequently, the number of particles decay in both days, but showed an increase at a radius of 0.24 μm for the spring and at 0.18 μm for the day in fall; here, the number of particles in each day is 4 x 10^{6} [cm^{-2}] and 3 x10^{6} [cm^{-2}] respectively. The maximum radius recorded for the spring day was 0.35 μm. For the fall day the maximum recorded radius was 0.22 μm, however, only very few particles are present in this size. Overall, the spring season showed more concentration of particles in all the sizes.

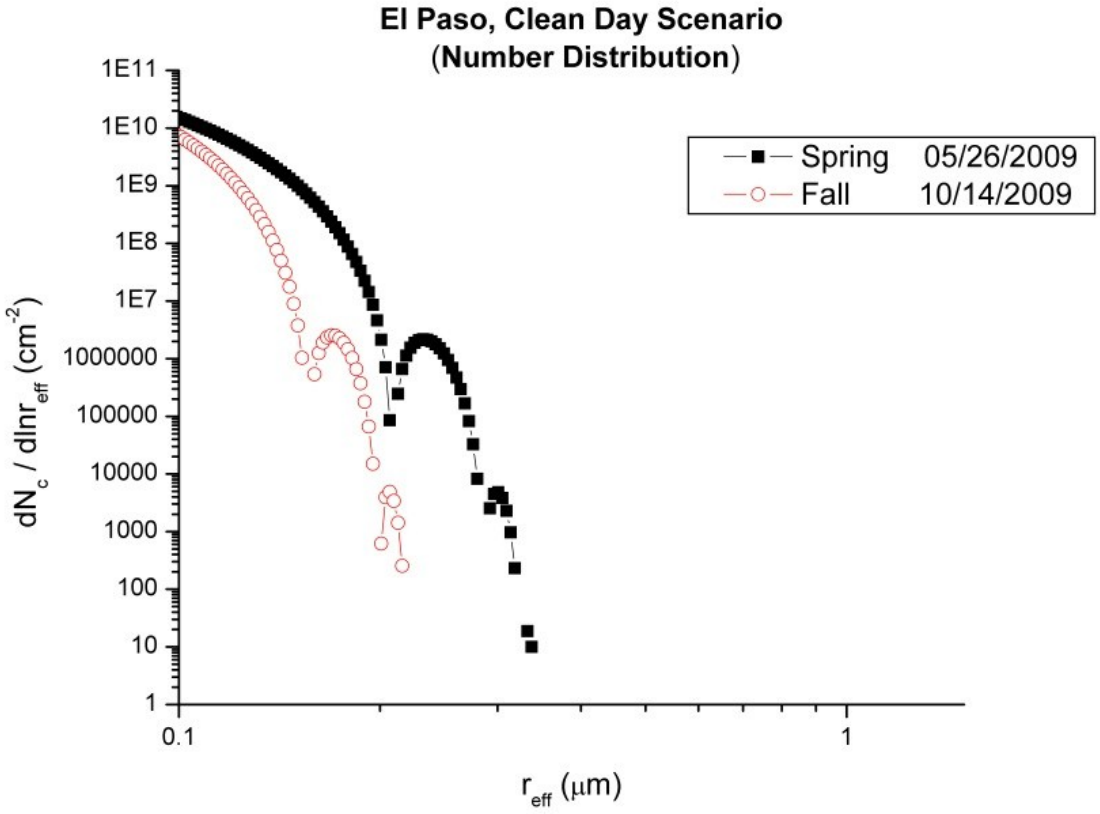

Figure 1-9. Columnar aerosol size distribution (number distribution) for the clean scenario in the spring and fall seasons (May 26, 2009 and October 14, 2009 respectively).

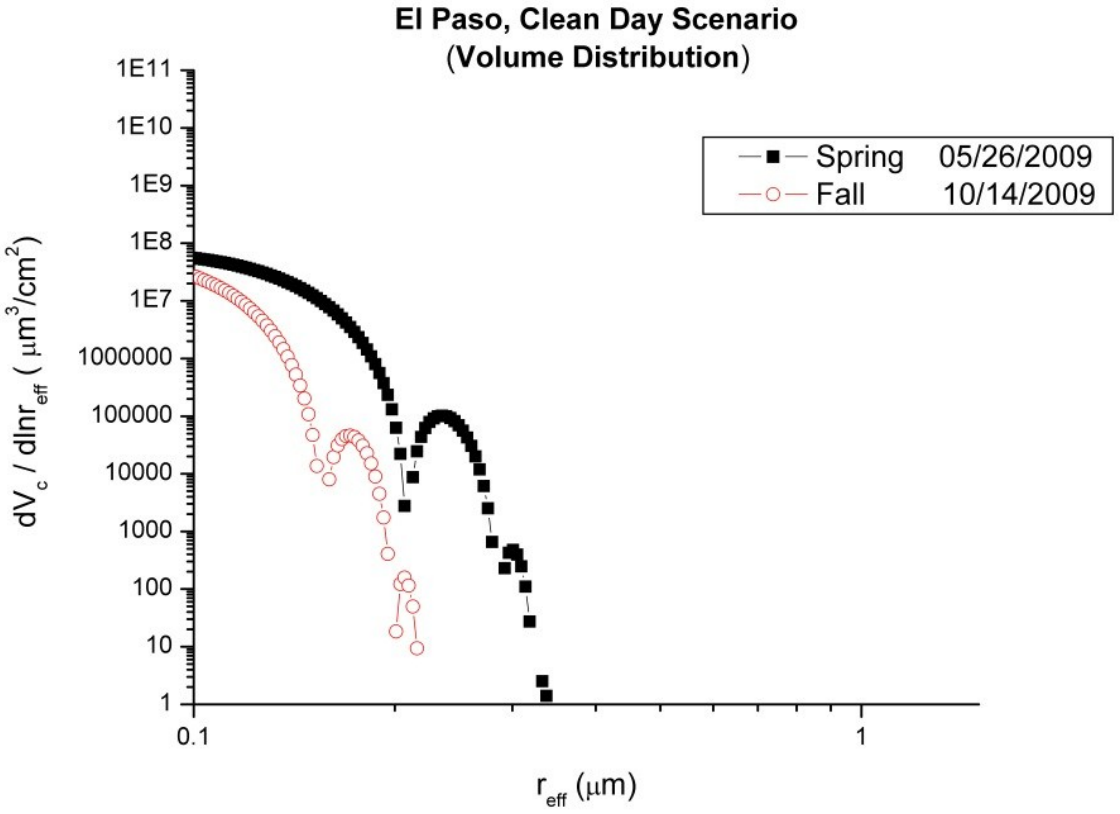

Figure 1-10. Columnar aerosol size distribution (volume distribution) for the clean scenario in the spring and fall seasons (May 26, 2009 and October 14, 2009 respectively).

Figure 1-11 shows the HYSPLIT backward trajectory for the clean day (May 26, 2009) of the spring season at 50, 500, 1,000 meters above ground level (AGL), showing that the air parcels came from the southern part of Arizona and New Mexico.

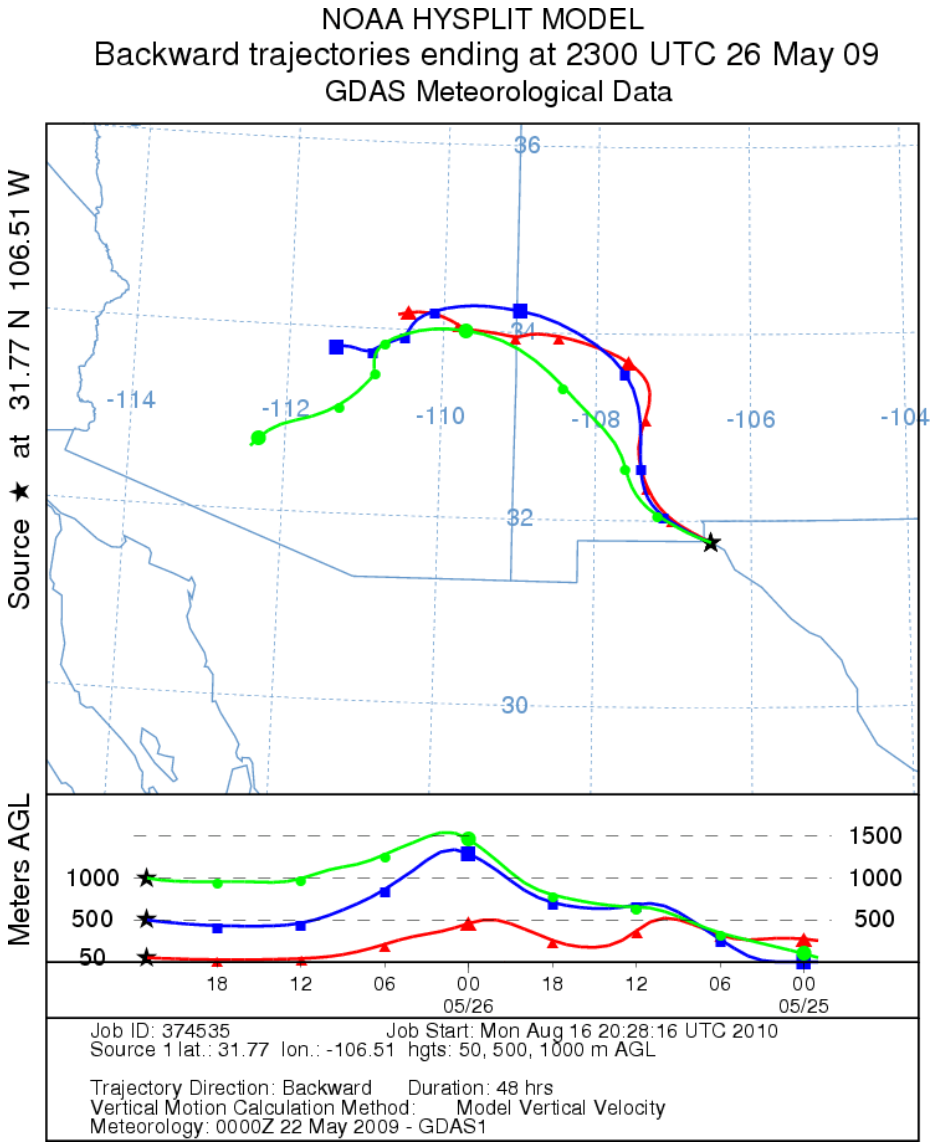

Figure 1-11. HYSPLIT 48-hour backward trajectory for a clean day in the spring (May 26, 2009) at 50, 500 and 1,000 meters above ground level (AGL).

Figure 1-12 depicts the HYSPLIT 48-hour backward trajectory for October 14, 2009. The air parcels at the three heights (50, 500, 1000 m AGL) originated in the southwest of El Paso, very close to the Pacific Ocean in the Mexican States of Sinaloa and Sonora, passing through the Chihuahuan desert.

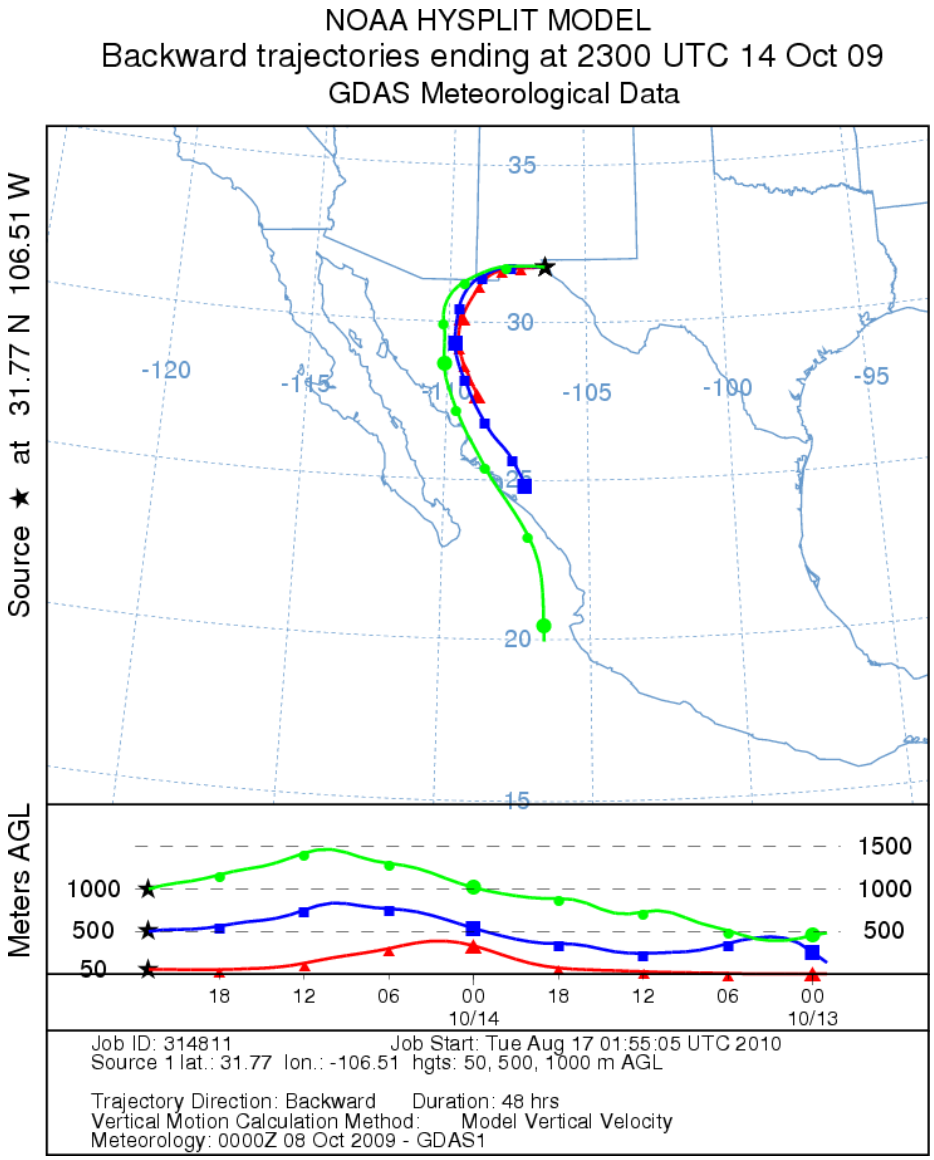

Figure 1-12. HYSPLIT 48-hour backward trajectory for a clean day in the fall (October 14, 2009) at 50, 500 and 1,000 meters above ground level (AGL).

Polluted day scenario

A polluted day scenario is characterized by high concentrations of $PM_{2.5}$. For this case, α was calculated at 415-500 nm wavelength range for the winter, summer, spring and fall days. The value of α for winter was 2.986 and for summer was 0.758. Therefore, the type of particulate matter (PM) in the winter was ascribed to the predominance of smaller size particles, such as

soot, whereas in the summer the high concentration of PM was attributable to larger particles, such as mineral dust. In the same fashion, the value of α for spring was 0.648 and for fall was 0.631. Hence, the PM in both seasons was ascribed to the predominance of larger size particles.

These aerosol size distributions, when compared to the values recorded at the surface by the CI-150t, exhibited correlations of 0.9883, 0.9991 and 0.9972 for winter, summer and spring cases respectively. Figures 1-13, 1-14 and 1-15 compare the size distributions between the Climet and EPIRM model for the winter, summer and spring seasons respectively.

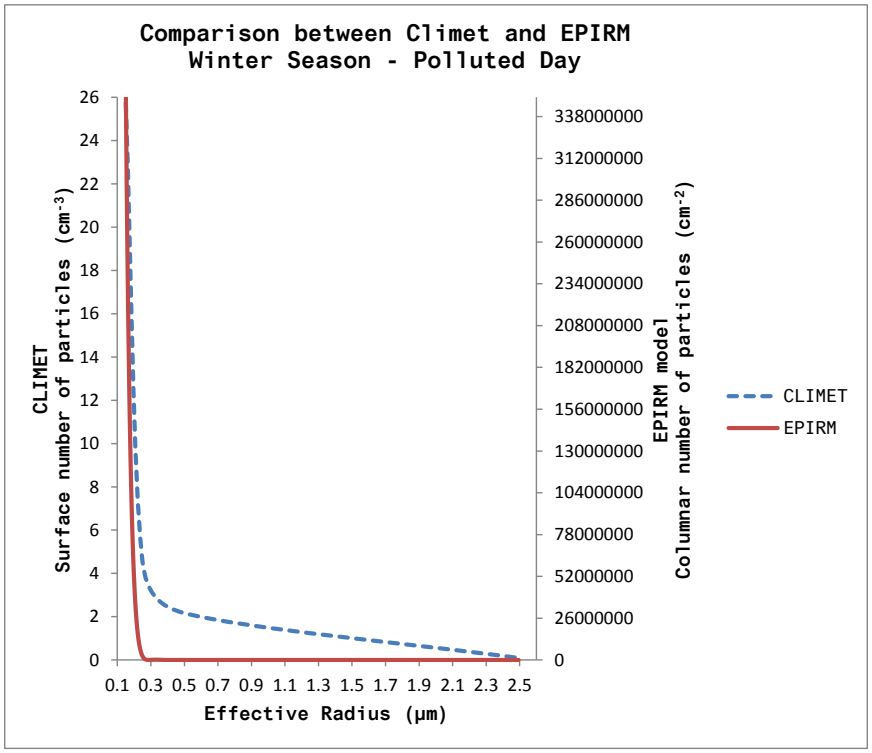

Figure 1-13. Comparison of aerosol size distribution between Climet (ground measurements) and the EPIRM model (columnar calculations) for the polluted day of the winter season.

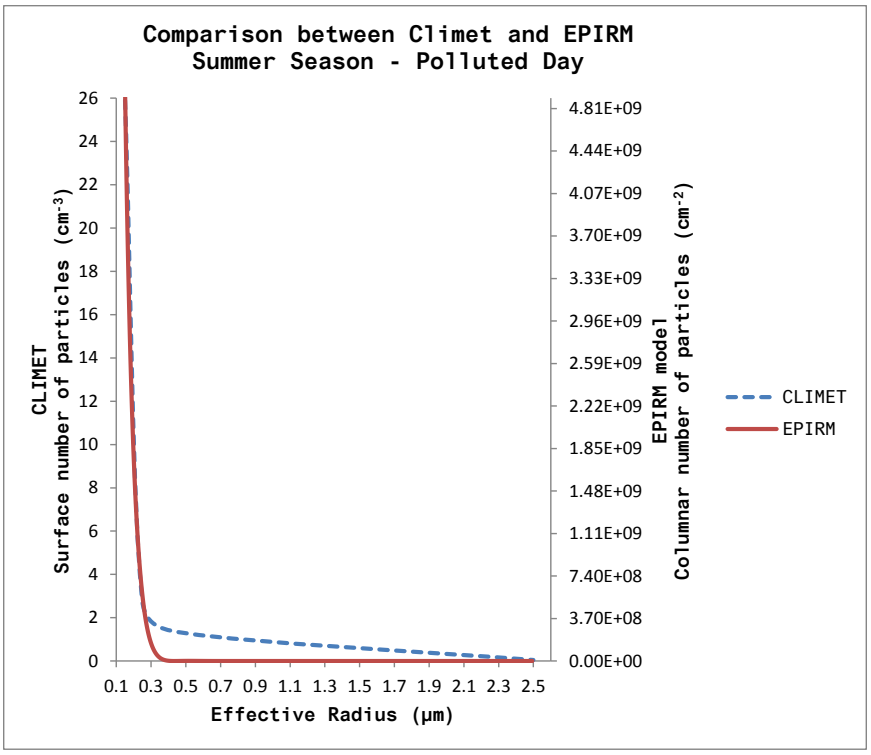

Figure 1-14. Comparison of aerosol size distribution between Climet (ground measurements) and the EPIRM model (columnar calculations) for the polluted day of the summer season.

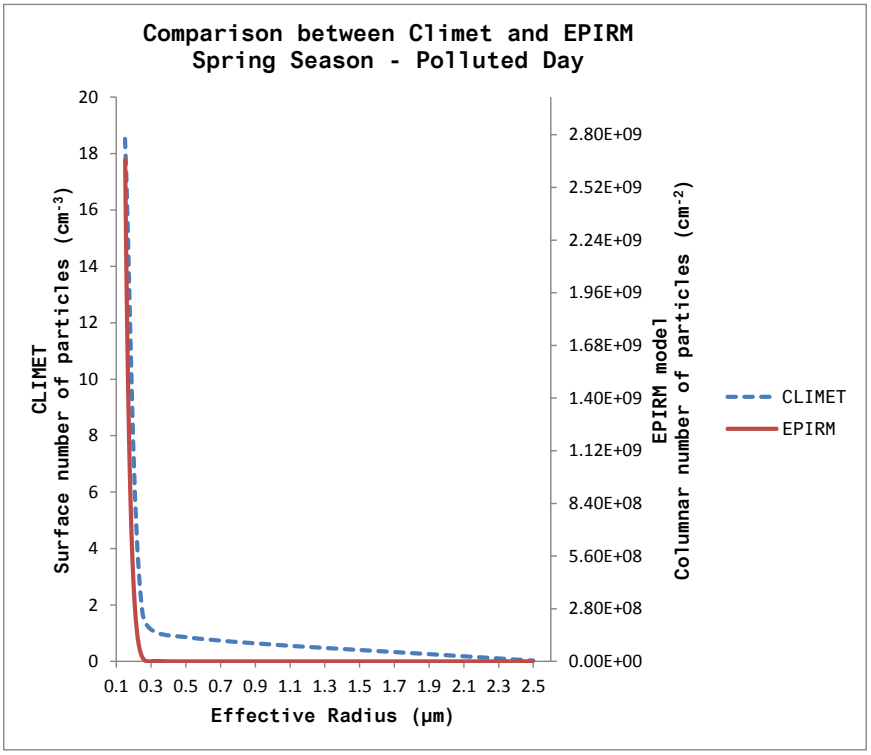

Figure 15. Comparison of aerosol size distribution between Climet (ground measurements) and the EPIRM model (columnar calculations) for the polluted day of the spring season.

Winter and summer comparison

Figure 1-16 illustrates the inter-comparison of columnar number aerosol size distribution and figure 1-17 shows the volume aerosol size distributions, for the winter and summer cases, for the polluted day scenario using the EPIRM model. Several maxima and minima are observed in this graph. At a particle radius of 0.1 μm, the figure shows a number concentration of 2 x 10^9 [cm^{-2}] for the winter and 1.5 x10^{10} [cm^{-2}] for the summer. The maximum particle radius for the winter day was 0.52 μm, while the maximum for the summer day was 1 μm.

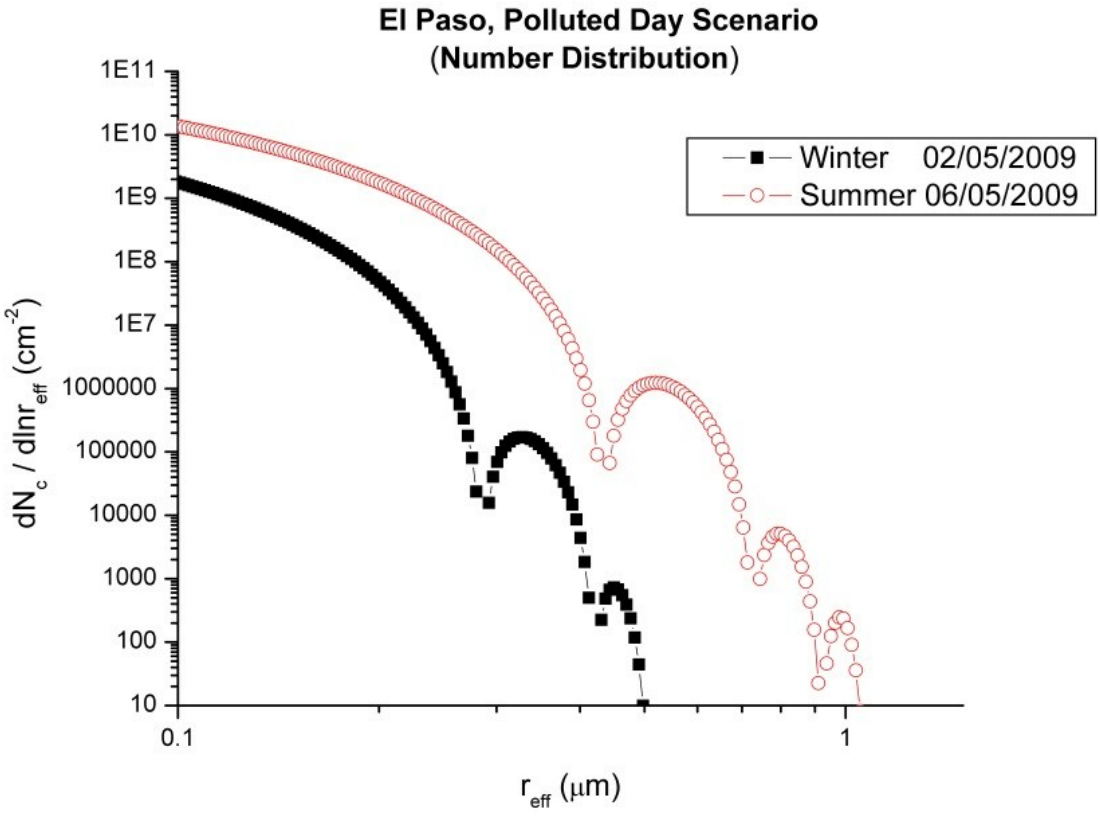

Figure 1-16. Columnar aerosol size distribution (number distribution) for the polluted scenario in the winter and summer seasons (February 5, 2009 and June 5, 2009 respectively).

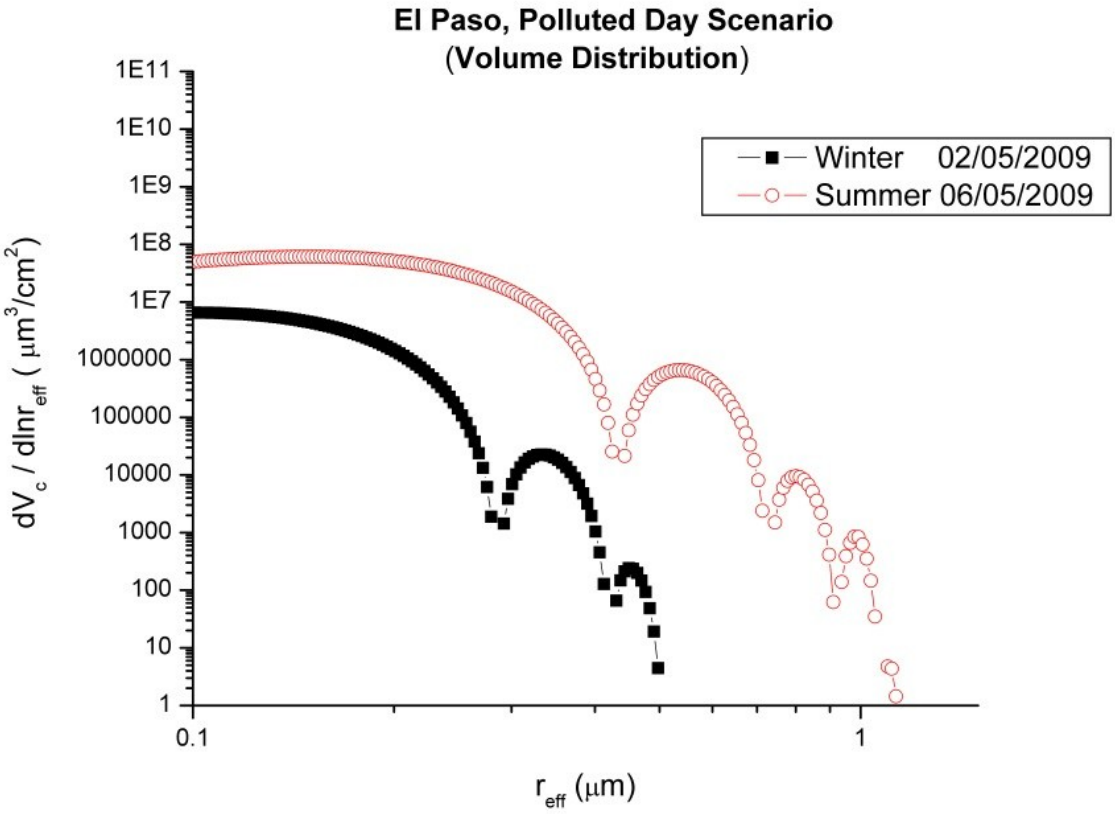

Figure 1-17. Columnar aerosol size distribution (volume distribution) for the polluted scenario in the winter and summer seasons (February 5, 2009 and June 5, 2009 respectively).

Figure 1-18 shows the HYSPLIT backward-trajectory for the winter polluted day. It was observed that the air parcels at each of the three predetermined heights came from the south of El Paso, with a slow flow at the end of the trajectories directly across industrialized Ciudad Juarez and into El Paso. It was inferred that the high particulate concentration was due primarily to influences of the El Paso-Juarez urban region, which resulted in a predominant concentration of smaller size particles. This is observed in figure 1-9 for the winter case, and is in agreement with the Angstrom exponent calculated for this day.

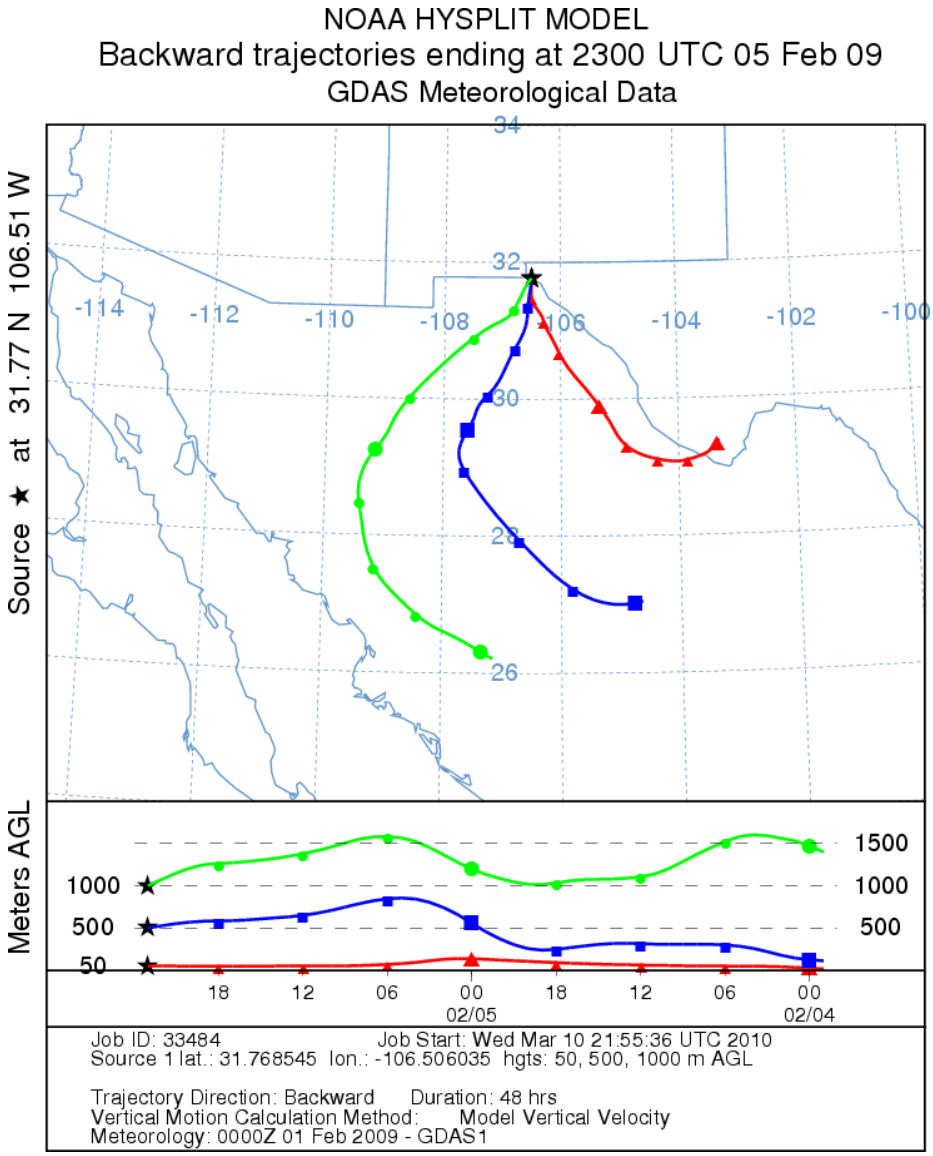

Figure 1-18. HYSPLIT 48-hour backward trajectory for a polluted day in the winter (February 5, 2009) at 50, 500 and 1,000 meters above ground level (AGL).

Figure 1-19 shows the HYSPLIT backward-trajectory for the summer polluted day. It is observed that air parcels came from near the Gulf of California and passed relatively swiftly across the Chihuahuan desert in a trajectory known to be associated with dust events (Rivera Rivera et al. 2009). From this trajectory it was inferred that mineral dust from the Chihuahuan desert was transported to the Paso del Norte Airshed, causing an increase in concentration of

larger size particles. This is seen in figure 1-17 for the summer case, and agrees with the Angstrom exponent calculated for this day.

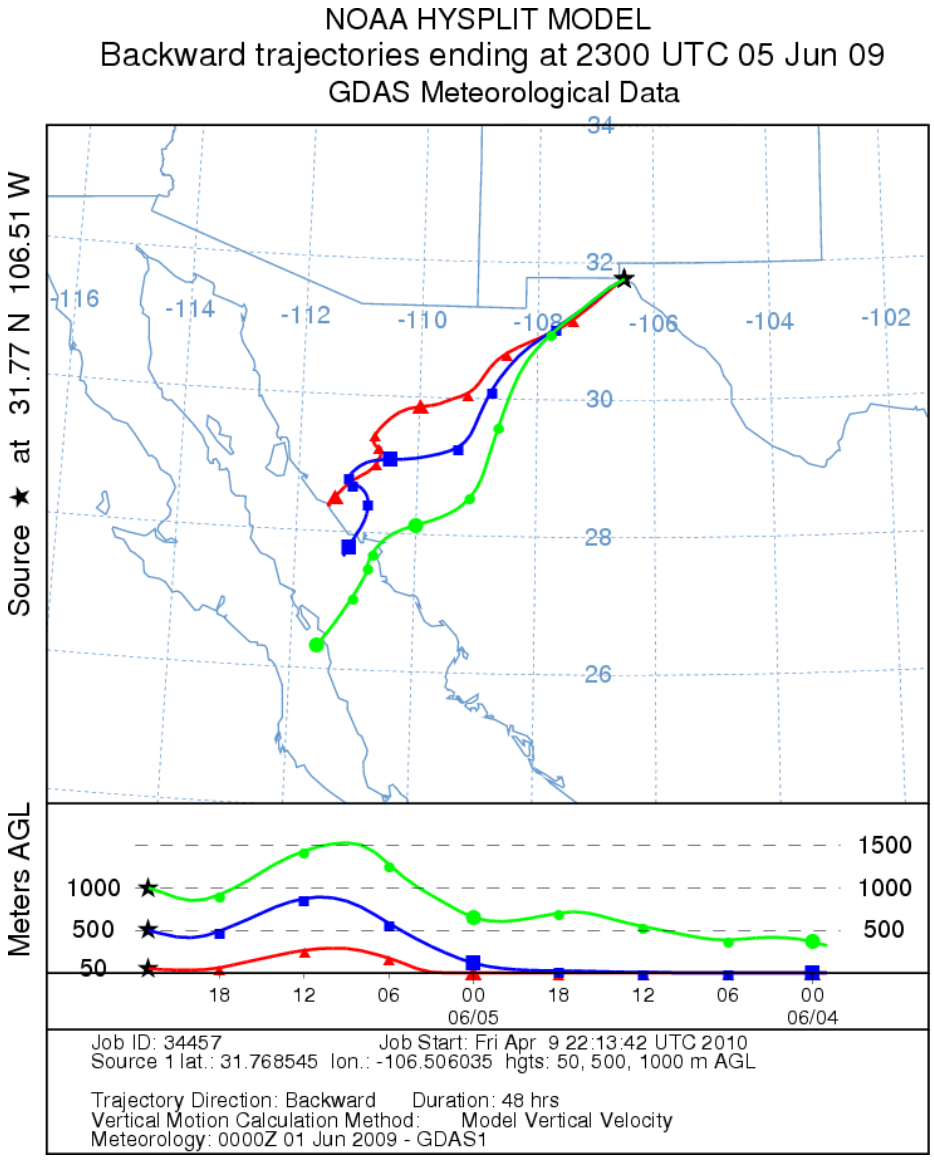

Figure 19. HYSPLIT 48-hour backward trajectory for a polluted day in the summer (June 5, 2009) at 50, 500 and 1,000 meters above ground level (AGL).

In summary, the HYSPLIT backward-trajectories provided evidence of the origin of the aerosol particles for each case study. It was noticeable that the air parcels during winter mainly originated in the urban region of El Paso-Juarez. The air parcels during the summer passed

across the Chihuahuan desert, transporting larger size particles through the city of Juarez and into the Paso del Norte Airshed.

Spring and fall comparison

Figure 1-20 and 1-21 show the comparison of the particle size distribution by number and volume respectively, for the spring (May 20, 200) and fall (November 28, 2009) polluted days. Both days presented very similar aerosol size distribution patterns. At 0.1 μm of radius, the spring day showed a slightly lower number of particles than the fall day, with 1.8 x 10^{10} [cm^{-2}]. Consequently, the number of particles decay both days, but show an increase at a radius of 0.24 μm for both the spring and fall days at 4 x 10^{6} [cm^{-2}]. The maximum radius recorded for the both days was 0.35 μm with few particles in the 1 μm radius.

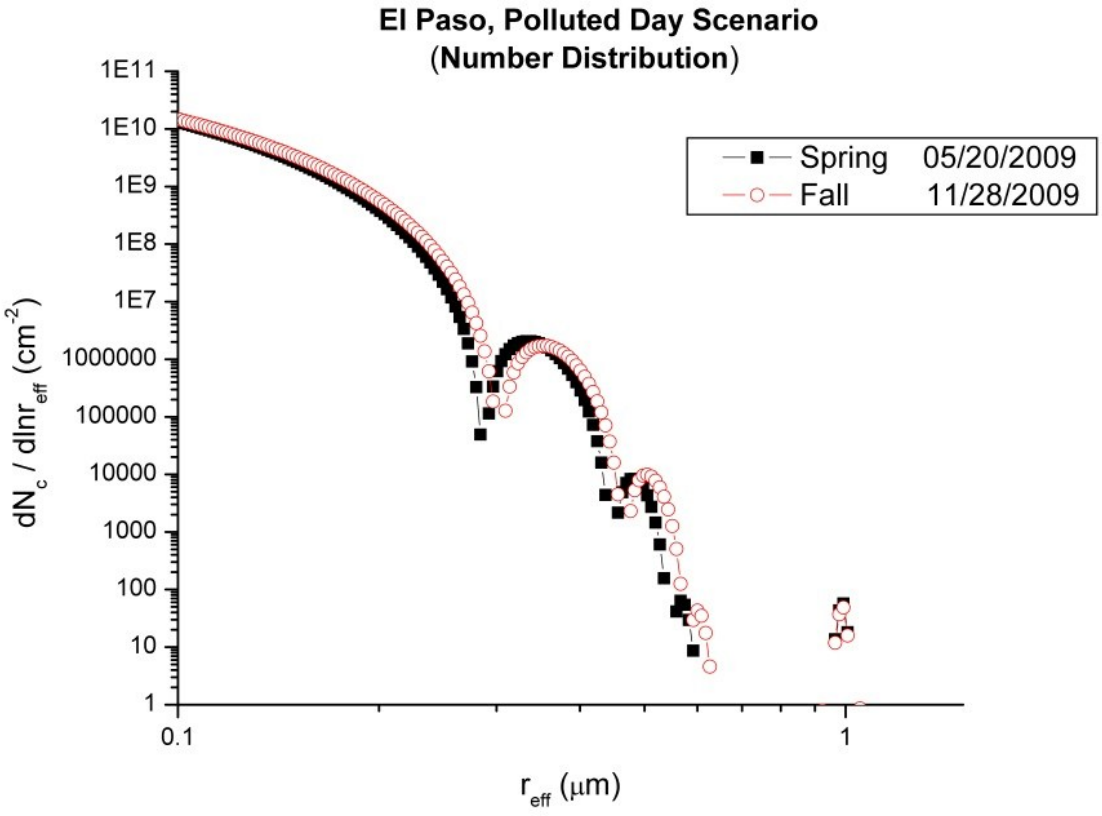

Figure 1-20. Columnar aerosol size distribution (number distribution) for the polluted scenario in the spring and fall seasons (May 20, 2009 and November 28, 2009 respectively).

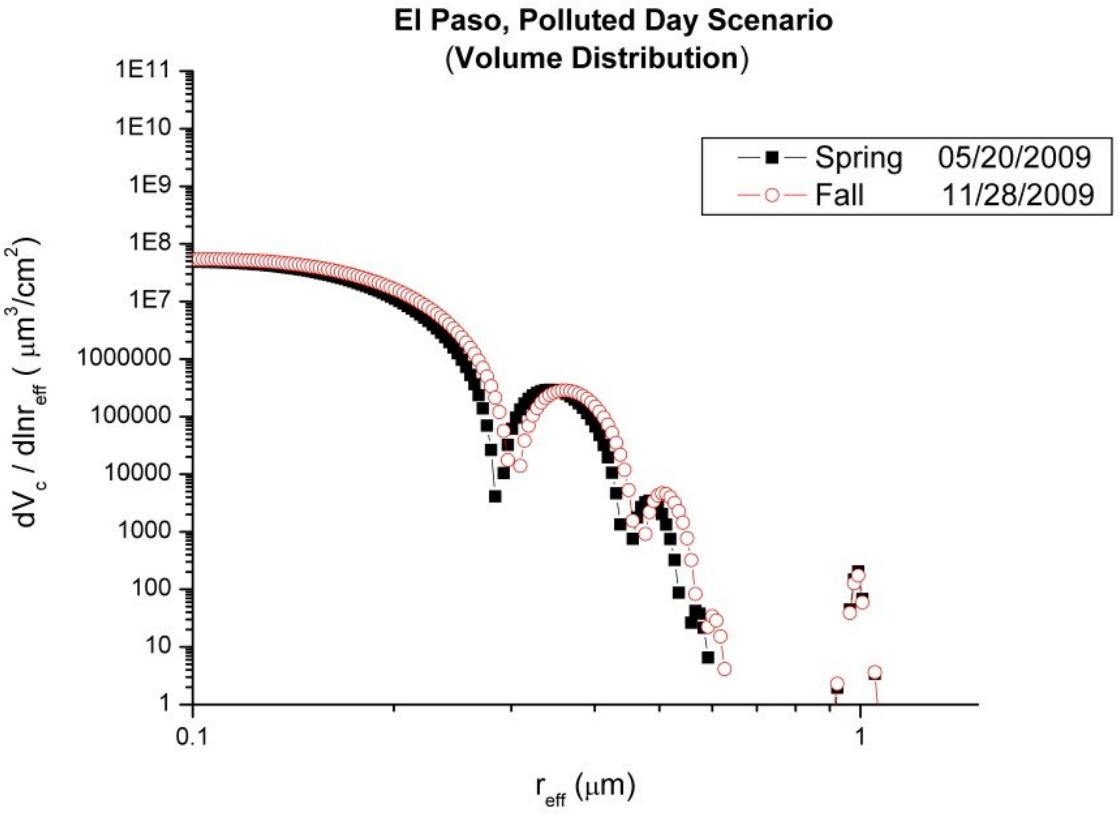

Figure 1-21. Columnar aerosol size distribution (volume distribution) for the polluted scenario in the spring and fall seasons (May 20, 2009 and November 28, 2009 respectively).

Figure 1-22 also depicts the HYSPLIT 48-hour backward trajectory for the polluted day (May 20, 2009). The air parcels came mostly from the Chihuahuan desert, where some mineral dust particles, as well as other particles, were lifted up and transported to El Paso.

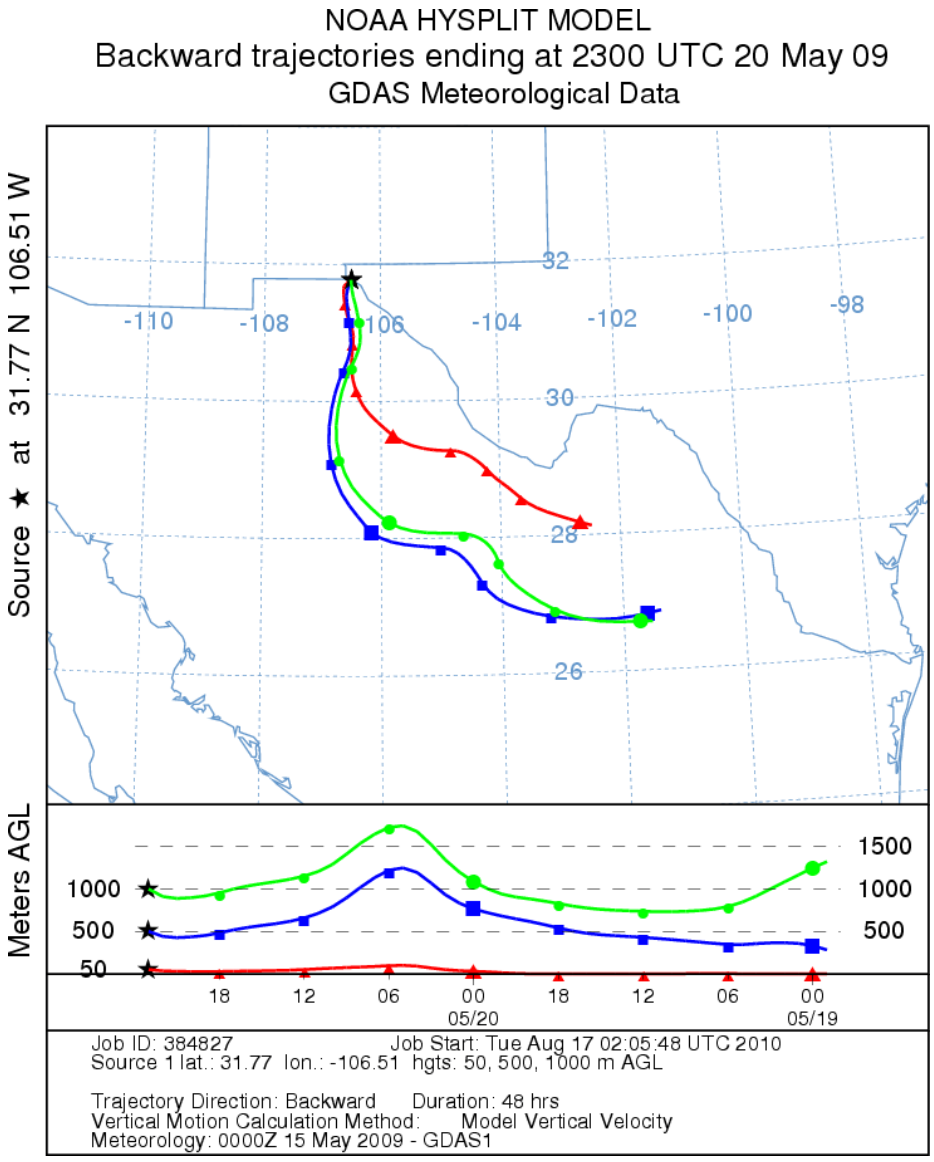

Figure 1-22. HYSPLIT 48-hour backward trajectory for a polluted day in the spring (May 20, 2009) at 50, 500 and 1,000 meters above ground level (AGL).

Figure 1-23 also portrays the HYSPLIT 48-hour backward trajectory for the polluted day (November 28, 2009). The air parcels came mostly from the Chihuahuan desert and passing from the state of Sonora, where some mineral dust particles were boosted up and conveyed to El Paso area.

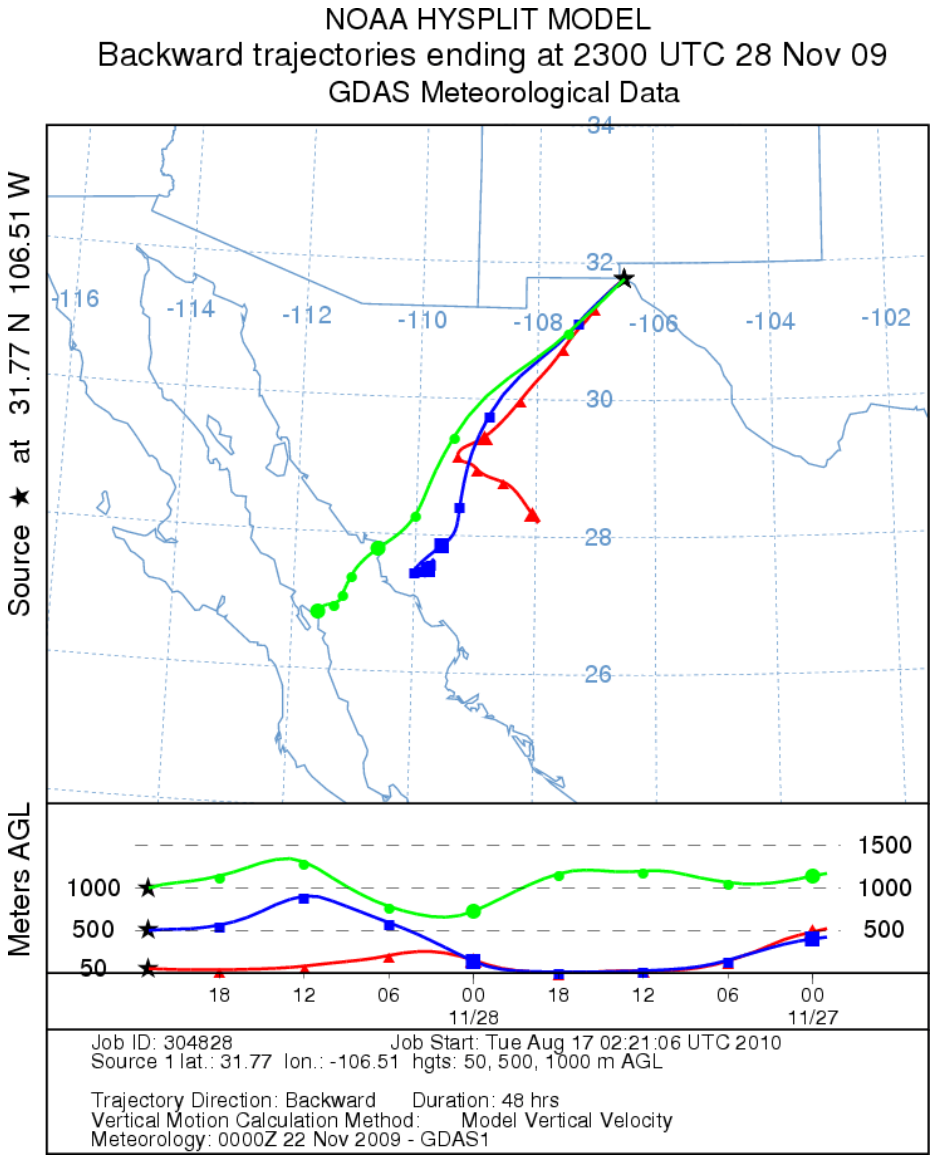

Figure 1-23. HYSPLIT 48-hour backward trajectory for a polluted day in the fall (November 28, 2009) at 50, 500 and 1,000 meters above ground level (AGL).

The HYSPLIT backward-trajectories provided evidence of the origin of the aerosol particles for each case study. It was perceptible that the air parcels during spring and fall seasons passed across the Chihuahuan desert, transporting larger size particles through the city of Juarez and into the Paso del Norte Airshed.

Conclusions

The inverse reconstruction model was successfully applied to the El Paso-Juarez Airshed. This model has an advantage over other techniques in that it can be used in the study of aerosols *in situ*. The methodology may be used in any area of the country, but is especially relevant to southwestern U.S cities such as El Paso, which experiences severe air pollution from fugitive dust source contaminants.

In this work it was observed that for the clean day scenario the summer case exhibited a greater concentration of smaller size particles than the winter case. This is attributable in part to the different regions from which the air parcels originated. Moreover, the air parcels moved more slowly in the summer case than in the winter case. For the summer day the air parcels passed across the more industrialized region of the Paso del Norte Airshed and this was interpreted as the cause of a higher concentration of small particles. Furthermore, it was noticeable that the spring case showed a greater concentration of particles in all the radius ranges.

The calculated Angstrom exponent in the polluted day scenario demonstrated that there is a predominance of smaller size particles in the winter than in the summer, as observed on the graphs. In contrast, the spring and fall days showed preponderance for larger size particles as well as high concentration of smaller size particles in both cases.

From the HYSPLIT backward-trajectories it was recognized that the air parcels during winter mainly originated at the urban region of Ciudad Juarez, Mexico, whereas the air parcels during the summer, spring and fall passed across the Chihuahuan desert.

In all four cases the correlation factors between the EPIRM model and the CI-150t instrument were above 0.98. The polymodality observed in the graphs is expected for an interface and complex region, such as the Paso del Norte region.

This research project will permit a better understanding of the environmental impact that natural and anthropogenic activities can generate, thus allowing a proper evaluation of the effectiveness of alternative air pollution control measures for regulatory compliance purposes.

CHAPTER 2

Intercomparison of optical depth data among MFRSR, MISR and AERONET in the Paso del Norte Region

Introduction

Aerosols are small particles present in the atmosphere in an ample size variation, concentration and chemical composition (Kaufman et al. 1997). Some aerosols are emitted directly into the atmosphere while others are formed from emitted compounds. Aerosols contain both naturally occurring compounds and those emitted as a result of human activities. Fossil fuel and biomass burning have increased aerosols containing sulfur compounds, organic compounds and black carbon (Ramanathan et al. 2001). Natural aerosols include mineral dust released from the earth's surface, sea salt aerosols, biogenic emissions from the land and oceans, as well as sulfate and soot aerosols produced by volcanic eruptions (Jacobson 1999). Aerosol particles influence radiative forcing directly through reflection and absorption of solar and infrared radiation in the atmosphere (Sokolik and Toon 1996). Some aerosols cause a positive forcing while other cause a negative forcing (Forster et al. 2007).

The use of satellite data has become an indispensable tool in the understanding of global climate change. Ground-based stations cannot assess trends in the global aerosol budget due to the short lifetime of aerosols and the corresponding spatial variations in the aerosol concentrations (Kaufman et al. 1997). Therefore, quotidian remote sensing of aerosols from satellites over the land and ocean is indispensable to account for the global radiative budget, and essential for the understanding of the aerosol radiative forcing of climate (Charlson et al. 1992). Contributions from satellite aerosol products, surface measurements, and aerosol transport

models are helping create a global picture of aerosol distributions for these applications (Kahn et al. 2005). These datasets play a fundamental role in remote sensing practices (Chopping et al. 2008), proving especially useful in areas where there are neither instruments nor monitoring networks that can provide terrestrial data for it analysis.

Daily satellite observations and continuous in situ measurements are needed to observe the emission and transport of dense aerosol plumes downwind of populated and polluted regions (urban haze), regions with vegetation fires (smoke), and desert (dust) (Kaufman, Tanré, and Boucher 2002). Comparisons of in situ measurements against those from global atmospheric models are complicated, due to differences in meteorological conditions. Furthermore, in situ measurements are representative of conditions mostly at or near the surface while the direct and indirect radiative forcing depends on the aerosol vertical profile (Forster et al. 2007). Besides, precise description of aerosol composition requires in situ chemical measurements that are restricted in time and location. However, it is possible to estimate the anthropogenic part of aerosols using a combination of satellite data, aerosol models, and information on urban and agricultural activities and fire practices (Kaufman, Tanré, and Boucher 2002).

Desert regions such as El Paso, Texas, tend to have high concentration of dust particles suspended in the air. The Paso del Norte Airshed is usually affected by anthropogenic and biogenic emissions as well as by dust particles (Noble et al. 2003); (Pearson, Fitzgerald, and Polanco 2007); (Esparza et al. 2011). The Paso del Norte metro area is isolated, more than 500 km away from the nearest urban area of comparable size, thus making it an ideal location for air quality studies of an isolated urban environment. The city of El Paso has a population of over 600,000, and is contiguous with the industrial city of Juarez, Mexico (population over 1 million) and some adjacent suburbs in the state of New Mexico. This area is one of the largest bi-national

metropolitan areas in the world, and one of the fifty largest metropolitan areas in the Western Hemisphere (Esparza et al. 2011). The climate is characterized by well-defined seasons, with hot summers and cold winters and with an average of approximately 22 cm of annual precipitation. The metropolitan area contains the Franklin Mountains which bisect the city of El Paso and the Sierra de Juarez in the city of Juarez as well as the river valley of the Rio Grande (Rio Bravo del Norte).

Aerosol optical depth (AOD) data obtained from satellites can be very useful in the aerosol characterization process for the region, since it can provide a wider coverage than in situ instruments, including places where data is sparse, such as the city of Juarez, in Mexico. This study includes a three-year (2006-2009) analysis of the aerosols' satellite data from the Multi-angle Imaging SpectroRadiometer (MISR) satellite instrument for the El Paso-Juarez Airshed. MISR has been providing tropospheric aerosol properties including aerosol optical depth (AOD), globally since February 2000 (Diner et al. 2001). Thus, comparisons of aerosol optical parameters between MISR, and ground data from a Multi-Filter Rotating Shadowband Radiometer (MFRSR) instrument in El Paso, Texas and from a near AERONET station located in White Sands, New Mexico, is presented.

Methodology

This study provides an analysis and comparison of the AOD data between ground-based instruments and satellite data. In this project, the ground-based instruments were a visible-spectrum MFRSR installed in the University of Texas at El Paso (UTEP) campus (31° 46' 06.79" N, 106° 30' 21.99" W) and the nearest sun photometer facility, NASA's Aerosol Robotic Network (AERONET), located at White Sands, New Mexico (32° 38' 06" N, 106° 20' 16" W).

Figure 2-1 shows the geographical location of these two stations and the MISR's swath. The linear distance between these two sites is about 60.90 miles. The satellite data was provided by the MISR instrument located in the Terra satellite. These measurements were taken within the latitude range of 31° 26' 45.6'' (31.446) and 31° 59' 5.9994'' (31.985) and the longitude range of 106° 8' 20.3994'' W (-106.139) and 106° 58'11.9994'' W (-106.97).

Figure 2-1. Geographical location of the AERONET-White Sands site (green), the UTEP MFRSR instrument (blue) and the MISR's swath (yellow rectangle).

The MISR's AOD measurements were provided at a wavelength of 558 nm. Therefore, interpolation in the MFRSR and AERONET measurements was required. This was achieved by using the Angstrom exponent (α), which describes the dependency of the AOD on wavelength. This dependency is expressed in equation 1.

$$\alpha = -\partial ln\tau / \partial ln\lambda \quad (1)$$

The criterion for an acceptable AOD comparison at a site required that MFRSR and AERONET data be available within a 1 hour window centered on the MISR overpass time. The relative error was calculated using the following approach (Abramowitz and Stegun 1972):

$$\delta x = \frac{\Delta x}{x} = \frac{x_0 - x}{x} \quad (2)$$

Where, δx is the relative error, Δx is the absolute error, x_0 is the measured value (i.e. MISR) and x is the true value (i.e. MFRSR or AERONET). With this equation it was realized if the MISR measurements are underestimating (negative) or overestimating (positive) with respect to the ground instruments.

Then, in order to get a positive error calculation in the range of 0 to 1, the following equivalent metric (Krause 1986) was applied:

$$X = \frac{|\delta x|}{1 + |\delta x|} \quad (3)$$

Where X is the error and δx is the relative error in equation 1.

In order to understand the likelihood of the error, the probability and cumulative density functions were calculated using the following definition:

$$P[a \leq X \leq b] = \int_a^b f(x)dx \quad (4)$$

Where,

$$f(x) = \frac{1}{\sqrt{2\pi\sigma^2}} e^{\frac{(x-\mu)^2}{2\sigma^2}} \quad (5)$$

In which μ is the mean and σ is the standard deviation of the data set; x is the evaluated data from the data set. Hence, if F is the cumulative distribution function of X, then:

$$F(x) = \int_{-\infty}^{x} f(u)du \quad (6)$$

And if f is continuous at x, then

$$f(x) = \frac{d}{dx}F(x) \quad (7)$$

Instruments

MISR

On December 18, 1999, NASA launched Terra, the first of a series of satellites within the Earth Observing System (EOS), a comprehensive program for monitoring the surface and atmosphere from remote sensing platforms and ground-based stations. Among the main objectives of EOS is improvement in our understanding of geophysical processes governing global changes in our planet's climate, including scattering and absorption of solar radiation by aerosols (Abdou et al. 2005).

The Multi-angle Imaging SpectroRadiometer (MISR) provides global, radiometrically calibrated, geo-rectified, and co-registered imagery at nine discrete viewing angles and four visible/near infrared spectral bands. (Diner et al. 1997) Radiant energy reflected and emitted by the Earth carries with it a signature of the atmospheric and surface properties. By measuring the wavelength, angular and polarization properties of this energy, satellite sensors can quantify several atmospheric and surface properties. The amount of light escaping the top of the atmosphere is affected by the angle at which the light was reflected by the surface or atmosphere.

MISR takes advantage of this fact by detecting the reflected light at different viewing angles (nadir to 70 degrees forward and backward) along the satellite's track in a narrower spectral range (440-860 nm) (Kalashnikova and Kahn 2008). It is thus able to separate the aerosol signal from that of surface reflectance, and determine the aerosol properties.

The independent aerosol retrieval strategies and algorithms used by MISR exploit the complementary multiangle nature of their measurements. Within a 7-min period, MISR observes the same point on Earth in nine different angles and four spectral bands.

AOD biases can arise from a variety of sources, including faulty assumptions in the retrieval algorithms, imperfect cloud screening, selection or prescription of inappropriate aerosol models, or errors in calibration. Martonchik et al., found that for desert sites the values of MISR AOD were biased high with respect AERONET by about 0.08 at 17.6 km spatial resolution and 0.05 at 52.8 km spatial resolution (Martonchick et al. 2004); (Diner et al. 2004).

The current set of MISR aerosols models used by the operational algorithm has known deficiencies, particularly with regard to dust particle properties and variety in the bimodal particle mixture. Once these aerosol model improvements are implemented, more detailed validation studies can be conducted to address additional aerosol properties including particle size, sphericity, and absorption (Martonchick et al. 2004).

AERONET

The Aerosol Robotic Network (AERONET) is a global network of ground-based sun photometers which measure atmospheric aerosol properties. This network was developed as a prospect for the fully understanding of the aerosols influence on climate forcing as wells as for

satellite data validation using ground-based sun photometers (Holben et al. 1998). Aerosol radiative forcing is one of the largest uncertainties in climate change studies.

The measurement system is a solar-powered CIMEL Electronique 318A spectral radiometer that measures the extinction of direct beam spectral solar radiation. Robots approximately 18" high with a 1-foot diameter base are used in conjunction with a data logger, data transmission device, batteries, solar panels, and antenna for data transmission. Four spectral wavelengths (500, 675, 870 and 1020 nm) are provided by this radiometer.

AERONET can provide continuous measurements of AOD, an important climate forcing agent. AOD is needed in satellite validation and atmospheric correction, and AERONET stations are used to calibrate the instruments since the low and stable AOD are ideal for this purpose. Long term particle size distribution comparisons will provide validation of the radiometric inversion scheme.

Currently there is no AERONET station in El Paso-Juarez area. There are three stations in the vicinity of the city. The closest station is located in La Jornada, New Mexico, which comprehends the Paso del Norte region. However, this site had AOD values from January 1997 to December 2007 only. The other station is located at Los Alamos, New Mexico, but as well as La Jornada, it only had values of AOD from January 2003 to December 2006. Consequently, the only station in close proximity to the city was the White Sands station, hitherto, is not located within the MISR's swath boundaries.

The White Sands facility houses the ground-based network of AERONET instrumentation, which measures aerosols and atmospheric properties on a continual basis. Solar

energy and optical properties were collected and derived from AERONET instruments, obtained from the level 2.0 data product on the AERONET website.

MFRSR

The Multi-Filter Rotating Shadowband Radiometer (MFRSR) is located at the UTEP campus, measuring solar irradiance in the visible regions at five narrowband wavelengths (415, 500, 610, 665 and 860 nanometers) (Esparza et al. 2011). Total optical depths were calculated using the standard Beer's Law approach (Bigelow et al. 1998); (Hand et al. 2004). In these calculations, the optical depth due to water and other molecules as well as Rayleigh and ozone optical depths are subtracted from total optical depth to obtain aerosol optical depth (Slusser et al. 2000), as shown in equation 3.

$$\tau_A = \tau_T - \tau_R - \tau_O - \tau_{WM} \quad (8)$$

In addition, this MFRSR is linked to a nationwide of MFRSR radiometers (Bigelow et al. 1998). At present, this network is part of the USDA UV-B Monitoring Program, which includes thirty five locations in the U.S. (including Alaska and Hawaii), two in Canada and one in New Zealand (Mckenzie et al. 2006).

Results

In an effort to associate the MISR retrievals, AOD data from the MFRSR and AERONET instrument were compared against the MISR's AOD data for the Paso del Norte Airshed from November 18, 2006 to November 19, 2009.

Figure 2-2 shows the comparison between the MISR's AOD at a wavelength of 558 nm and the MFRSR's AOD interpolated at wavelength of 558 nm using the 500 and 610 nm AOD values.

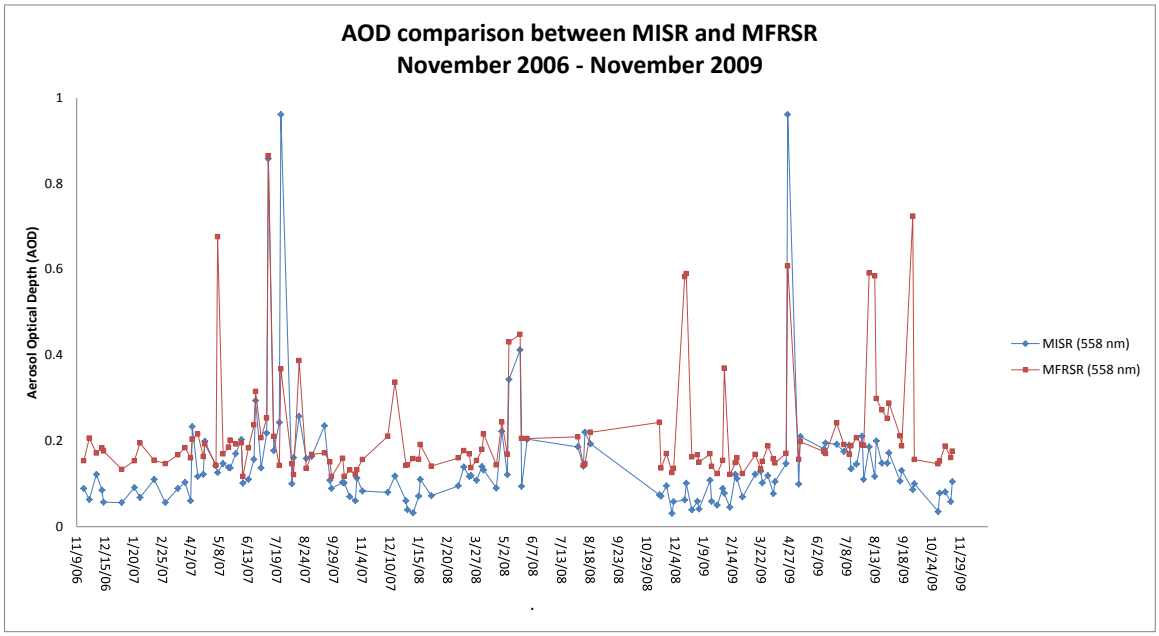

Figure 2-2. AOD data from MISR and MFRSR from selected days from November 2006 to November 2009.

Figure 2-3 shows the comparison of the observed MISR values against the MFRSR values. This comparison provided a linear correlation of 0.52, in which MISR underestimated the ground values of the MFRSR.

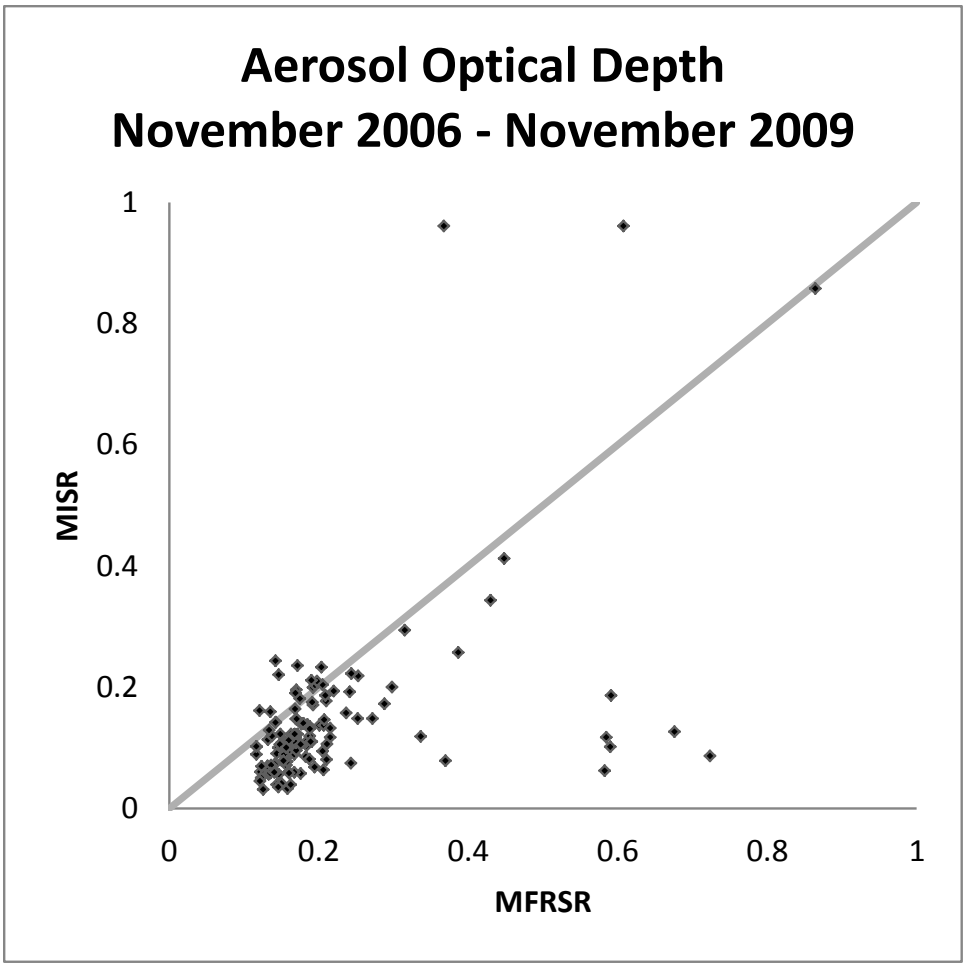

Figure 2-3. Scatter plot of MISR vs MFRSR AOD for the entire dataset.

Figure 2-4 shows the percentage error in the measurements, having the MFRSR values as the true values and obtaining the absolute value. The average error is 26.13% with a standard deviation of 12.69%. The maximum recorded error was 61.73% and the minimum was 0.54%.

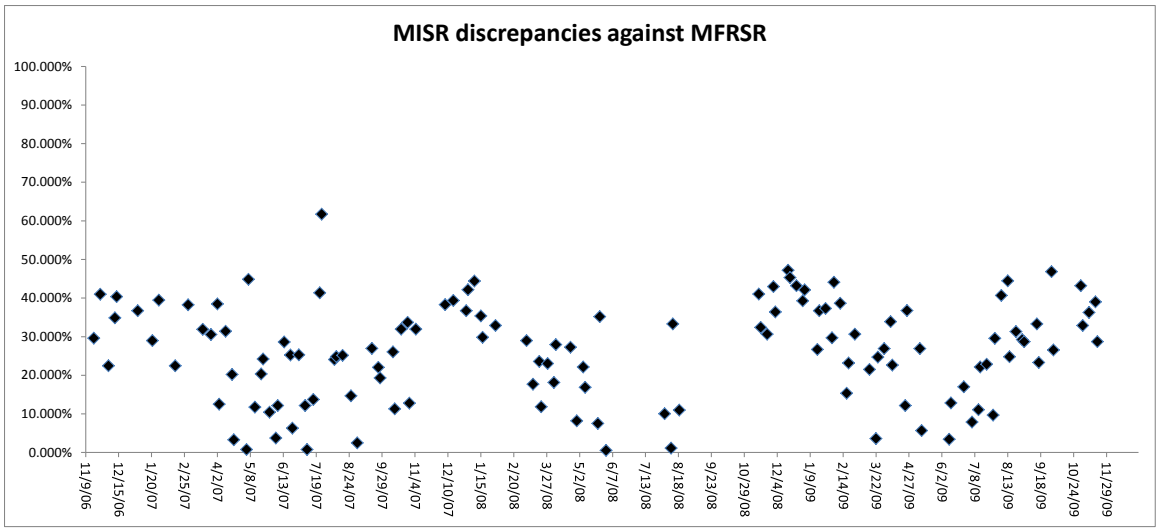

Figure 2-4. Error percentage of the AOD data from MISR and MFRSR from selected days from November 2006 to November 2009.

Figure 2-5 shows the probability and cumulative density functions of the error between MISR and MFRSR. This described the relative likelihood for the error to occur at a given point.

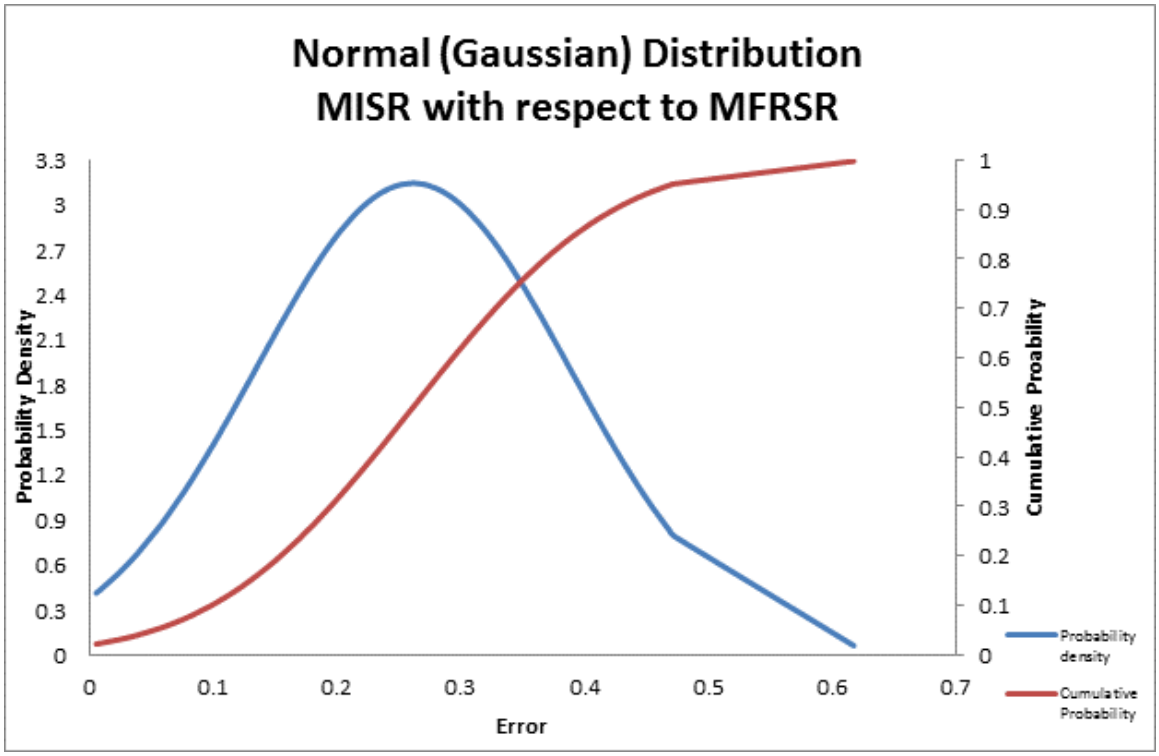

Figure 2-5. Probability density function and cumulative probability for the error between MISR and MFRSR AOD measurements.

Table 2-1 summarizes the seasonal modality of the error. During the winter season, 97% of the error measurements were in the 20 to 50% range. In the spring season, the error concentrated in the 20 to 40% error range, yet 32% of the total measurements fell below the 15% error. For the summer season 44% of the measurements had 15% or less error, the other 40% of the measurements were in 20 to 30% error. For the fall season, only 12% of the measurements fell below the 15% error, and 84% of the measurements were in the range of 20 to 50% error. Overall, 7% of the measurements had less than 5% error; 4.7% were between 5 and 10%; 11.8% were between 10-15%; 4.7% were between 15-20%; 31.5% were between 20-30%; 26% were between 30-40%; 13.4% were between 40-50%; and less than 0.9% was located in the 60-80%

Table 2-1. Seasonal summary of the number of measurements categorized by percentage error bins.

Error %	<5%	5-10%	10-15%	15-20%	20-30%	30-40%	40-50%	50-60%	60-80%	80-100%	TOTAL
Winter											
2006-2007	0	0	0	0	3	3	1	0	0	0	7
2007-2008	0	0	0	0	1	5	2	0	0	0	8
2008-2009	0	0	0	1	3	6	5	0	0	0	15
Season Total	***0***	***0***	***0***	***1***	***7***	***14***	***8***	***0***	***0***	***0***	***30***
Spring											
2007	2	0	3	0	3	5	1	0	0	0	14
2008	1	2	1	3	6	1	0	0	0	0	14
2009	1	1	1	0	5	2	0	0	0	0	10
Season Total	***4***	***3***	***5***	***3***	***14***	***8***	***1***	***0***	***0***	***0***	***38***
Summer											
2007	2	1	4	0	6	0	1	0	1	0	15
2008	1	0	2	0	0	1	0	0	0	0	4
2009	1	2	2	1	6	1	2	0	0	0	15
Season Total	***4***	***3***	***8***	***1***	***12***	***2***	***3***	***0***	***1***	***0***	***34***
Fall											
2006	0	0	0	0	1	0	1	0	0	0	2
2007	1	0	2	1	3	3	0	0	0	0	10
2008	0	0	0	0	0	2	2	0	0	0	4
2009	0	0	0	0	3	4	2	0	0	0	9
Season Total	***1***	***0***	***2***	***1***	***7***	***9***	***5***	***0***	***0***	***0***	***25***
TOTAL	**9**	**6**	**15**	**6**	**40**	**33**	**17**	**0**	**1**	**0**	***127***

From the previous graphs it was observed that mostly MISR underestimates the ground measurements performed by the MFRSR. However, it is noticeable that the minimum errors occurred during the summer months of each of the three years.

Figure 2-6 shows the AOD data obtained from MISR data at a wavelength of 558 nm and the AERONET at White Sands (WS) data interpolated at a wavelength of 558 nm using the 500 and 675 nm wavelengths.

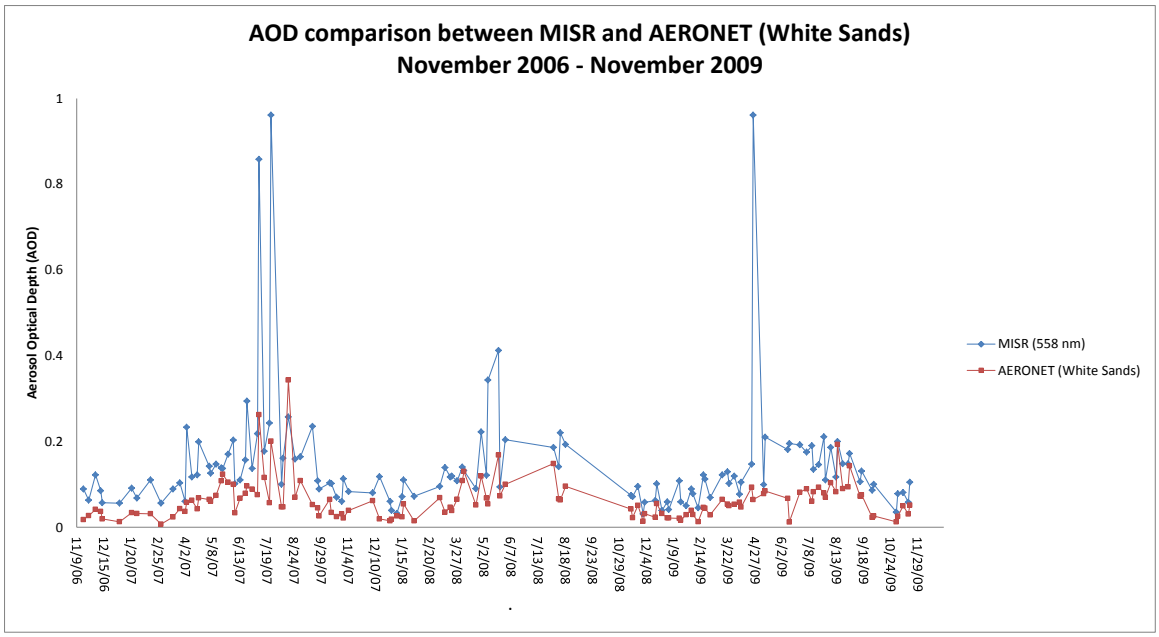

Figure 2-6. AOD data from MISR and AERONET at White Sands, NM from selected days from November 2006 to November 2009.

Figure 2-7 shows the comparison of the observed MISR values against the AERONE-WS values. This comparison provided a linear correlation of 0.58, in which MISR overestimated the ground values of the AERONET-WS.

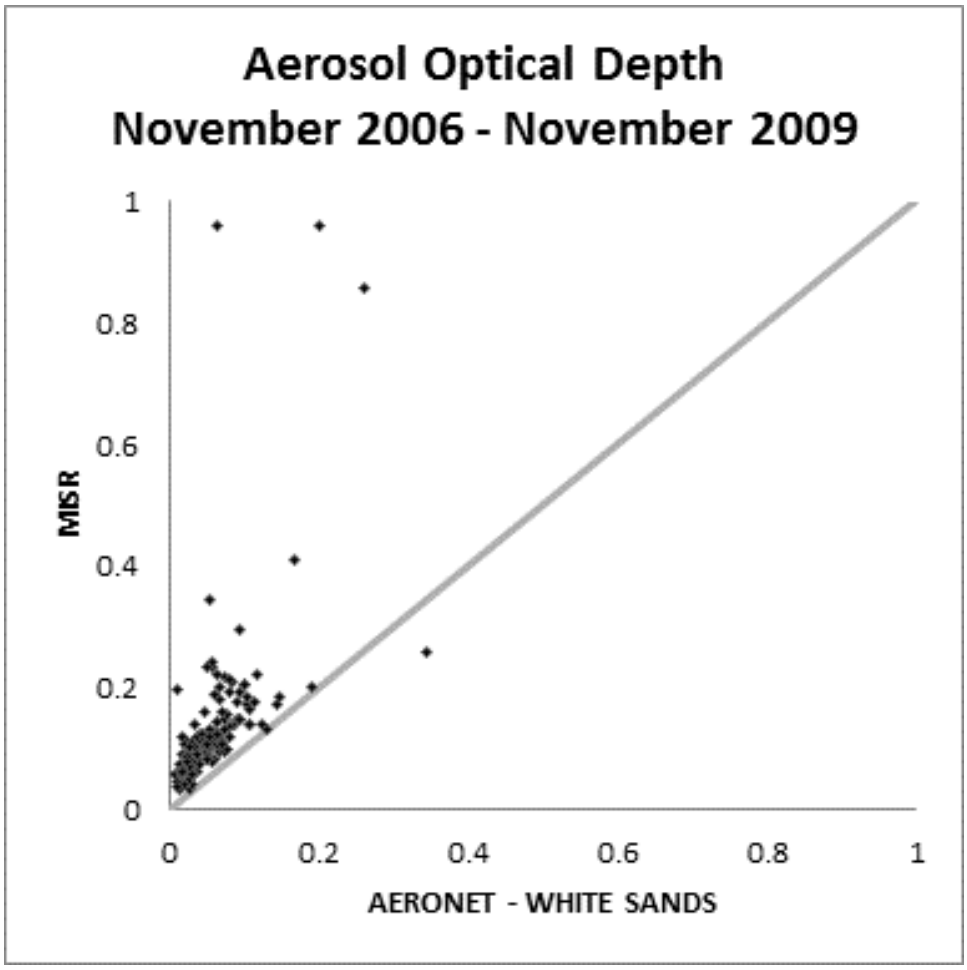

Figure 2-7. Scatter plot of MISR vs AERONET-White Sands AOD for the entire dataset.

Figure 2-8 shows the percentage error in the measurements, having the AERONTE-WS values as the true values and obtaining the absolute value. The average error is 53.36% with a standard deviation of 18.98%. The maximum recorded error was 93.87% and the minimum was 1.51%.

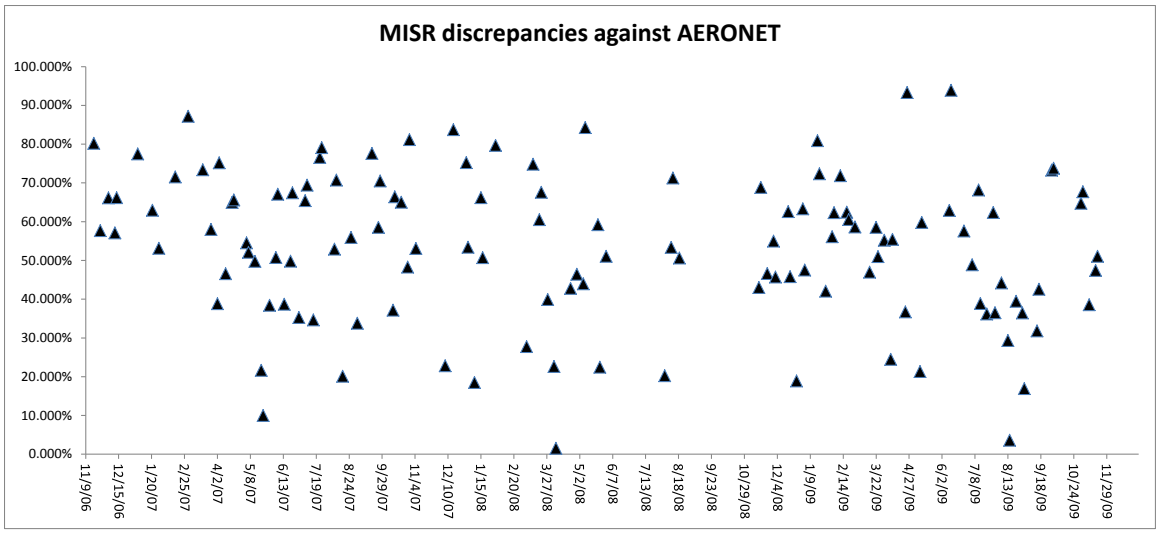

Figure 2-8. Error percentage of the AOD data from MISR and AERONET at White Sands from selected days from November 2006 to November 2009.

Figure 2-9 shows the probability and cumulative density functions of the error between MISR and AERONET-WS.

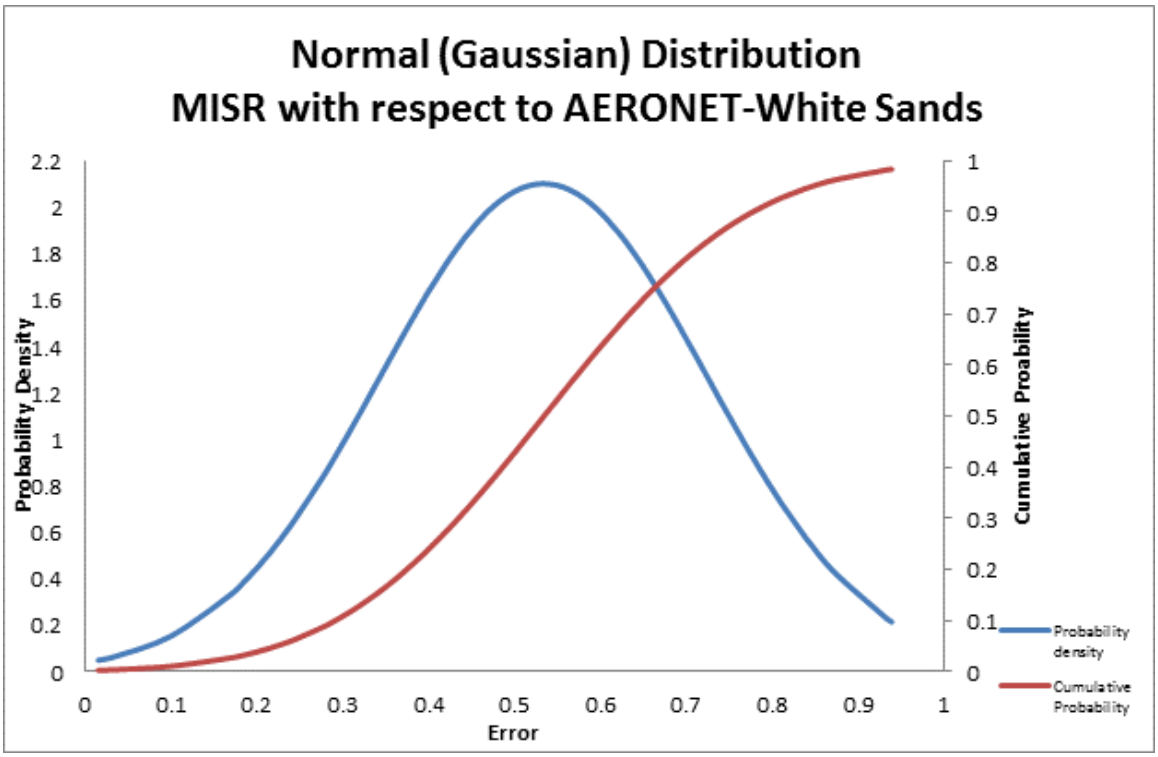

Figure 9. Probability density function and cumulative probability for the error between MISR and AERONET-WS AOD measurements.

Table 2-2 summarizes the seasonal modality of the error. During the winter season, 90% of the error measurements were in the range of greater than 50% error. In the spring season, the error concentrated in the 40 to 80% error range with 60.5% of the total measurements, hitherto 5.3% of the total measurements fell below the 10% error. For the summer season 23.5% of the measurements were in the 30-40% error range, while 32.4% were in 60-80% error range. In the fall season there were no measurements with error less than 30%; only 16% of the measurements were in the error range of 30-40%, while 64% of the measurements had errors greater than 50%. Overall, 1.6% of the measurements had less than 5% error; 0.8% was between 5 and 10%; 0% was between 10-15%; 2.4% were between 15-20%; 7.9% were between 20-30%; 12.6% were between 30-40%; 14.2% were between 40-50%; 21.3% were between 50-60%; 33.1% were between 60-80%; and the remaining 6.1% were in the 80-100% error region.

Table 2-2. Seasonal summary of the number of measurements categorized by percentage error bins.

Error %	< 5%	5-10%	10-15%	15-20%	20-30%	30-40%	40-50%	50-60%	60-80%	80-100%	TOTAL
Winter											
2006-2007	0	0	0	0	0	0	0	2	5	0	7
2007-2008	0	0	0	1	1	0	0	2	3	1	8
2008-2009	0	0	0	1	0	0	4	2	7	1	15
Season Total	***0***	***0***	***0***	***2***	***1***	***0***	***4***	***6***	***15***	***2***	***30***
Spring											
2007	0	1	0	0	1	2	2	3	4	1	14
2008	1	0	0	0	3	1	3	2	3	1	14
2009	0	0	0	0	2	1	1	5	0	1	10
Season Total	***1***	***1***	***0***	***0***	***6***	***4***	***6***	***10***	***7***	***3***	***38***
Summer											
2007	0	0	0	0	1	3	1	3	7	0	15
2008	0	0	0	0	1	0	0	2	1	0	4
2009	1	0	0	1	1	5	2	1	3	1	15
Season Total	***1***	***0***	***0***	***1***	***3***	***8***	***3***	***6***	***11***	***1***	***34***
Fall											
2006	0	0	0	0	0	0	0	1	0	1	2
2007	0	0	0	0	0	2	1	2	4	1	10
2008	0	0	0	0	0	0	2	1	1	0	4
2009	0	0	0	0	0	2	2	1	4	0	9
Season Total	***0***	***0***	***0***	***0***	***0***	***4***	***5***	***5***	***9***	***2***	***25***
TOTAL	**2**	**1**	**0**	**3**	**10**	**16**	**18**	**27**	**42**	**8**	***127***

It was observed that mostly MISR overestimates the ground measurements performed by the AERONET-WS. The season with the least minimum errors was the spring season, followed by the summer.

Despite of AERONET-WS's slightly better linear correlation, the MFRSR instrument provided results with less error when compared to the MISR data.

Figure 2-10 shows the scatter plot of the MFRSR and AERONET-WS in terms of AOD for the entire data set. From this graph it can be observed that MFRSR values were greater than the values from the AERONET. This comparison provided a linear correlation of 0.41.

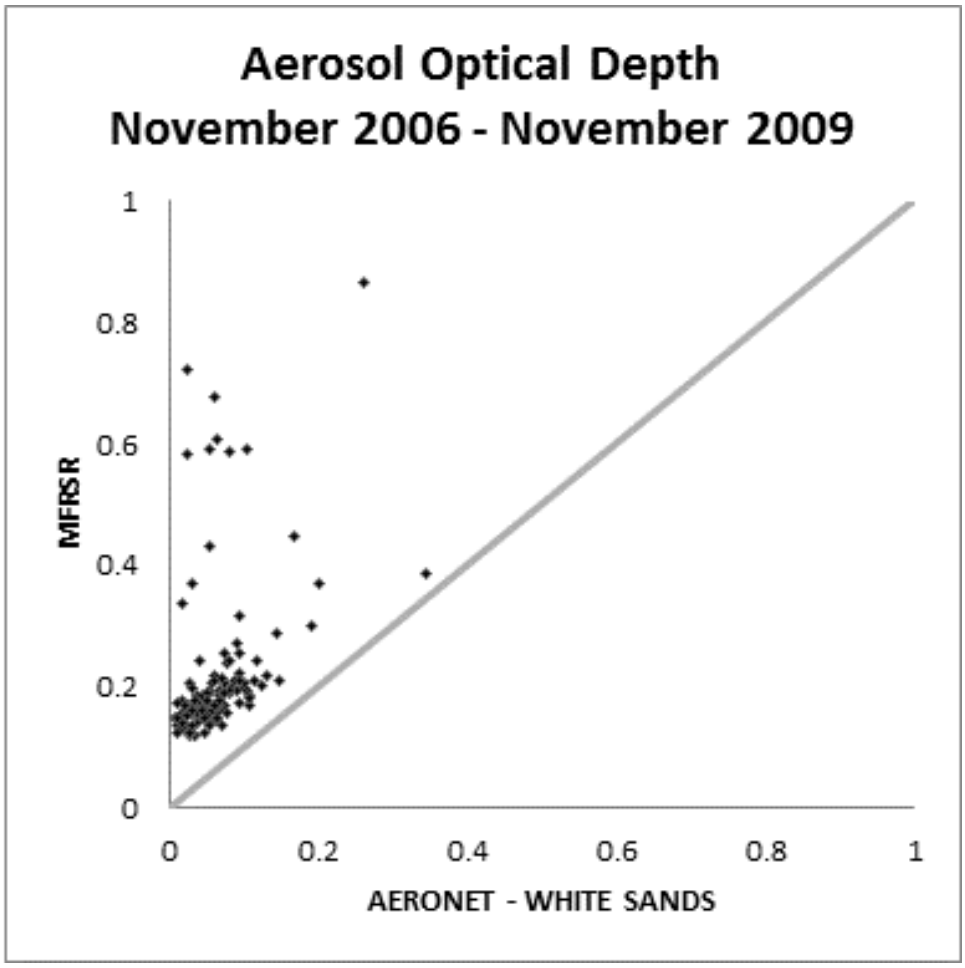

Figure 2-10. Scatter plot of MFRSR vs AERONET-White Sands AOD for the entire dataset.

In order to provide greater contrast between the values retrieved on each of the instruments, figure 2-11 portrays the three different measurements in the time series for the first year. As previously stated, the MISR instruments mostly underestimated the MFRSR and mostly overestimated the AERONET-WS values. However, during the spring and summer seasons, the gap between the three curves narrowed.

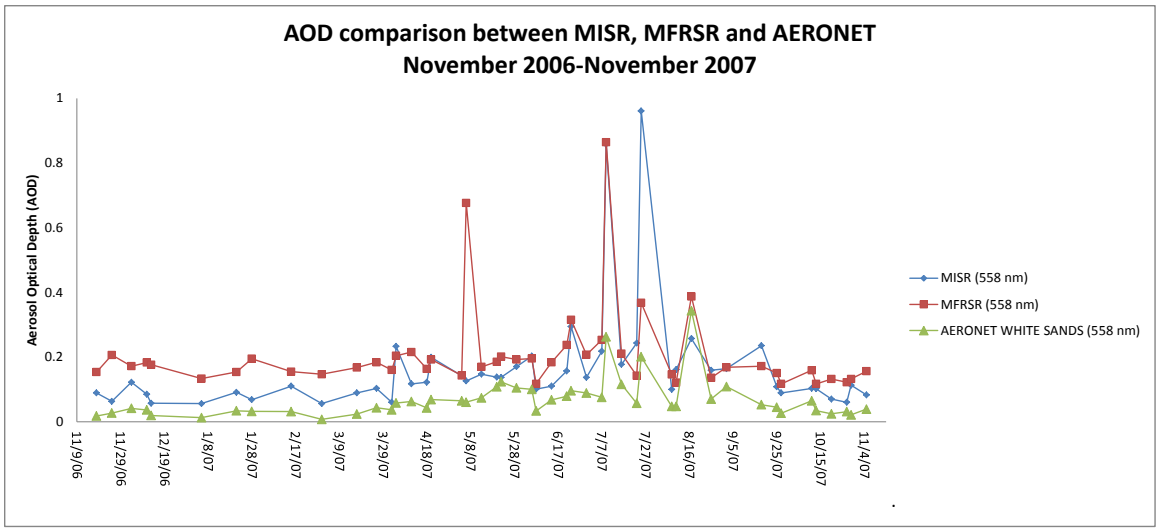

Figure 2-11. AOD data from MISR, MFRSR and AERONET from selected days from November 2006 to November 2007.

Figure 2-12 depicts the time series of the three instruments for the 2007-2008 year. Again, the spring and summer months showed the greatest correlation, while the spread for the rest of the months became larger.

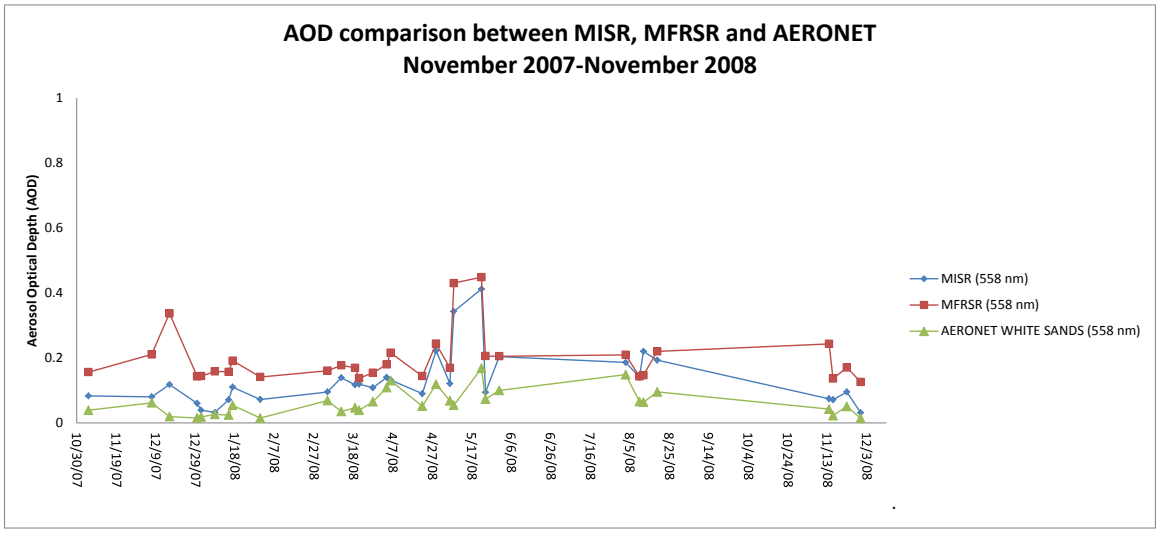

Figure 2-12. AOD data from MISR, MFRSR and AERONET from selected days from November 2007 to November 2008.

Figure 2-13 depicts intercomparison for the 2008-2009 year. The spring and summer months showed good correlation. However, the rest of the year the MFRSR data shows some discrepancy with the MISR data, even though a similar pattern is observed.

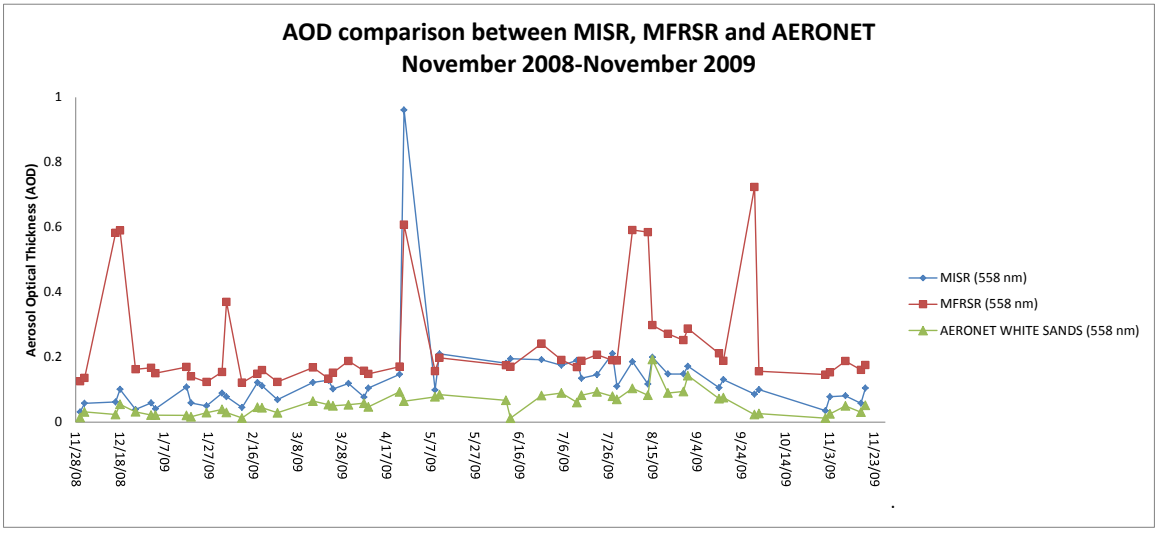

Figure 2-13. AOD data from MISR, MFRSR and AERONET from selected days from November 2008 to November 2009.

Conclusions

AOD data obtained from satellites can be very useful in the aerosol characterization due to its capability of covering wider areas than in situ instrument. However, in situ instruments provide continual measurements.

This project attempted to relate the MISR satellite data by comparing the values against the MFRSR (El Paso, TX) and AERONET (White Sands, NM) ground values. The MISR instrument underestimated the columnar values of the MFRSR ground instrument and yielded a

linear correlation of 0.52. The average error is 26.13% with a standard deviation of 12.69%. The maximum recorded error was 61.73% and the minimum was 0.54%. The linear correlation of MISR when compared to AERONET-WS was 0.58, in which MISR overestimated the columnar values of the AERONET-WS. The average error is 53.36% with a standard deviation of 18.98%. The maximum recorded error was 93.87% and the minimum was 1.51%.

Overall, the seasons with the minimum errors were the spring and summer seasons. It has been understood that in the ultraviolet regime, aerosol retrievals over deserts are favorable enabled due to the low surface reflectance at these wavelengths. However, in the visible and near IR, the desert environment can be highly reflective and accurate retrievals of AOD are extremely difficult to achieve using single view multispectral satellite instruments due to their general inability to measured radiances (Martonchick et al. 2004).

The spring and summer months showed good correlation. However, the rest of the year the MFRSR data shows some discrepancy with the MISR data, even though a similar pattern was observed.

CHAPTER 3

Retrieval of $PM_{2.5}$ Concentration at the Surface Using MISR Satellite Data and an Empirical Model

Introduction

Airborne particulate matter consists of a mixture of liquid and solid particles suspended in the air. Several research studies have found that there is a relationship among frequent exposure to fine particulate matter and a range of respiratory illnesses (Shwartz and Neas 2000); (Johnson and Graham 2005); (Dominici et al. 2006); (Pope III, Ezzati, and Dockery 2009); (Sheffield et al. 2011). In addition, these particles are able to penetrate deep into the lungs and are capable of being transported over great distances by the wind (Harrison, Deacon, and Jones 1997). Most of these studies have been conducted in urban areas, where daily particulate matter (PM) variability predominates. A study performed in Phoenix, Arizona showed that the $PM_{2.5}$ (particulate matter with an aerodynamic diameter of less than 2.5 μm) anthropogenic contribution to air pollution were mainly due to traffic, sulfate and a copper smelter. These were found to be the most consistently associated with cardiovascular mortality across the several Phoenix source allotment analyses (Mar et al. 2006).

The assessment of PM of a certain geographic region is a very important task in the understanding of the anthropogenic activities air-land interaction and its effects on human health. However, this implies the necessity of an organized network that performs various fundamental operations such as the data retrieval, quality control, as well as the acquisition, service and maintenance of the instruments that can provide us with $PM_{2.5}$ information. Therefore, the cost of operation and maintenance of this type of network is very high. Consequently, in some

developing countries the implementation of monitoring stations is not considered a top priority, causing limited in situ assessments of the PM interaction. Though, air quality models can be implemented in the absence of monitoring stations but the accuracy may be strayed due to model assumptions and absence of background information about the characteristics of ubiquitous particles.

Satellites have the ability to provide global atmospheric and environmental data for the assessment of air pollution problems. Temporal correlations between satellite measurements and in situ instruments have been studied since 1979 when the Total Ozone Mapping Spectrometer (TOMS) was launched (Chun et al. 2003). More recently, the relationship between aerosol optical depth (AOD) and surface PM concentrations has received considerable attention. As a result, several studies have explored the relationship between column AOD derived from Moderate Resolution Imaging SpectroRadiometer (MODIS) and ground fine particulate matter (Wang and Christopher 2003); (Hutchison, Smith, and Faruqui 2005). With the Multi-angle Imaging SpectroRadiometer (MISR) inception, more studies linking the AOD and ground PM have been performed (Liu et al. 2007);(van Donkelaar et al. 2010).

The use of atmospheric monitoring stations helps in the understanding of the aerosol loading ambient interaction of a particular region. Each air monitoring station is designed to determine representative concentrations of the air's composition for a particular area. The increase of linked monitoring stations will provide a larger coverage and a better understanding of the ambient dynamics. Monitoring stations of the Texas Commission on Environmental Quality (TCEQ) make daily records of different atmospheric parameters including $PM_{2.5}$ in the state of Texas, including the city of El Paso (Texas Commission on Environmental Quality 2009). The El Paso-Juarez metropolitan area is frequently affected by desert particles and

biogenic and anthropogenic emissions (Esparza et al. 2011). Hence, the TCEQ monitoring network plays an important role in understanding the atmospheric conditions and aerosols' behavior in this area. Thus, the target of this project was to link ground information with columnar satellite data. This was achieved by developing an empirical model capable of assigning parameters to the characteristic variables of the region with the purpose of predicting $PM_{2.5}$ ground concentrations from satellite values of AOD, thus providing a supplemental data source to ground measurements.

Methodology

The complete understanding between satellite and ground-level measurements will provide a solid basis to remotely sense events of high particulate matter concentrations. Liu et al., has developed an empirical model that delivers a regression between daily $PM_{2.5}$ concentrations and AOD values from satellite measurements for the eastern United States in the year 2001 (Liu et al. 2005). In another study, a method that uses total and fractional column AOD from satellite measurements to estimate ground level concentrations of fine PM was performed, by treating aerosol components as individual predictor variables (Liu, Koutrakis, and Kahn 2007).

In this research, the study area is the Paso del Norte Airshed. The limits of the area are depicted in figure 3-1.

Figure 3-1. Limits of the Paso del Norte Airhsed

This study relies on satellite and ground instruments information. Thus, the data collection and its proper processing is an indispensable joint operation that determines the accuracy of the results.

Model

The empirical model was intended to include particular characteristics of the area such as the type of region and its location, as well as the daily varying ambient parameters such as AOD, relative humidity (RH), planetary boundary layer (PBL) and $PM_{2.5}$.

The optical depth relates to the quantity of light removed from a beam by absorption and scattering during its path through a medium (vertical path from Earth's surface to outer space), being an indicator of the abundance of particles in the vertical air column. The total optical depth (τ_T) is defined by the following equation:

$$\frac{I}{I_O} = e^{-\tau} \quad (1)$$

Where, I is the observed intensity after a given path, I_O is the intensity of radiation at the source. The AOD (τ_A) is obtained by subtracting the optical depths due to Rayleigh, ozone and water vapor, from the total optical depth as shown in equation 2.

$$\tau_A = \tau_T - \tau_R - \tau_O - \tau_{wv} \quad (2)$$

This value of AOD can be also retrieved using satellite instruments, in which at a wavelength of 558 nm (green band) obeys the following equation:

$$\tau_A = \int_0^\infty \int_0^\infty C_{ext}(r, \lambda, m) n(r, z) dz dr \quad (3)$$

Where C_{ext} (r, λ, m) is the particle extinction cross-sections and n(r,z) is the height-dependent aerosol number density, r is the radius of particle, λ is the wavelength of the incident light and m is the index of refraction.

Water is ubiquitous in the atmosphere. Consequently, ambient particles frequently include some liquid water, provoking a partitioning of any individual organic compound into a liquid aerosol phase depending not only on the amounts and properties of the aerosols in the phase but also on the amount of water present (Seinfeld et al. 2001). According to Seinfeld et al. as the RH increases, some of the partitioning organic compounds will tend to be in the aerosol phase, as well as portions of some of the more hydrophobic compounds may tend to be out of the aerosol phase and back into the gas phase (Seinfeld et al. 2001). Thus, RH was included in the model.

One of the physical phenomena influencing surface particulate and other gases concentrations in the Paso del Norte area is the planetary boundary layer (PBL) above the surface (surface-based mixing height) (MacDonald et al. 2001). The PBL is the zone in the atmosphere where the fluxes of energy, momentum, and matter between the atmosphere and land are regulated (Baklanov et al. 2011). Consequently, PBL values were included in the model.

The model solves the following empirical regression equation:

$$[PM_{2.5}] = \left(e^{\varepsilon_0+\varepsilon_1(\text{variable}_1)+\varepsilon_2(\text{variable}_2)+\cdots+\varepsilon_n(\text{variable}_n)} \right) \times \left(e^{\varepsilon_{RH}(RH)}\right)(AOD)^{\varepsilon_{AOD}}(PBL)^{\varepsilon_{PBL}} \quad (4)$$

Where ε_0 through ε_n are regression coefficients for each definite variable and ε_{RH}, ε_{AOD} and ε_{PBL} are the coefficients for RH, AOD and PBL respectively. Here, the linkage between the ground measurements of $PM_{2.5}$, the atmospheric factors and the definite variables is by the retrieval of each parameter (ε) for each definite variable. These variables are listed in the following table.

Table 3-1. Description of the definite variables used in the model.

Variable	Value	Level
Region	1	Mediterranean
	2	Humid subtropical
	3	Humid continental
	4	Semiarid
	5	Arid
	6	Tropical wet and dry
	7	Tropical wet
Season	1	Spring (March-May)
	2	Summer (June-August)
	3	Fall (September-November)
	4	Winter (December-February)
Location	1	Rural
	2	Suburban
	3	Urban

By transforming equation 4 and defining each variable, then equation 5 is formed and expressed as follows:

$$\ln([PM_{2.5}]) = \varepsilon_1(\text{region}) + \varepsilon_2(\text{season}) + \varepsilon_3(\text{site}) + \varepsilon_{RH}(RH) + \varepsilon_{AOD}\ln(AOD) + \varepsilon_{PBL}\ln(PBL) \qquad (5)$$

Equation 5 is the linearized equation that was solved by the model.

Satellite data

Aerosol optical depth (AOD) data is from MISR level 2 aerosol data collection, which is processed at the Atmospheric Sciences Data Center at NASA Langley Research Center (Abdou et al. 2005). These measurements were taken within the latitude range of 31° 26’ 45.6’’ (31.446)

and 31° 59’ 5.9994’’ (31.985) and the longitude range of 106° 8’ 20.3994’’ W (-106.139) and 106° 58’11.9994’’ W (-106.97). Figure 3-2 depicts the corner points of the MISR’s overpasses.

Figure 3-2. MISR’s latitude and longitude overpass range.

MISR observes the same point on Earth in nine different angles (from nadir up to 70.5° fore and aft of the local vertical) and four spectral bands (446, 558, 672 and 866 nm) (Diner et al. 2001). MISR retrievals are performed over 16 x 16 arrays of 1.1 km x 1.1 km Space Oblique Mercator grid pixels, comprising 17.6 x 17.6 km area.

During the timeframe selected for the study, MISR produced 167 experimental values of AOD for the area, being all these approximately at 11-hour local time.

Ground data

For the ground $PM_{2.5}$ and relative humidity measurements, three monitoring stations were selected, being these the CAMS 12, 40 and 41. Then, each value was recorded at the same date and time as the MISR's measurements. A total of 167 gravimetrically based hourly average $PM_{2.5}$ measurements were collected from November 2006 to November 2009. Next, an average of the three values per day was calculated and used as input value into the model. The same procedure was employed in the retrieval of RH values, since the three monitoring stations also count with this sensor.

For the PBL data, each value was selected by matching the MISR's measurements date and time. Then, the values were retrieved by inspecting each graph provided by the Global Systems Division of the Earth System Research Laboratory (ESRL) (NOAA-ESRL-GSD/MADIS CAP Profile n.d.). Figure 3-3 shows one of the graphs used to retrieve the PBL height.

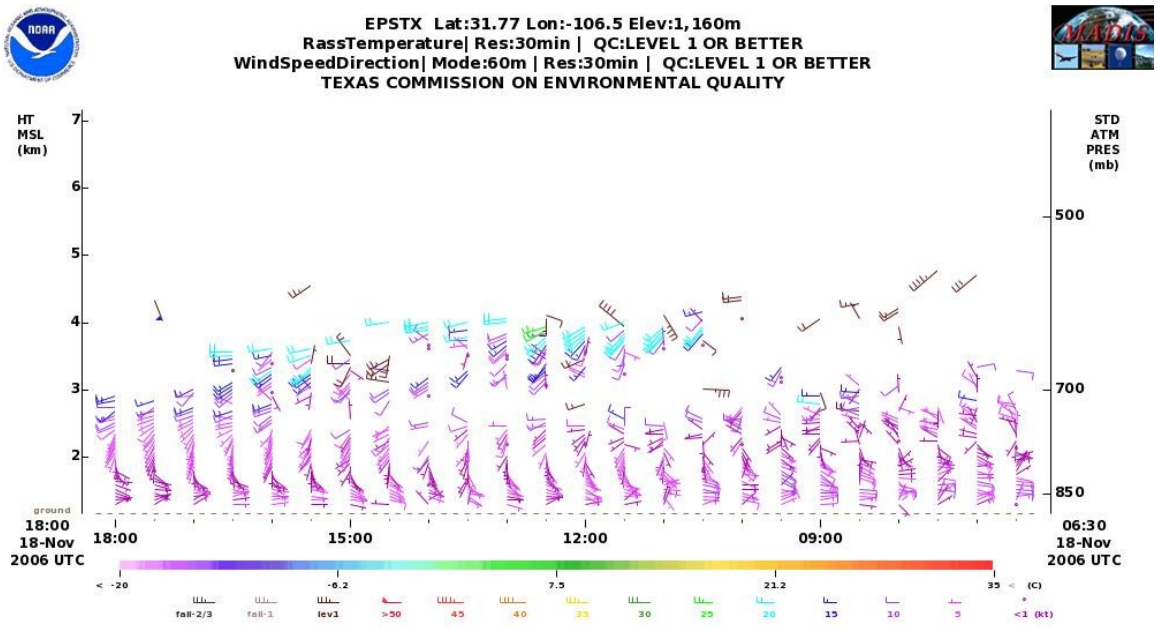

Figure 3-3. PBL height information.

Results

The histograms for the frequency of the various parameters showed that the values of AOD and $PM_{2.5}$ are unimodal, while RH and PBL also showed a unimodal distribution regardless of the additional peaks.

Figure 3-4 shows the histogram for the 167 selected AOD values from November 2006 to November 2009. The arithmetic and geometric means for the 167 values in this 3-year study was 0.14 and 0.12 respectively. The geometric mean, unlike an arithmetic mean (average), tends to dampen the effect of very high or low values. The maximum values recorded were in the spring and summer seasons (0.961), while the greatest arithmetic and geometric means were recorded in the spring season (.22 and .18 respectively). Detailed results for this parameter are shown in table 3-2.

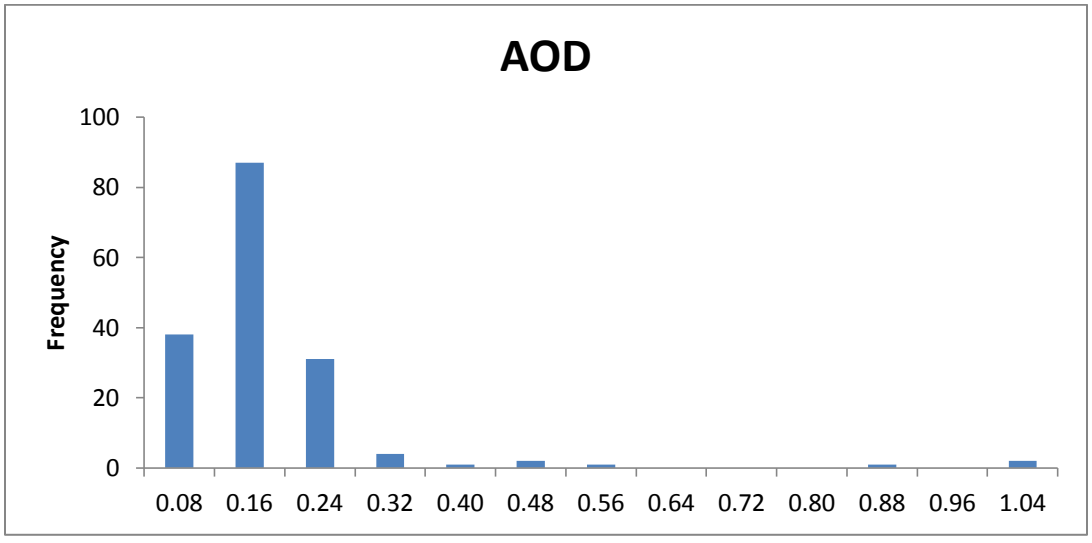

Figure 3-4. Histogram using 167 values for the AOD variable.

Figure 3-5 shows the histogram for the $PM_{2.5}$ values measured at ground level at three different stations. The mode was in the range of 5.5 to 8.3 $\mu g/m^3$. The three-year arithmetic and geometric means were 6.58 and 5.37 $\mu g/m^3$ respectively. The maximum value of 34.86 $\mu g/m^3$ was recorded in the winter month, while the largest arithmetic and geometric means were recorded in the spring and summer months. Thorough results for this parameter are shown in table 2.

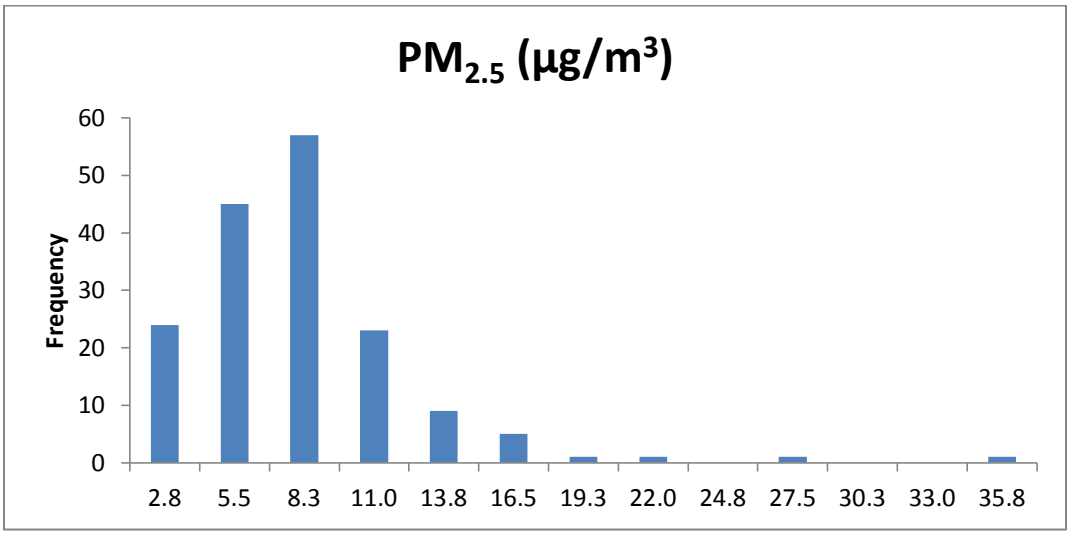

Figure 3-5. Histogram using 167 values for the $PM_{2.5}$ variable.

The histogram for the RH is shown in figure 3-6. These values were retrieved from the same ground monitoring station used for the $PM_{2.5}$. Characteristic of the region, the highest frequency for this parameter is located in the 15% and 25% size bins. The three-year mean of the RH was 23.41%. The seasonal behavior of the RH had its higher average value in winter (28.31%), followed by summer (25.61%), fall (24.85%) and spring (16.12%). The

minimum value was recorded in the spring (5.65%) followed by a day in the winter (6.45%). Complete results for this parameter are shown in table 3-2.

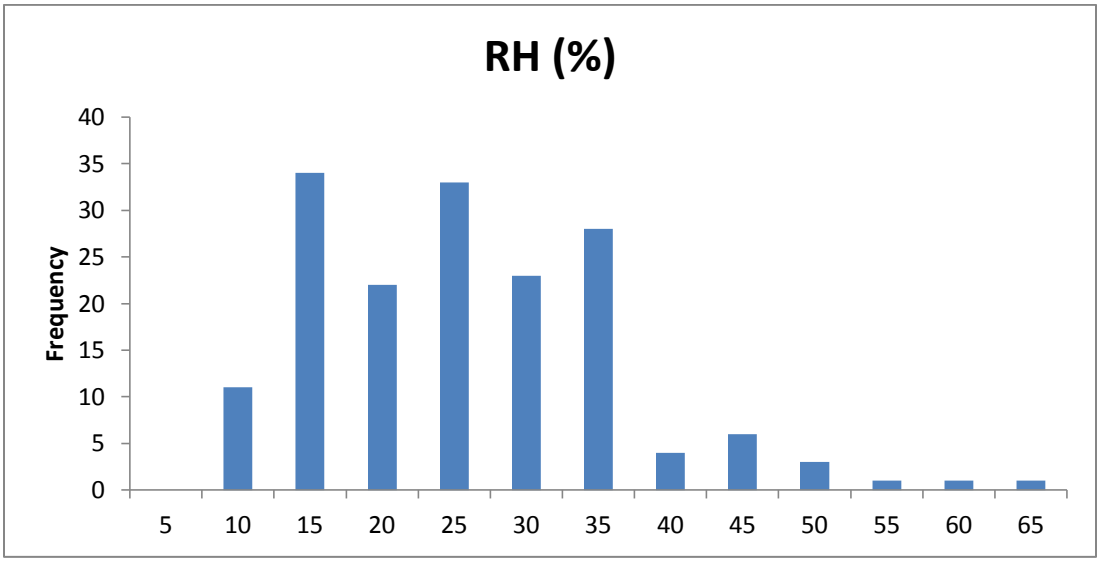

Figure 3-6. Histogram using 167 values for the RH variable.

The PBL height's histogram is depicted in figure 3-7. These values were retrieved at sea level, while the elevation of the study area was 1.16 km. The three-year average was 2.65 km, having its highest average during the summer season, followed by fall, spring and winter. The winter season recorded the lowest value, a clear sign of morning inversion (Brown et al. 2001). Thorough results for this parameter are shown in table 3-2.

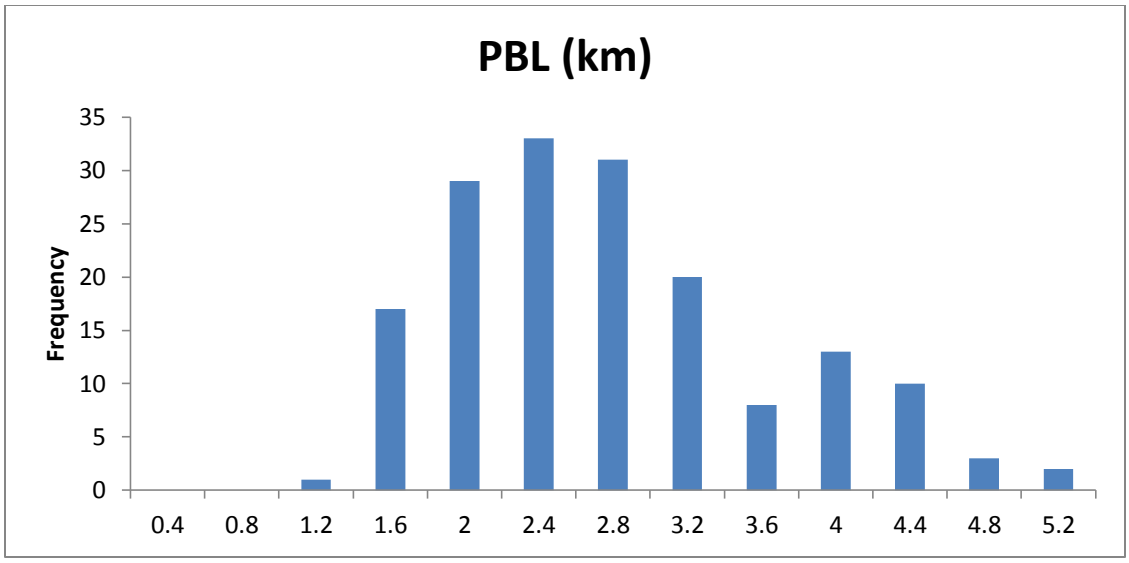

Figure 3-7. Histogram using 167 values for the PBL variable.

Table 3-2. Statistical summary of each of variable used in the model allocated by season and by the 3-year period.

Variable	Season	Maximum	Minimum	Arithmetic Mean	Arithmetic Std. deviation	Geometric Mean	Geometric Std. deviation	AM-GM inequality
AOD (Unitless)	Spring	0.96	0.06	0.16	0.14	0.14	1.63	0.02
	Summer	0.96	0.09	0.22	0.18	0.18	1.65	0.04
	Fall	0.24	0.03	0.10	0.04	0.09	1.51	0.01
	Winter	0.25	0.03	0.09	0.04	0.08	1.57	0.01
	3-year	0.96	0.03	0.14	0.13	0.12	1.78	0.02
PM2.5 ($\mu g/m^3$)	Spring	19.38	1.56	7.24	3.48	6.43	1.68	0.81
	Summer	15.58	2.52	7.21	3.01	6.69	1.47	0.52
	Fall	13.07	0.74	5.62	2.95	4.81	1.84	0.81
	Winter	34.86	0.60	5.95	6.73	3.81	2.59	2.14
	3-year	34.86	0.60	6.58	4.38	5.37	1.98	1.21
RH (%)	Spring	32.65	5.65	16.12	7.44	14.58	1.57	1.54
	Summer	43.60	10.90	25.61	8.37	24.20	1.42	1.41
	Fall	48.10	11.00	24.85	8.97	23.35	1.43	1.50
	Winter	63.75	6.45	28.31	12.12	25.71	1.59	2.60
	3-year	63.75	5.65	23.41	10.43	21.09	1.61	2.32
PBL (km)	Spring	3.80	1.40	2.27	0.61	2.19	1.32	0.08
	Summer	5.00	2.20	3.42	0.77	3.34	1.25	0.08
	Fall	4.80	1.50	2.81	0.93	2.66	1.40	0.15
	Winter	4.00	1.20	2.18	0.56	2.12	1.27	0.06
	3-year	5.00	1.20	2.65	0.87	2.52	1.38	0.13

The implementation of the empirical model was done by using the data for each variable described in equation 5. In general, the model described 38% of the variability. Initially, this value was 24% while counting the whole set. Figure 3-8 shows the model results against the observed values describing the linear variability for the entire data set (from November 2006 to November 2009).

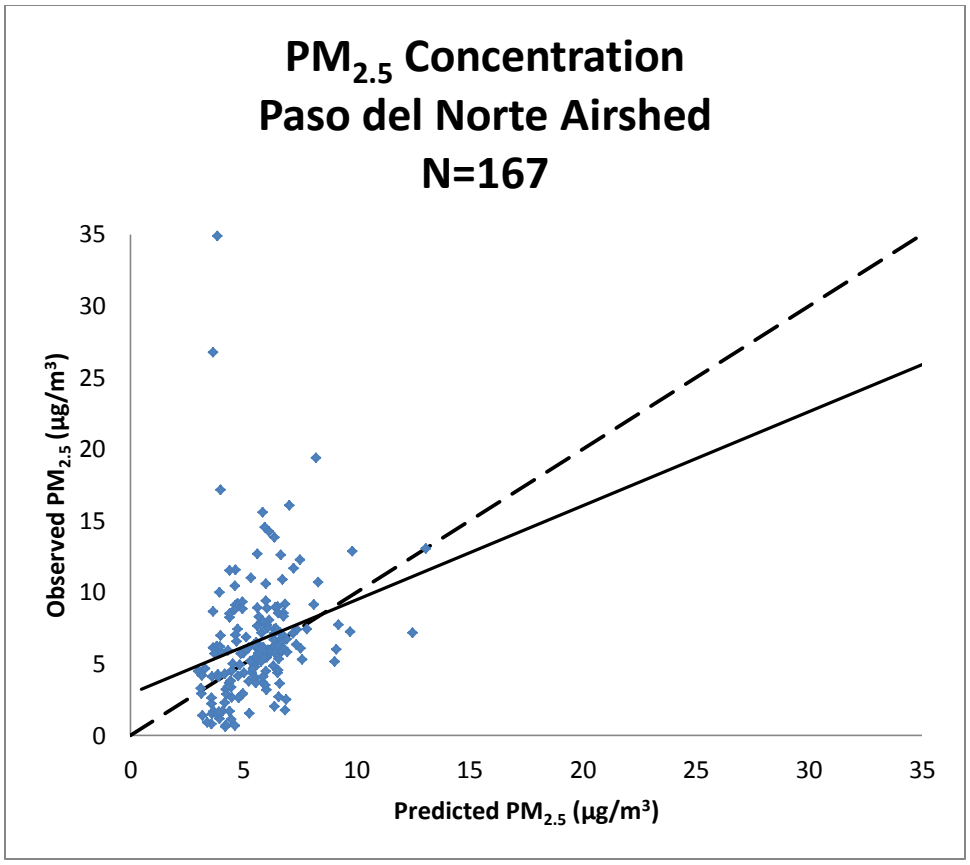

Figure 3-8. Linear relationship between the observed and predicted $PM_{2.5}$ values for 167 available dates from November 2006 to November 2009.

When the values that exceeded 15 µg/m^3 were removed (6 values), the linear correlation increased to 0.43, yet using the retrieved parameters of the whole set. By running the model with values less than 15 µg/m^3 (N=161), the linear correlation was 0.38. Figure 3-9 depicts these results comprising November 2006 through November 2009 time span. Table 3-3 lists the values for the retrieved parameters.

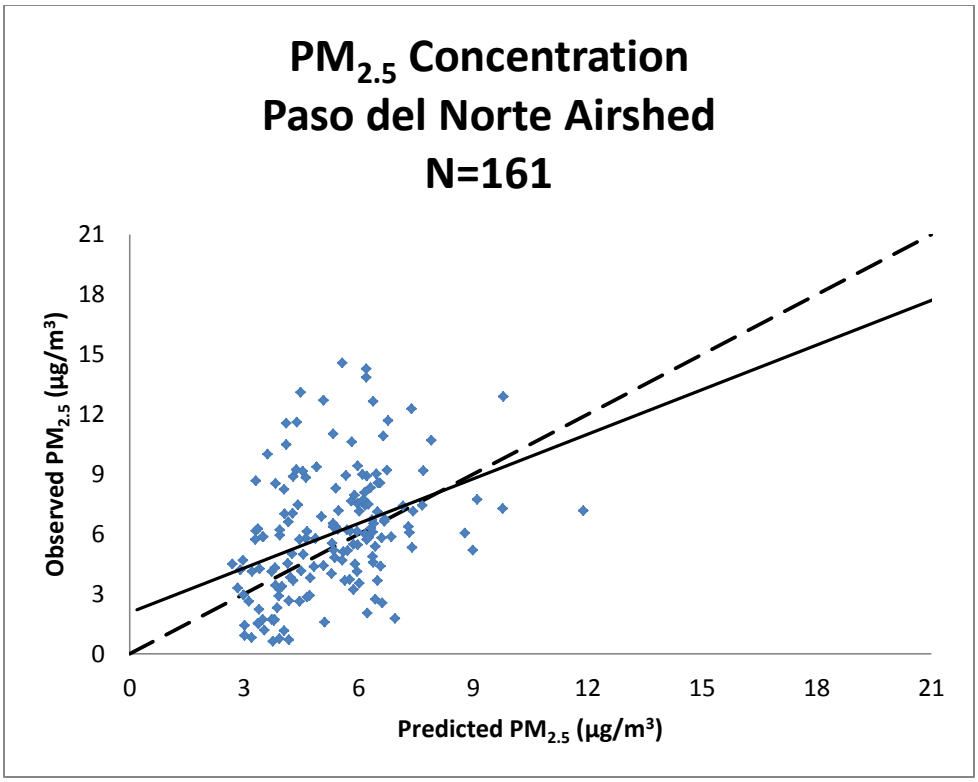

Figure 3-9. Linear relationship between the observed and predicted $PM_{2.5}$ values for 161 available dates from November 2006 to November 2009.

The Paso del Norte has the four season well defined (Rincon et al. 2005). Therefore, it was very congruent to have seasonal parameters derived from each seasonal analysis. Figure 3-10 shows a plot between the observed and predicted $PM_{2.5}$ values for the spring season. Here the linear correlation was 0.26 for a sample size of 46 points. Table 3-3 shows the retrieved parameters for each of the variables.

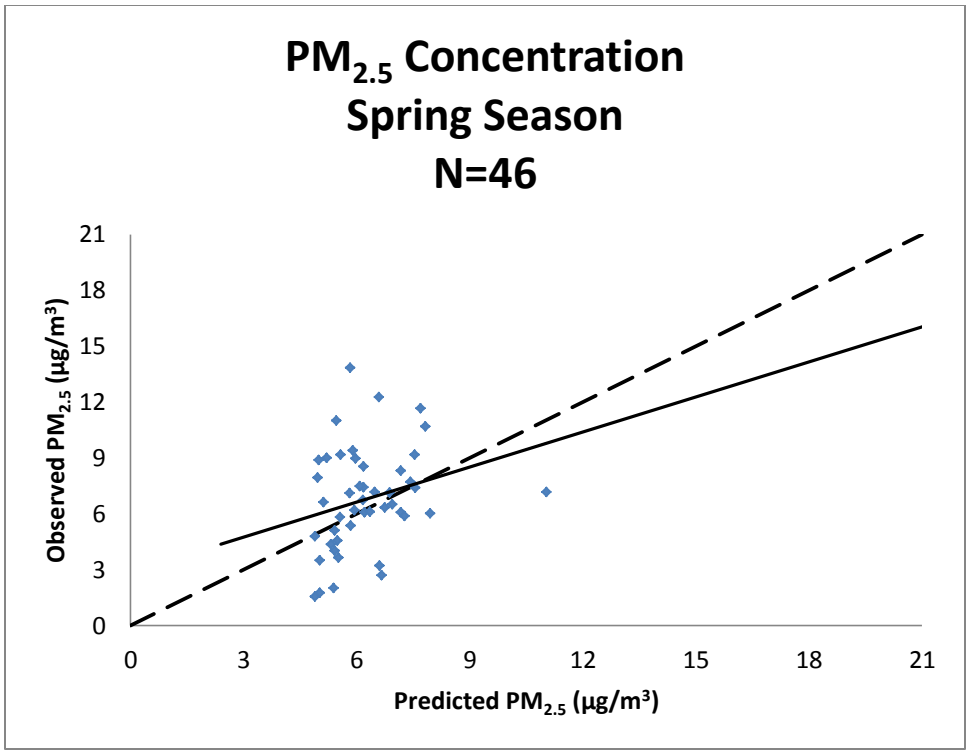

Figure 3-10. Linear relationship between the observed and predicted $PM_{2.5}$ values for 46 available dates for the spring seasons from November 2006 to November 2009.

Figure 3-11 is the graph showing the linear correlation between the observed and predicted $PM_{2.5}$ concentrations for the summer season. Here the linear correlation was 0.32, of a sample size of 42. This season showed the largest average concentration, with a value of 7.01 $\mu g/m^3$ and a root mean squared (RMS) error of 2.61 $\mu g/m^3$.

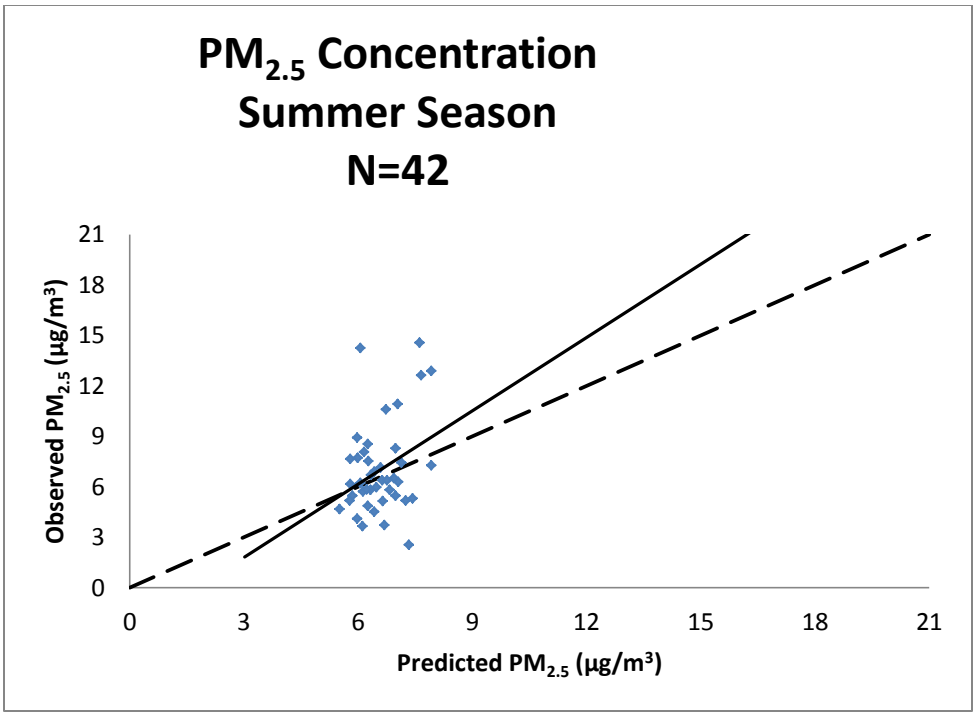

Figure 3-11. Linear relationship between the observed and predicted $PM_{2.5}$ values for 42 available dates for the summer seasons from November 2006 to November 2009.

The relationship between the observed and predicted $PM_{2.5}$ concentrations for the fall season is depicted in figure 3-12. Here the linear correlation was 0.25, being this the lowest correlation value among the four seasons.

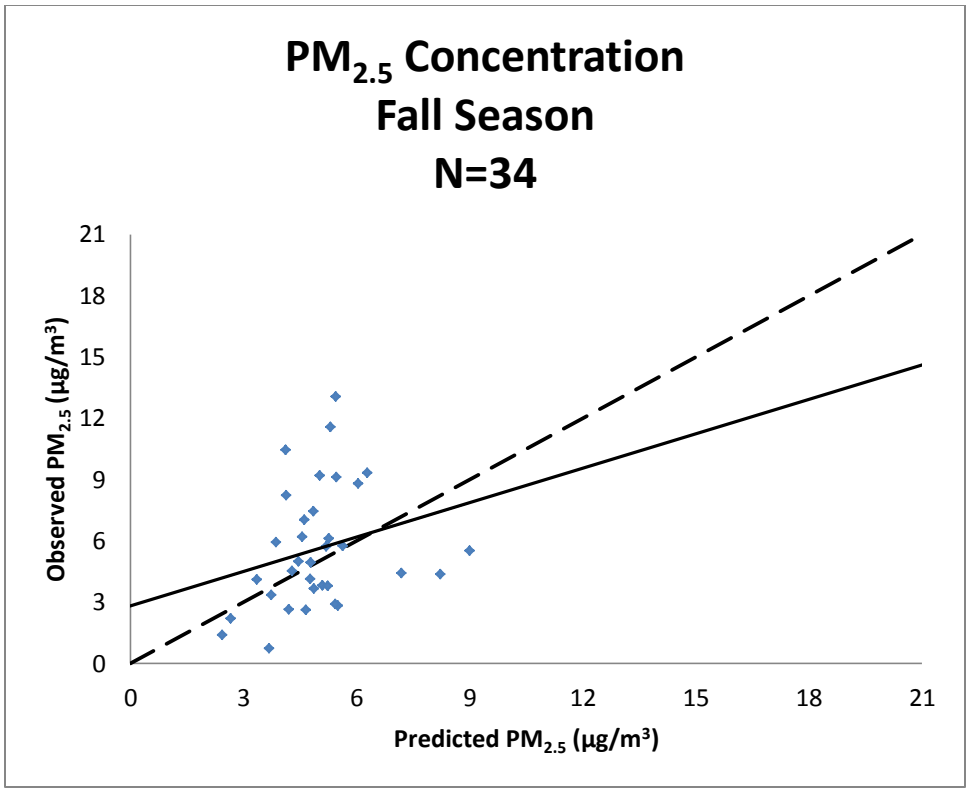

Figure 3-12. Linear relationship between the observed and predicted $PM_{2.5}$ values for 34 available dates for the fall seasons from November 2006 to November 2009.

The comparison graph for the winter season is illustrated in figure 3-13. Here, with a sample size of 39, the linear correlation was 0.42, the highest of the four seasons. It also showed the lowest average concentration of the four seasons (4.38 $\mu g/m^3$) but the largest RMS error (3.07$\mu g/m^3$).

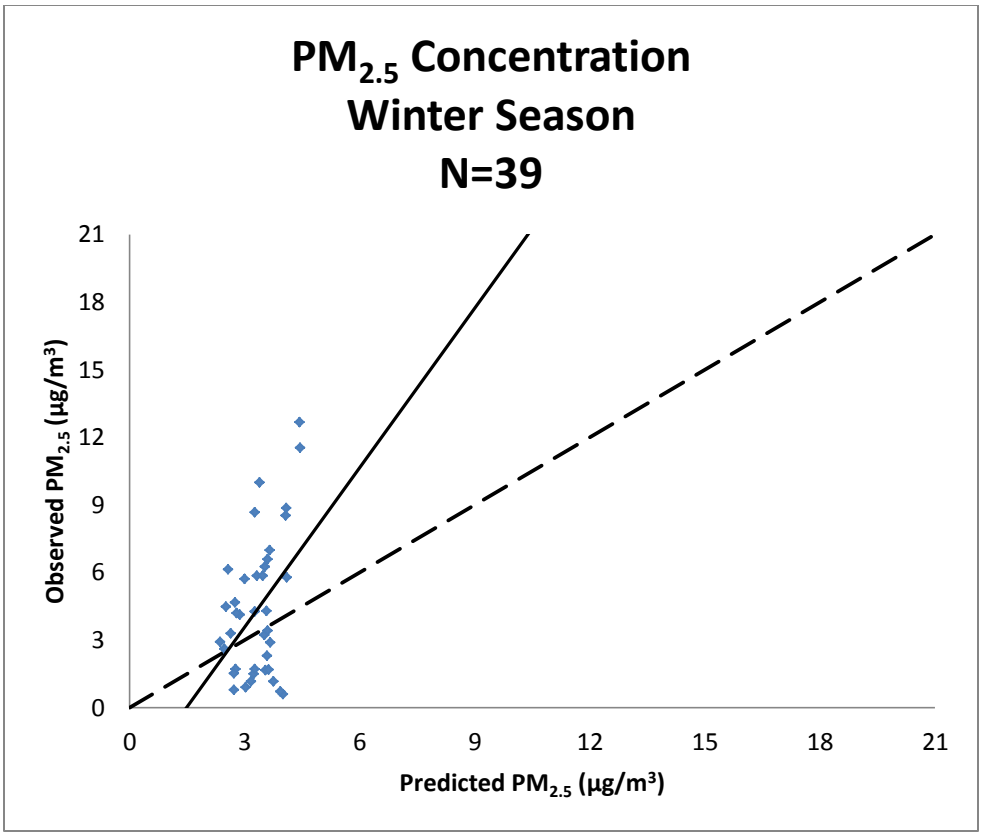

Figure 3-13. Linear relationship between the observed and predicted $PM_{2.5}$ values for 39 available dates for the winter seasons from November 2006 to November 2009.

Table 3-3 summarizes the values for the parameters for each of the five scenarios, as well as their average concentrations, RMS errors and linear correlations.

Table 3-3. Summary for each of the five scenarios listing the retrieved parameters, root mean squared error and the linear correlation.

	Entire Set	Refined Set (< 15 μg/m^3)	Individual Parameters by Season			
			Spring	*Summer*	*Fall*	*Winter*
Sample Size	167	161	46	42	34	39
Region	0.4335	0.5277	0.5163	0.5059	0.6281	0.3791
Season	-0.0992	-0.1296	0	0	0	0
Site	0.2629	0	0	0	0	0
RH	-0.0068	-0.0047	-0.0047	-0.0063	-0.0004	-0.0095
AOD	0.2874	0.2976	0.1897	0.0966	0.65	0.2671
PBL	-0.0057	0.0549	-0.3945	-0.2693	0.0186	0.324
Average concentration (μg/m^3)	6.57	6.02	6.79	7.01	5.62	4.38
RMS error (μg/m^3)	4.39	2.92	2.70	2.61	2.94	3.07
Linear correlation	0.24	0.38	0.26	0.32	0.25	0.42

The negative parameter of the RH indicates that the same AOD values would correspond to higher $PM_{2.5}$ concentrations as RH decreases, showing a correction for the hydrophilic effect on particle light extinction.

The positive parameter of AOD indicates that the surface $PM_{2.5}$ concentrations varied linearly with MISR AOD values. In figure 3-14 it can be observed that the during this time series both parameter behave linearly, although few values for the AOD were out of the established norm.

The negative sign of the PBL in the spring and summer seasons indicates that the fine particles emitted at the surface are diluted within the boundary layer as the PBL increases, resulting in lower $PM_{2.5}$ concentration. The positive sign of the PBL for the fall and winter season may indicate the opposite, less dilution of particles regardless of the increment in the PBL height.

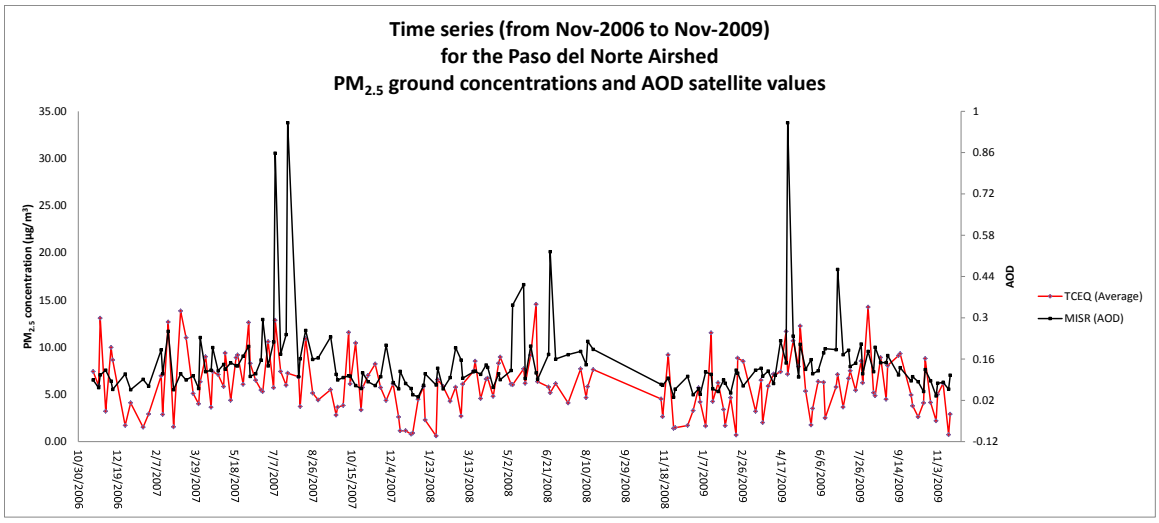

Figure 3-14. Time series for the Paso del Norte Airshed comparing the ground values of $PM_{2.5}$ and the satellite AOD values from November 2006 to November 2009.

Conclusion

The objective of this research, which was to estimate ground $PM_{2.5}$ by using the MISR's satellite AOD data through the implementation of an empirical model, was successfully achieved. This model addressed seven variables within the region. The purpose was to create a model that can be replicated in other regions.

For this project, selected days in a three-year span were analyzed. Overall the model explained 38% of the variability. The greater variability of the observed AOD values is likely attributable to the fact the satellite measures the particles in the entire atmospheric column, including particles that not necessarily affect ground concentrations.

During the seasonal analysis, winter showed the greatest linear correlation. This result could be associated to the PBL height, which for this season showed the lowest average, meaning more mixing at lower altitudes.

With the inclusion of more data points per season, a better correlation could be achieved. In addition, the inclusion of more variables such as vertical profile and aerosol composition will enhance the correlation. Consequently, a more descriptive range of parameter values and more accurate estimations will be obtained.

SUMMARY AND CONCLUSIONS

Urban regions are by their nature concentrations of humans, materials and activities. They therefore exhibit both the highest levels of pollution and the largest targets of direct impacts.

On the urban scale there is often, but not always, a reasonable relation between local emissions and resulting local pollution levels. In contrast to regional and global pollution, local efforts to mitigate urban-scale air pollution may therefore generally have direct and observable effects (Baltensperger et al. 2009).

Particle size is the most important parameter for characterizing the behavior of aerosols. All properties of aerosols depend on particle size, some very strongly. Light scattering provides and extremely sensitive tool for the measurement of aerosol concentrations and particle size. A single particle as small as 0.1 μm produces a detectable scattered light signal. Light-scattering techniques have the advantages of minimally disturbing the aerosol and providing instantaneous information that is often suitable for continuous monitoring. A disadvantage of light-scattering instruments is that the scattering may be sensitive to small changes in refractive index, scattering angle, particle size, or particle shape, which can lead to confusing or misleading results (Hinds 1998).

This dissertation work brought a well understanding of the aerosols in the Paso del Norte Airshed. Each of the three objectives fulfilled the general aim in different but complimentary ways, and by having a holistic vision of the study it is evident that there was an intertwined relationship in which one objective cannot be fully understood without the other two.

There is a firm conviction that this research is has a significant relevance for the atmospheric physics field, as well as for the remote sensing and air pollution modeling areas. Intrinsically, there is an academic benefit in which the research institution, the University of Texas at El Paso, demonstrates its leadership and research capacity in the optical characterization of aerosols for the Paso del Norte region.

This study has brought short-term benefits by amplifying the current knowledge of aerosols in the zone. Hitherto, it is imperative to have a continual study on this field due to the high complexity and constant change of the atmospheric conditions. However, there is no doubt that the advancement in new technology and improved methodologies will permit a more specific understanding of the aerosols and its interaction with the environment and their effects on climate. Therefore, this research has set another silo that will produce social, economic and health related benefits. A social benefit could arise from the improved understanding of aerosol dynamics and the social and health problem that they could represent. Hence, this understanding could lead to the implementation of better regulations that seek the welfare of the community. Inherently, there could be an economic benefit by addressing the main responsible entities of the emissions of aerosols and possibly obtain monetary proceeds from them to remediate the social and health damages.

LIST OF REFERENCES

1. Abdou, Wedad A., David J. Diner, John V. Martonchik, Carol J. Bruegge, Ralph A. Kahn, Barbara J. Gaitley, Kathleen A. Crean, Lorraine A. Remer, and Brent Holben. 2005. "Comparison of coincident Multiangle Imaging Spectroradiometer and Moderate Resolution Imaging Spectroradiometer aerosol optical depths over land and ocean scenes containing Aerosol Robotic Network sites." *Journal of Geophysical Research* 110(D10S07):1-12.

2. Abramowitz, Milton and Irene A. Stegun, eds. 1972. *Handbook of Mathematical Funcitons: with formulas, graphs, and mathematical tables*. New York: Dover.

3. Alexandrov, Mikhail D., Peter Kiedron, Joseph J. Michalsky, Gary Hodges, Connor J. Flynn, and Andrew A. Lacis. 2007. "Optical depth measurements by shadow-band radiometers and their uncertainties." *Applied Optics* 46(33):8027-8038.

4. Alexandrov, Mikhail D., Andrew A. Lacis, Barbara E. Carlson, and Brian Cairns. 2008. "Characterization of atmospheric aerosols using MFRSR measurements." *Journal of Geophysical Research* 113(D08204):1029-1052.

5. Baklanov, Alexander A., Branko Grisogono, Robert Bornstein, Larry Mahrt, Sergej S. Zilitinkevich, Peter Taylor, Soren E. Larsen, Mathias W. Rotach, and H.J.S. Fernando. 2011. "The nature, theory, and modeling of atmospheric planetary boundary layers." *Bulleting of the American Meteorological Society* (February):1-6.

6. Baltensperger, Urs, Janet Barlow, Peter Brimblecombe, Hugh Coe, Jes Fenger, Atul Jain, Roland Leigh, John Lockwood, Rob Mackenzie, Paul Monks, Dudley Shallcross, Richard

Wayne, and Paul I. Williams. 2009. *Atmospheric Science for Environmental Scientists*. Wiley-Blackwell.

7. Baltensperger, Urs, Charles Clement, Ian Colbeck, Markus Furger, Irena Grgic, Ari Laaksonen, Mihalis Lazardis, Kari Lehtinen, Rob Mackenzie, David Topping, and Jay Turner. 2008. *Environmental Chemistry of Aerosols*. Blackwell Publishing.

8. Bigelow, D S., J R. Slusser, A F. Beaubien, and J H. Gibson. 1998. "The USDA ultraviolet radiation monitoring program." *Bulletin of the American Meteorological Society* 79:601-615.

9. Blackman, Allen and Alejandra Palma. 2002. "Scrap tires in Ciudad Juárez and El Paso: Ranking the Risks." *Journal of Environment & Development* 11(3):247-266.

10. Charlson, R. J., S. E. Schwartz, J. M. Hales, R. D. Cess, J. A. Coakley, Jr., J. E. Hansen, and D. J. Hofmann. 1992. "Climate forcing by anthropogenic aerosols." *Science* 255:423-430.

11. Cho, Hi K., Myeong J. Jeong, and Jhoon Kim. 2003. "Dependence of diffuse photosynthetically active solar irradiance on total optical depth." *Journal of Geophysical Research* 108(4):1-10.

12. Chopping, Mark, Lihong Su, Albert Rango, John V. Martonchik, Debra P. Peters, and Andrea Laliberte. 2008. "Remote sensing of woody shrub cover in desert grasslands using MISR with a geometric-optical canopy reflectance model." *Remote Sensing of Environment* 112:19-34.

13. Chun, D. A., Y. J. Kaufman, G. Zibordi, J. D. Chem, Jietai Mao, Chengcai Li, and B. N. Holben. 2003. "Global monitoring of air pollution over land from the Earth Observing System-Terra Moderate Resolution Imaging Spectroradiometer (MODIS)." *Journal of Geophysical Research* 108(D21):4-1-4-18.

14. Diner, D. J., W. A. Abdou, C. J. Bruegge, J. E. Conel, K. A. Crean, B. J. Gaitley, M. C. Helmlinger, R. A. Kahn, J. V. Martonchik, and S. H. Pilorz. 2001. "MISR aerosol optical depth retrivals over southern Africa during the SAFARI-2000 dry season campaign." *Geophysical Research Letters* 28(16):3127-3130.

15. Diner, David J., Jewel C. Beckert, Terrence H. Reilly, Carol J. Bruegge, James E. Conel, Ralph A. Kahn, John V. Martonchik, Thomas P. Ackerman, Roger Davies, Siegfried A. Gerstl, Howard R. Gordon, Jan-Peter Muller, Ranga Myneni, Piers J. Sellers, Bernard Pinty, and Michel M. Verstraete. 1997. "Multi-angle Imaging SpectroRadiometer (MISR) Instrument Description and Experiment Overview." *IEEE Transactions on Geoscience and Remote Sensing*.

16. Diner, David J., Ralph A. Kahn, Carol J. Bruegge, V. M. Jonh, Wedad A. Abdou, Barbara J. Gaitley, Mark C. Helmlinger, Olga V. Kalashnikova, and Wen-Hao Li. 2004. "Refinements to MISR's radiometric calibration and implications for establishing a climate-quality aerosol observing system." *Passive Optical Remoet Sensing of the Atmosphere and Clouds IV* 5652:57-65.

17. Dominici, Francesca, Roger D. Peng, Michelle L. Bell, Luu Pham, Aidan McDermont, Scott L. Zeger, and Jonathan M. Samet. 2006. "Fine particulate air pollution and hospital

admission for cardiovascular and respiratory diseases." *Journal of American Medical Association* 295(10):1127-1134.

18. Draxler, R R. and G D. Rolph. 2010. "NOAA Air Resources Laboratory Silver Spring MD." HYSPLIT (HYbrid Single-Particle Lagrangian Integrated Trajectory) Model acces via NOAA ARL READY Website. Retrieved March 10, 2010 (http://ready.arl.noaa.gov/HYSPLIT.php).

19. Eck, T F., B N. Holben, J S. Reid, O Dubovik, A Smirnov, N T. O'Neill, I Slutsker, and S Kinne. 1999. "Wavelength dependence of the optical depth of biomass burning, urban, and desert dust aerosols." *Journal of Geophysical Research* 104:31333-31349.

20. Esparza, Angel E., Rosa M. Fitzgerald, Thomas E. Gill, and Javier Polanco. 2011. "Use of light extinction method and inverse modeling to sutdy aerosols in the Paso del Norte Airshed." *Atmospheric Environment* 45:7360-7369.

21. Forster, P, V Ramaswamy, P Artaxo, T Berntsen, R Betts, D W. Fahey, J Haywood, J Lean, D C. Lowe, G Myhre, J Nganga, R Prinn, G Raga, M Schulz, and R Van Dorland. 2007. "Changes in Atmospheric Constituents and in Radiative Forcing. In: Climate Change 2007: The Physical Science Basis. Contribution of Working Group I to the Fourth Assessment Report of the Intergovernmental Panel on Climate Change." *Cambridge University Press* 131-217.

22. Google. n.d. "Google Maps." Retrieved October 20, 2009 (http://maps.google.com/maps?f=q&source=s_q&hl=en&geocode=&q=el+paso,+texas&sll=37.0625,-

95.677068&sspn=40.137381,92.724609&ie=UTF8&hq=&hnear=El+Paso,+Texas&z=11
).

23. Gouveia, Nelson and Tony Fletcher. 2000. "Time series analysis of air pollution and mortality: effects by cause, age and socioeconomic status." *Journal of Epidemiological Community Health* (54):750-755.

24. Hand, J L., S M. Kreidenweis, J Slusser, and G Scott. 2004. "Comparisons of aerosol optical properties derived from sun photometry to estimates inferred from surface measurements in Big Bend National Park, Texas." *Atmospheric Environment* 38:6813-6821.

25. Hansen, Christian. 1992. "Analysis of discrete ill-posed problems by means of the l-curve." *Society for Industrial and Applied Mathematics* 34(4):561-580.

26. Hansen, Christian. 1994. "Regularization tools: a MATLAB package for analysis and solution of discrete ill-posed problems." *Numerical Algorithm* 6(1).

27. Harrison, Roy M., Andrew R. Deacon, and Marcus R. Jones. 1997. "Sources and Processes Affecting Concentrations of PM10 and PM2.5 Particulate Matter in Birmingham (U.K)." *Atmospheric Environment* 4103-4117.

28. Hinds, William. 1998. *Book of Aerosol Technology*.

29. Holben, B. N., T. F. Eck, I. Slutsker, Tanre D., J. P. Buis, A. Setzer, E. Vermote, J. A. Reagan, Y. J. Kaufman, T. Nakajima, F. Lavenu, I. Jankowiak, and A. Smirnov. 1998. "AERONET- A federated instrument network and data archive for aerosol characterization." *Remote Sensing Environment* 66:1-16.

30. Hutchison, Keith D., Solar Smith, and Shazia J. Faruqui. 2005. "Correlating MODIS aerosol optical thickness data with ground-based PM2.5 observations across Texas for use in a real-time air quality prediction system." *Atmospheric Environment* 39:7190-7203.

31. INEGI. n.d. "Instituto Nacional de Estadistica y Geografia." Retrieved November 20, 2009 (http://www.inegi.org.mx/lib/olap/general_ver4/MDXQueryDatos.asp?#Regreso&c=10401).

32. Jacobson, Mark Z. 1999. *Fundamentals of Atmospheric Modeling*. Cambridge University Press.

33. Johnson, Philip R. and John J. Graham. 2005. "Fine Particulate Matter National Ambient Air Quality Standards: Publich health impact on populations in the Northeastern United States." *Environmental Health Perspectives* 113(9):1140-1147.

34. Kahn, Ralp A., Barbara J. Gaitley, John V. Martonchik, David J. Diner, and Kathleen A. Crean. 2005. "Multiangle Imaging Spectroradiometer (MISR) global aerosol optical depth validation based on 2 years of coincident Aerosol Robotic Network (AERONET) observations." *Journal of Geophysical Research* D10S04.

35. Kalashnikova, Olga V. and Ralph A. Kahn. 2008. "Mineral dust plume evolution over the Atlantic from MISR and MODIS aerosol retrieval." *Journal of Geophysical Research* 113(D24204):1-17.

36. Kaufman, Yoram J., Didier Tanré, and Olivier Boucher. 2002. "A satellite view of aerosols in the climate system." *Nature* 419:215-223.

37. Kaufman, Y. J., D. Tanré, H. R. Gordon, T. Nakajima, J. Lenoble, R. Frouin, H. Grassl, B. M. Herman, M. D. King, and P. M. Teillet. 1997. "Passive remote sensing of tropospheric aerosol and atmospheric correction for the aerosol effect." *Journal of Geophysical Research* 102(D14):16815-16830.

38. Kaufman, Y. J., D. Tanré, L. A. Remer, E. F. Vermote, A. Chu, and B. N. Holben. 1997. "Operational remote sensing of tropospheric aerosol over land from EOS moderate resolution imaging spectroradiometer." *Journal of Geophysical Research* 102(D14):17051-17067.

39. Kokhanovsky, Alexander A. 2008. *Aerosol Optics: Light Absorption and Scattering by Particles in the Atmosphere*. Praxis Publishing.

40. Krause, Eugene F. 1986. *Taxicab geometry: An adventure in non-euclidean geometry*. New York: Dover.

41. Ligon, David A., Tuan W. Chen, and James B. Gillespie. 1996. "Determination of aerosols parameters from light-scattering data using an inverse Monte Carlo technique." *Applied Optics* 35(21):4297-4303.

42. Li, Wen-Whai, Ruben Orquiz, Jose H. Garcia, Tania T. Espino, Nicholas E. Pingitore, Jorge Gardea-Torresdey, Judith Chow, and John G. Watson. 2001. "Analysis of temporal and spatial dichotomous PM air samples in the El Paso-Cd. Juarez air quality basin." *Journal of Air & Waste Management Association* (51):1551-1560.

43. Li, Wen-Whai, Ruben Orquiz, Jose H. Garcia, Tania T. Espino, Nicholas E. Pingitore, Jorge Gardea-Torresdey, Judith Chow, and John G. Watson. 2001. "Analysis of temporal and spatial dichotomous PM air samples in the El Paso-Cd. Juarez air quality basin." *Journal of the Air & Waste Management Association* 50:1551-1560.

44. Liu, Yangyang, W P. Arnott, and John Hallett. 1999. "Particle size distribution retrieval from multispectral optical depth: influences of particle nonsphericity and refractive index." *Journal of Geophysical Research* 104:31753-31762.

45. Liu, Yang, Petros Koutrakis, and Ralph Kahn. 2007. "Estimating fine particulate matter component concentrations and size distributions using satellite-retrieved fractional aerosol optical depth: Part 1-Method development." *Journal of Air & Waste Management Association* 57:1351-1359.

46. Liu, Yang, Petros Koutrakis, Ralph Kahn, Solene Turquety, and Robert M. Yantosca. 2007. "Estimating fine particulate matter component concentrations and size distributions using satellite-retrieved fractional aerosol optical depth: Part 2-A case study." *Journal of Air & Waste Management Association* 57:1360-1369.

47. Liu, Yang, Jeremy A. Sarnat, Vasu Kilaru, Daniel J. Jacob, and Petros Koutrakis. 2005. "Estimating Ground-Level PM2.5 in the Eastern United States Using Satellite Remote Sensing." *Environmental Science and Technolog* 3269-3278.

48. Lynch , Amanda H. and John J. Cassano. 2006. *Applied Atmospheric Dynamics*. John Wiley & Sons, Ltd.

49. MacDonald, Clinton P., Paul T. Roberts, Hilary H. Main, Timothy S. Dye, Dana L. Coe, and James Yarbrough. 2001. "The 1996 Paso del Norte Ozone study: analysis of meteorological and air quality data that influence local ozone concentrations." *The Science of the Total Environment* 276:93-109.

50. Malm, William C. and Jenny L. Hand. 2007. "An examination of the physical and optical properties of aerosols collected in the IMPROVE program." *Atmospheric Environment* (41):3407-3427.

51. Mar, Therese F., Kazuhiko Ito, Jane Q. Koenig, Timothy V. Larson, Delbert J. Eatough, Ronald C. Henry, Eugene Kim, Francine Laden, Ramona Lall, Lucas Neas, Matthias Stolzel, Pentti Paatero, Philip K. Hopke, and George D. Thurston. 2006. "PM source apportionment and health effects. 3. Investigation of inter-method variations in associations between estimated source contributions of PM2.5 and daily mortality in Phoenix, AZ." *Journal of Exposure Science and Environmental Epidemiology* 16:311-320.

52. Martonchick, J. V., D. J. Diner, R. Kahn, and B. Gaitley. 2004. "Comparison of MISR and AERONET aerosol optical depths over desert sites." *Geophysical Research Letters* 31:1-4.

53. Mckenzie, Richard, Greg Bodeker, Gwen Scott, Jim Slusser, and Kathleen Lantz. 2006. "Geographical differences in erythemally-weighted UV measured at mid-latitude USDA sites." *Photochemical & Photobiological Sciences* 5:343-352.

54. Mishchenko, Michael I., Larry D. Travis, and Daniel W. Mackowski. 1996. "T-matrix computations of light scattering by nonspherical particles: a review." *Journal of Quantitative Spectroscopy and Radiative Transfer* 55:535-575.

55. Mishchenko, Michael I., Nadia T. Zakharova, Gordon Videen, Nikolai G. Khlebtsov, and Thomas Wriedt. 2010. "Comprehensive T-matrix reference database: A 2007 -2009 update." *Journal of Quantitative Spectroscopy & Radiative Transfer* 111:650-658.

56. Murr, L. E., K. F. Soto, K. M. Garza, P. A. Guerrero, F. Martinez, E. V. Esquivel, D. A. Ramirez, Y. Shi, J. J. Bang, and J. I. Venzor. 2006. "Combustion-generated nanoparticulates in the El Paso, TX, USA/Juarez, Mexico Metroplex: Their comparative characterization and potential for adverse health effects." *International Journal of Environmental Research and Public Health* 3(1):48-66.

57. National Weather Service Weather Forecast Office. 2009. "Extremes (and some normals) of El Paso Weather from 1879." Retrieved April 27, 2010 (http://www.srh.noaa.gov/epz/?n=elpaso_extreme_weather).

58. Noble, Christopher A., Shaibal Mukerjee, Melissa Gonzales, Charles E. Rodes, Philip A. Lawless, Sanjay Natarajan, Eric A. Myers, Gary A. Norris, Luther Smith, Haluk Ozkaynak, and Lucas M. Neas. 2003. "Continuous measurement of fine and ultrafine particulate matter, criteria pollutants and meteorological conditions in urban El Paso, Texas." *Atmospheric Environment* 37:827-840.

59. Ordieres, J B., E P. Vergara, R S. Capuz, and R E. Salazar. 2005. "Neural network prediction model for fine particulate matter (PM2.5) on the US-Mexico border in El Paso

(Texas) and Ciudad Juarez (Chihuahua)." *Environmental Modeling and Software* 547-559.

60. Pearson, Roderick, Rosa M. Fitzgerald, and Javier Polanco. 2007. "An inverse reconstruction model to retrieve aerosol size distribution from optical depth data." *Journal of Optics A: Pure and applied optics* 9:56-59.

61. Pope III, Arden C., Majid Ezzati, and Douglas W. Dockery. 2009. "Fine-particulate air pollution and life expectancy in the United States." *The New England Journal of Medicine* 360(4):376-386.

62. Ramanathan, V., P. J. Crutzen, J. T. Kiehl, and D. Rosenfeld. 2001. "Aerosols, Climate, and the Hydrological Cycle." *Science* 294:2119-2124.

63. Rivera Rivera, Nancy I., Thomas E. Gill, Kristi A. Gebhart, Jenny L. Hand, Max P. Bleiweiss, and Rosa M. Fitzgerald. 2009. "Wind modeling of Chihuahuan Desert dust outbreaks." *Atmospheric Environment* 43:347-354.

64. Rodriguez, G. and D. Theis. 2005. "An algorithm for estimating the optimal regularization parameter by the L-curve." *Rendiconti di Matematica* 25(7):69-84.

65. Seinfeld, John N., Garnet B. Erdakos, William E. Asher, and James F. Pankow. 2001. "Modeling the formation of secondary organic aerosol (SOA). 2. The predicted effects of relative humidity on aerosol formation in the Pinene, Pinene, Sabinene, Carene and Cyclohexene-ozone systems." *Environmental Science and Technology* 35:1806-1817.

66. Seinfield, John H. and Spyros N. Pandis. 2006. *Atmospheric Chemistry and Physics*. 2nd ed. John Wiley & Sons.

67. Sheffield, Perry, Angkana Roy, Kendrew Wong, and Leonardo Trasande. 2011. “Fine particulate matter pollution linked to respiratory illness in infants and increased hospital costs.” *Health Affairs* 30(5):871-878.

68. Shwartz, Joel and Lucas Neas. 2000. “Fine particles are more strongly associated than coarse particles with acute respiratory health effects in schoolchildren.” *Epidemiology* 11(1):6-10.

69. Slusser, James, James Gibson, David Bigelow, Donald Kolinski, Patrick Disterhoft, Kathleen Lantz, and Arthur Beaubien. 2000. “Langley method of calibrating UV filter radiometers.” *Journal of Geophysical Research* 105:4841-4849.

70. Slusser, James, James Gibson, David Bigelow, Donald Kolinski, Wanfeng Mou, Gloria Koenig, and Arthur Beaubien. 1999. “Comparison of column ozone retrievals by use of an UV multifilter rotating shadow-band radiometer with those from Brewer and Dobson spectrophotometers.” *Journal of Applied Optics* 38(9):1543-1551.

71. Sokolik, Irina N. and Owen B. Toon. 1996. “Direct radiative forcing by anthropogenic airborne mineral aerosols.” *Nature* 381:681-683.

72. Staniswalis, Joan G., Norris J. Parks, Julia O. Bader, and Yolanda Muñoz Maldonado. 2005. “Temporal Analysis of Airborne Particulate Matter Reveals a Dose-Rate Effect on Mortality in El Paso: Indications of Differential Toxicity for Different Particle Mixtures.” *Journal of Air & Waste Management Association* (55):893-902.

73. Stohl, Andreas. 1998. “Computation, accuracy and applications of trajectories: a review and bibliography.” *Journal of Atmospheric Environment* 106:18015-18027.

74. Sun, Wenbo and Bing Lin. 2006. “Optical characterization of metallic aerosols.” *Journal of Quantitative Spectroscopy & Radiative Transfer* (100):359-372.

75. Texas Commission on Environmental Quality. 2009. “Texas Commission on Environmental Quality.” SIP Revision: El Paso, PM10, November 1991. Retrieved March 5, 2010 (http://www.tceq.state.tx.us/implementation/air/sip/nov1991elpaso.html).

76. Toledano, C., M. Wiegner, M. Garhammer, M. Seefeldner, J. Gasteiger, D. Muller, and P. Koepke. 2009. “Spectral aerosol optical depth characterization of desert dust during SAMUM 2006.” *Tellus* 61B:216-228.

77. Twomey, S. 1977. *Introduction to the Mathematics of inversion in remote sensing and indirect measurements*. Amsterdam: Elsevier Scientific Publishing Company.

78. US Census Bureau. n.d. “Population estmates.” Retrieved November 20, 2009 (http://www.census.gov/popest/estimates.html).

79. van Donkelaar, Aaron, Randall V. Martin, Michael Brauer, Ralph Kahn, Robert Levy, Carolyn Verduzco, and Paul J. Villeneuve. 2010. “Global estimates of ambient fine particulate matter concentrations from satellite-based aerosol optical depth: Development and application.” *Environmental Health Perspectives* 118(6):847-855.

80. Verma, S., C. Venkataraman, O. Boucher, and S. Ramachandran. 2007. “Source evaluation of aerosols measured during the Indian Ocean Experiment using combined chemical transport and back trajectory modeling.” *Journal of Geophysical Research* 112(D11210).

81. Wang, Jun and Sundar A. Christopher. 2003. “Intercomparison between satellite-derived aerosol optical thickness and PM2.5 mass: Implications for air quality studies.” *Geophysical Reserach Letters* 30(21):1-4.

CURRICULUM VITA

Angel E. Esparza was born in Ciudad Juárez, México in February 18, 1983. Due to the proximity with El Paso, Texas, he raised in both sides of the border. In the year 2000, he entered The University of Texas at El Paso and graduated in May 2004 with a Bachelor of Science in Industrial Engineering. In the following semester he obtained a second Bachelor of Science in Mechanical Engineering from UTEP. Subsequently, after being accepted into the Master of Science program in Mechanical Engineering, he worked as a lecturer at the Universidad Autónoma de Ciudad Juárez. Towards the Masters completion, he obtained a full-time job as an Industrial Engineer at the United Parcel Service (UPS) located in El Paso. He graduated in December 2006 and in September 2007 he got accepted into the Master in Science in Industrial Engineering at the New Mexico State University. While pursuing this degree, he obtained a full-time job with the Border Environment Cooperation Commission. He graduated in December 2008 and got accepted into Environmental Science and Engineering Ph.D. program at the University of Texas at El Paso. While in the Ph. D. program, he was working as a research assistant in the Environmental Physics Research group supported by the NOAA/EPP grant. He has presented his work at several conferences and has published two papers on his work.

Permanent Address:

2340 Robert Wynn

El Paso Texas, 79936

angel.esparza@gmail.com